GEOFORSCHUNGSZENTRUM POTSDAM

STIFTUNG DES ÖFFENTLICHEN RECHTS

Scientific Technical Report

Yuriy Maystrenko

Evolution and structure of the Glueckstadt Graben by use of borehole data, seismic lines and 3D structural modelling, NW Germany

_____

vom Fachbereich Geowissenschaften

der Freien Universität Berlin

zur Erlangung des akademischen Grades eines

Dr. rer. nat

genehmigte Dissertation

Berlin, 2005

Scientific Technical Report STR05/14

Evolution and structure of the Glueckstadt Graben by use of borehole data, seismic lines and 3D structural modelling, NW Germany

Diplom-Geophysiker

Yuriy Maystrenko

vom Fachbereich Geowissenschaften

der Freien Universität Berlin

zur Erlangung des akademischen Grades eines

Dr. rer. nat

genehmigte Dissertation

Berlin, 2005

*When a man has no longer any
conception of excellence
above his own,
his voyage is done, he is
dead*

Henry Ward Beecher

Contents

I

List of figures

IV

V

VI

Acknowledgments

Abstract

The Central European Basin System is one of the basins where the sedimentary cover is strongly affected by salt tectonics. The most significant stage of salt movement occurred during the Triassic. The largest Triassic subsidence occurred in the different sub-basins surrounding the Ringkoebing-Fyn High such as the Horn Graben, the Danish Basin and the Glueckstadt Graben. Furthermore, the thickest Triassic succession is observed in the Glueckstadt Graben where it reaches more than 9000 m. In the present study, the structure and the Permian to recent evolution of the Glueckstadt Graben are investigated by use of borehole data, seismic lines and 3D structural modelling.

The evaluation of the diverse deformation patterns of the sedimentary cover and their relations to salt structures show that the strongest salt movements occurred at the beginning of the Keuper when the Gluckstadt Graben was affected by extension. The onlap patterns of the Jurassic sediments onto the top of the Keuper succession indicate essential changes of the sedimentation style during the Jurassic. Thick Jurassic sediments are only observed around salt structures and are thinning away from salt walls or salt stocks. The Upper Cretaceous strata have an approximately constant thickness and the parallel reflections patterns indicate a quiet tectonic setting with very minor salt movements in the Late Cretaceous. Renewed salt flow during the Paleogene-Neogene caused rapid subsidence along the marginal parts of the Central Triassic Graben in the Westholstein, the Eastholstein and the Hamburger troughs. The thick Paleogene-Neogene strata within the marginal troughs may also be related to a regional component of tectonic subsidence in the area, contemporary with rapid subsidence in the North Sea.

The 3D modelling approach has been used to determine salt distribution at certain paleo-levels in response to unloading due to sequential removing of the stratigraphic layers. The modelling approach was also aimed to reconstruct the original Permian salt distribution immediately after deposition. The initial salt thickness varies from 1300 m at the flanks of the basin up to 3000 m within the central part and demonstrates a clear NNE-SSW trend of the basin. The regional trend of the restored salt distribution points to a westward continuation of the Permian salt basin.

The formation of the deep Central Triassic Graben and the subsequent Jurassic-Cenozoic marginal troughs was strongly controlled by the development of salt structures through time. It is shown that the depocentre of sedimentation was moving away from the central part of the of the original Graben structure towards its margins. The evaluation of the available data and results of the 3D reverse modelling demonstrate that a greater amount of subsidence occurred close to the active salt structures, and may have resulted in gradual depletion of Permian salt. Thus, this study indicates that the source of such long-term subsidence is derived from gradual depletion of the Permian salt, which started within the axial part of the basin and moved towards the basin flanks with time. In this sense, the Glueckstadt Graben was formed at least partially as a "basin-scale rim syncline" during post-Permian times. Therefore, the results show that salt withdrawal may have played an important role during the Meso-Cenozoic evolution and that the effects of salt-driven subsidence during the Meso-Cenozoic can be considered the main reason for the formation of the deep Central Triassic Graben and the subsequent Jurassic-Cenozoic marginal troughs.

Zusammenfassung

Das zentraleuropäische Beckensystem ist eines der Becken, in denen die Sedimentdecken stark durch Salztektonik beeinflusst sind. Die stärksten salztektonischen Aktivitäten traten während der Trias auf. Die größte triassische Subsidenz erfolgte in den verschiedenen Unterbecken rund um das Ringköbing-Fünen Hoch (Horn Graben, Dänisches Becken, Glückstadt Graben). Die mächtigste triassische Abfolge wurde im Glückstadtgraben beobachtet, wo sie mehr als 9000 m Mächtigkeit erreicht. In der vorliegenden Studie wurden die Struktur sowie die Entwicklung des Glückstadt Grabens vom Perm bis heute mit Hilfe von Bohrdaten, seismischen Linien und 3D-Strukturmodellierung untersucht.

Die Auswertung der verschiedenen Deformationsmuster der Sedimentdecke und ihr Bezug zu Salzstrukturen zeigen, dass die stärksten Salzbewegungen am Beginn des Keupers, während einer Dehnung des Glückstadt Graben auftraten. Die jurassischen Sedimente zeigen dann eine grundlegende Änderungen der Sedimentationsart während des Jura an. Mächtige jurassische Sedimente treten nur rund um Salzstrukturen auf und dünnen mit zunehmender Entfernung von Salzmauern oder Salzstöcken aus. Die Oberkreideschichten haben eine annähernd konstante Mächtigkeit, und die parallelen Reflektionsmuster weisen auf eine ruhige tektonische Subsidenz mit geringen Salzbewegungen in der Oberkreide hin. Erneute Salzbewegungen während des Paläogens-Neogens verursachten schnelle Subsidenz entlang der Randbereiche des zentraltriassischen Grabens, den Westholstein, Ostholstein und Hamburger Trögen. Die mächtigen paläogen-neogenen Schichten innerhalb der Randtröge sind eventuell auch mit einer regionalen Komponente tektonischer Subsidenz verbunden, zeitgleich mit schneller Subsidenz in der Nordsee.

Der 3D-Modellierungsansatz wurde genutzt, um die Salzverteilung für verschiedenen Paläolevels als Reaktion auf Entlastung durch sequentielles Entfernen der stratigraphischen Schichten zu bestimmen. Mit dem Modellierungsansatz wurde auch versucht, die ursprüngliche permische Salzverteilung unmittelbar nach der Ablagerung zu rekonstruieren. Die ursprüngliche Salzmächtigkeit variiert zwischen 1300 m an den Beckenflanken und bis zu 3000 m innerhalb des zentralen Teils und zeigt einen klaren NNO-SSW-Trend innerhalb des Beckens.

Die Bildung des tiefen zentraltriassischen Grabens und der nachfolgenden jurassisch-känozoischen Randtröge wurde stark durch die langandauernde Entwicklung von Salzstrukturen kontrolliert. Es wird gezeigt, dass das Sedimentationszentrum sich vom Zentralteil der ursprünglichen Grabenstruktur in Richtung ihrer Ränder verlagerte. Die Auswertung der verfügbaren Daten und die Ergebnisse der 3D-Rückwärtsmodellierung zeigen, dass der größte Teil der Subsidenz nahe aktiver Salzstrukturen auftrat, und eventuell zu einer graduellen Abwanderung permischer Salze führte. Daher zeigt die Studie, dass die Ursache der langzeitigen Subsidenz die graduelle Abwanderung permischen Salzes ist, welche im axialen Teil des Beckens begann und sich im Laufe der Zeit in Richtung der Beckenflanken bewegte. In diesem Sinne wurde der Glückstadtgraben zumindest teilweise in nachpermischer Zeit als "basin-scale rim syncline" geformt. Daher zeigen die Ergebnisse, dass dieser Salzrückzug während der meso-känozoischen Evolution eine bedeutende Rolle gespielt haben dürfte, und dass die Effekte salzgesteuerter Subsidenz während des Meso-Känozoikums als Hauptursache der Bildung des tiefen zentraltriassischen Grabens und die nachfolgenden jurasso-känozoischen Tröge angesehen werden kann.

Chapter I

INTRODUCTION

The study of basin evolution is an aim, which is difficult to achieve in areas of strong salt tectonics. Postdepositional salt flow complicates the recognition of basin evolution both in the local and regional scale. This problem has been analyzed in many different ways. The interpretation of 2D seismic lines is difficult because the seismic pattern is complicated by salt movements. Two main questions of salt tectonics are: (1) the triggering mechanism and (2) the changes in the basin architecture caused by salt flow. Understanding these processes is essential and has to be analyzed by use of additional methods, such as analogue experiments or numerical physical modellenig. During the last decades, 2D and 3D numerical modelling of salt movements together with structural information from seismics has been used for resolving some problems of salt tectonics in basins such as the Gulf of Mexico, North Sea basins, Precaspian basin, Dniepr-Donets basin and many others (e.g. Woidt, 1978; Schmeling, 1987; Roemer and Neugebauer, 1991; Poliakov et al., 1993; Daudre and Cloetingh, 1994; Kaus and Podladchikov, 2001; Stovba et al., 2003; Scheck et al. 2003; Ismail-Zadeh et al., 2004). The Glueckstadt Graben (GG) is one of the sedimentary basins where the sedimentary cover has been strongly affected by salt tectonics. This means that salt movements had an important impact on sedimentation and the subsequent deformation of Mesozoic and Cenozoic strata.

The GG is located between the North Sea and the Baltic Sea, at a transition between areas of different crustal structures (Abramovitz et al., 1999; Meissner et al., 2002; Krawczyk et al., 2002), and between the Ringkoebing-Fyn High in the north and Elbe Fault Zone in the south. Consequently, the GG overprints major structural units in the transition area between Baltica and Caledonian-Variscan Europe. Since the 1990s and until now, the Thor Suture (or Caledonian Deformation Front, Fig. 1.1) has been usually considered as the contact between Baltica and Central Europe (e.g. Pharaoh et al., 1997), while Cocks et al. (1997) favoured the Elbe Line as the major contact zone. A more detailed model of a wedge-like piece of Baltic crust continuing from the Ringkoebing-Fyn High to the Elbe Line has been suggested by the BASIN'96 experiment (DEKORP-BASIN Research Group, 1999) and favoured by Bayer et al. (1999, 2002). Southward of the GG, a block with a low velocity zone in the lower crust was documented between the Elbe Line and the Elbe Fault Zone (e.g.

Aichroth et al., 1992; Thybo, 2001; Scheck et al. 2002). Similar results, concerning the EOL as the southernmost boundary of Baltica have been derived from the TOR-experiment, however, the interpretation is not straight forward and the southern margin of the Ringkoebing-Fyn High may serve as an alternative candidate for the Baltica margin at the level of the upper mantle (Gregersen et al., 2002).
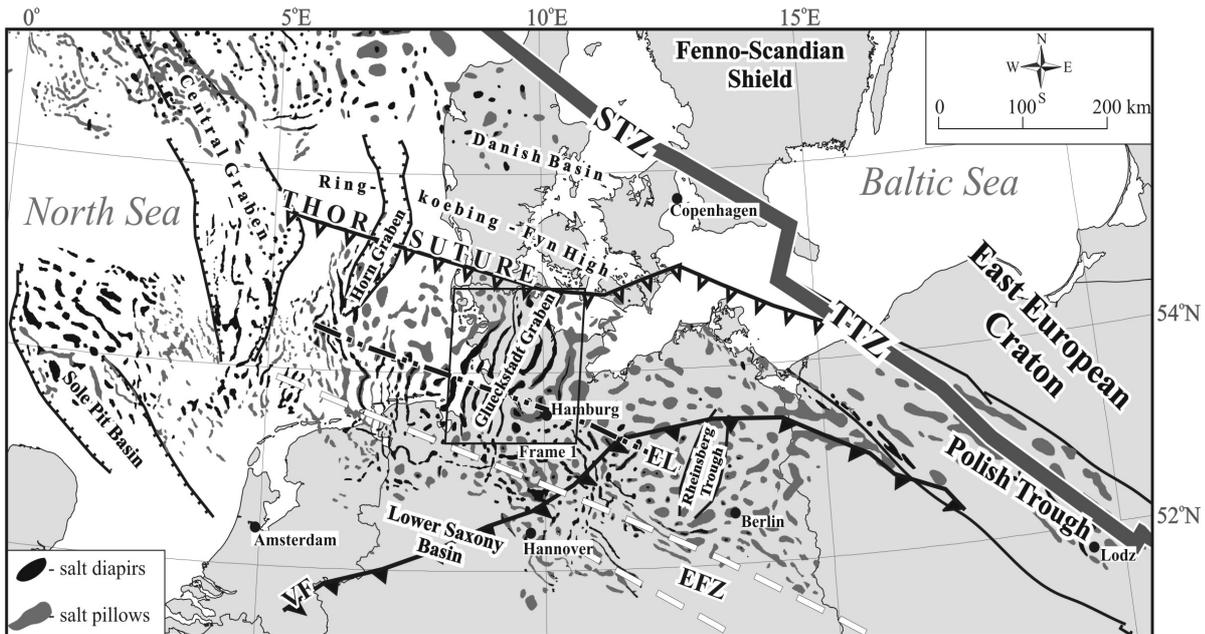
Figure 1.1. Location of the study area (frame 1) in relation to major structural units within the Central European Basin System (compiled after Ziegler, 1990b; Lockhorst et al., 1998; Pharaoh, 1999, Bayer et al., 2002). STZ: Sorgenfrei-Tornqist Zone, TTZ: Teisseyre-Tornquist Zone, EOL: Elbe-Odra Line, EFZ: Elbe Fault Zone, VF: Variscan Front.

The Southern Permian basin, the Danish Basin and the Mid-Polish Trough together with the superimposed Mesozoic graben and basin structures (e.g. the GG, the Horn Graben, the Rheinsberg Trough and the Lower Saxony Basin) form the Central European Basin System (CEBS). The sedimentary cover of the CEBS is pierced by Permian salt, which has been mobilized during the Mesozoic and Cenozoic to form a variety of salt structures (walls, stocks and pillows). One of the significant stages of salt movements occurred during the Triassic. The Triassic corresponds to a period of global plate boundary and plate kinematics

reorganization, marking the beginning of the break-up of Pangea (Ziegler, 1990). From the thickness map of the Triassic in the CEBS it is obvious that sediments extended from the western part of the North Sea to Eastern Poland (Fig. 1.2). The largest Triassic subsidence occurred in the different sub-basins surrounding the Ringkoebing-Fyn High (Fig. 1.2), in the
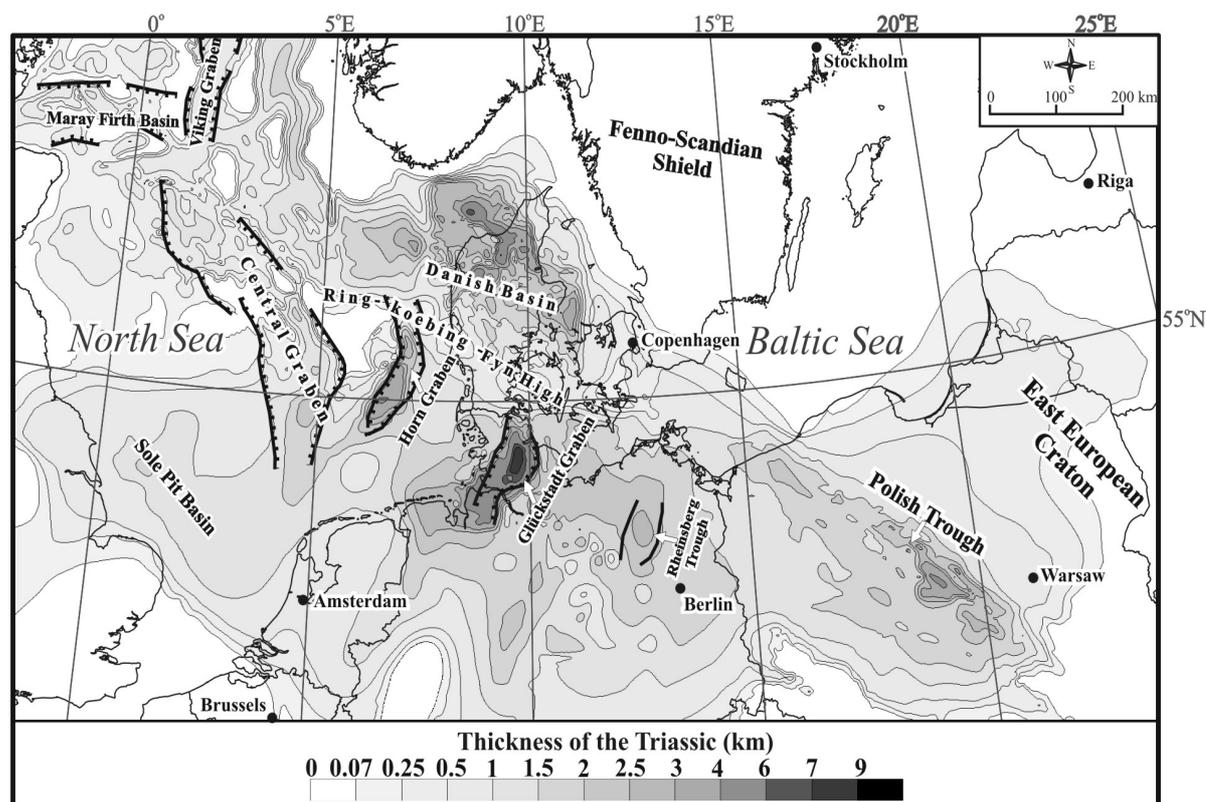
Figure 1.2. Location of the study area in relation to major Triassic subsidence centers within the Central European Basin System (compiled after Van Horn, 1987; Ziegler, 1990; Britze and Japsen, 1991; Vejbaek and Britze, 1994; Baldschuhn et al., 1996 and 2001; Šimkevičius et al., 2001; Evans et al., 2003; Scheck et al., 2003; Dadlez, 2003; Bayer et al., 2003; Sliaupa, 2004; Lamarche and Scheck-Wenderoth, 2005).

Horn Graben, the GG and the Danish Basin. Another center of Triassic subsidence is located within the Polish Trough where the thickness of Triassic reaches up to 5000 m. The Sole Pit Basin, the Central Graben and the Rheinsberg Trough are characterized by minor thickening of the Triassic strata in comparison with the mentioned Triassic basins. The thickest Triassic succession is observed in the GG where it reaches about 9000 m (Fig. 1.2). The last strong

tectonic event before the Triassic took place during the end of Late Carboniferous-Early Permian times and was accompanied by extensive igneous activity and faulting within the entire CEBS (Gast, 1988; Plein, 1990; Ziegler, 1990b; Dadlez et al., 1995; Bachmann et al., 1997; Bayer et al., 1999; Abramovitz and Thybo, 1999). Apparently, the Late Carboniferous - Early Permian rifting initiated the deposition of a thick Upper Permian succession that is stratigraphically complex and contains thick salt layers. Later, the Permian salt was mobilized, creating significant space for additional sedimentation in the Triassic. This period of salt tectonics was associated with extension, reflecting a discrete pulse of tectonic activity in the Triassic (Ziegler, 1990; Vejbaek, 1990; Kockel, 2002; Scheck et al., 2003; Krzywiec, 2004; Maystrenko et al., in press). Particularly, the area of the GG is not only the thickest Triassic structure within the CEBS, but it provides a large "natural laboratory" concerning the effects of salt tectonics in space and time. Although the large-scale tectonic evolution of the region has been highlighted by Sannemann (1968), Brink et al. (1990), Brink et al. (1992), Baldschuhn et al. (1996), Bachmann and Hoffmann (1997), Baldschuhn et al. (2001), Kockel (2002), the relation between salt movements and tectonic events is still poorly understood.

The main objective of this work is to examine the evolution of the GG, with emphasis on the influence of salt tectonics during the Mesozoic and Cenozoic periods. The origin and development of large salt walls and intrabasinal structural features in the region are analyzed by selected deep wells, 2D reflection seismic lines and a 3D structural modelling approach.

In particular, the ultimate aim of this study is to analyze the following aspects of the post-Carboniferous basin evolution:

(1) the recognition of the major tectonic events;

(2) the timing of salt movements;

(3) the relationship between salt structures and styles of sedimentation both in time and in space;

(4) the development of salt structures through time;

(5) the initial thickness distribution of the Permian (Rotliegend and Zechstein) salt within the basin.

1.1. Geological setting

1.1.1. Structural framework

The basin structure and fill of the GG have been systematically studied since the beginning of the last century, mainly in the view of oil and gas exploration. Some results of the scientific investigations within this area have been discussed in several publications (Sannemann, 1968; Dohr et al., 1989; Brink et al., 1990, 1992; Baldschuhn et al., 1996, 2001; Kockel, 2002). Nevertheless, it is useful to discuss some aspects of the major structures since they are important for understanding basin development.
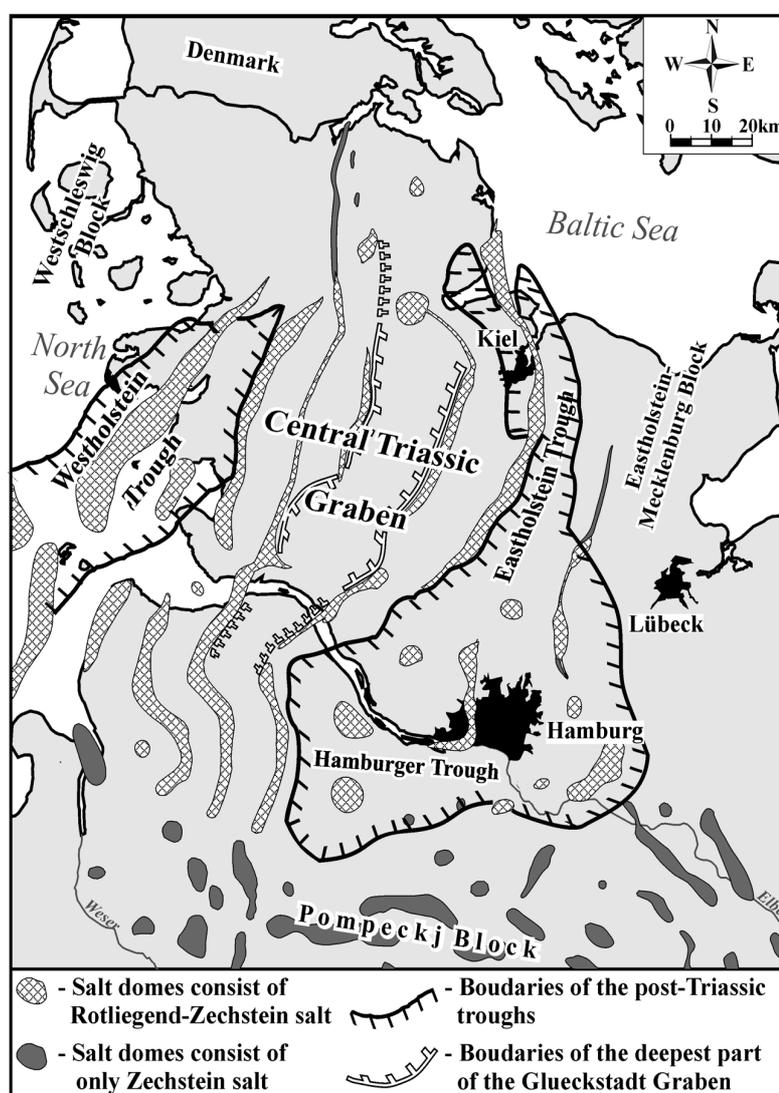
Figure 1.3. Tectonic map of the Glueckstadt Graben (frame 1 in the Fig. 1.1; position of salt domes after Baldschuhn et al., 1996).

The GG is mainly located in Schleswig-Holstein and in the northern part of Lower Saxony, NW Germany. It can be subdivided into three structural domains (Fig. 1.3):

(1) the central Triassic graben;

(2) the marginal Jurassic and Cenozoic troughs – Westholstein, Eastholstein and Hamburger;

(3) the flanks of the basin – Westschleswig and Eastholstein-Mecklenburg blocks.

Direct information on the nature of the lower crust is scarce, but available indirect evidence indicates that the crust below GG was consolidated during the Caledonian orogeny (Bayer et al., 2002) and that the structural grain within the Caledonian basement may have influenced later structural development of the crust in the Schleswig-Holstein area. According to the interpretation of an east-west running reflection line, the central part of the GG is characterized by a thinned lower crust due to a Moho uplift of up to 25 km in comparison with the flanks where the Moho is located at a depth of more than 30 km (Dohr et al., 1989; Brink et al., 1992). This Moho uplift is associated with a steep gravity gradient culminating in a broad maximum located in the GG area, which appears in the gravity field, reduced to the base of Zechstein (Dohr et al., 1989).

The isopach map of the Meso-Cenozoic sedimentary cover, provided in Fig. 1.4a, illustrates the variation of sediment thickness across the different sub-basins of the GG. The Central Triassic Graben is by far the deepest part of the GG. In its central area, the base of Triassic sediments is located at more than 10000 m depth (Fig. 1.4b). At its south-eastern margin, the Triassic depocenter is separated from the Eastholstein-Mecklenburg block by the Eastholstein and Hamburger Troughs (Fig. 1.4b), which exhibit increased thicknesses of Jurassic (more than 1900 m) and Cenozoic (more than 3300 m) sediments. The Westholstein marginal through is also characterized by thick Jurassic (more than 2400 m) and Cenozoic (more than 5000 m) deposits and separates the Central Triassic Graben from the Westschleswig block (Fig. 1.4b). The Westschleswig and Eastholstein-Mecklenburg blocks bound the GG from the northwest and the southeast accordingly and are covered by post-Permian sediments of up to 4000 m thickness. These structural zones have small dip (sometimes almost horizontal) at the base of Upper Permian (Fig. 1.4b), little salt mobilisation and the salt overburden is characterized by relatively undeformed rocks.
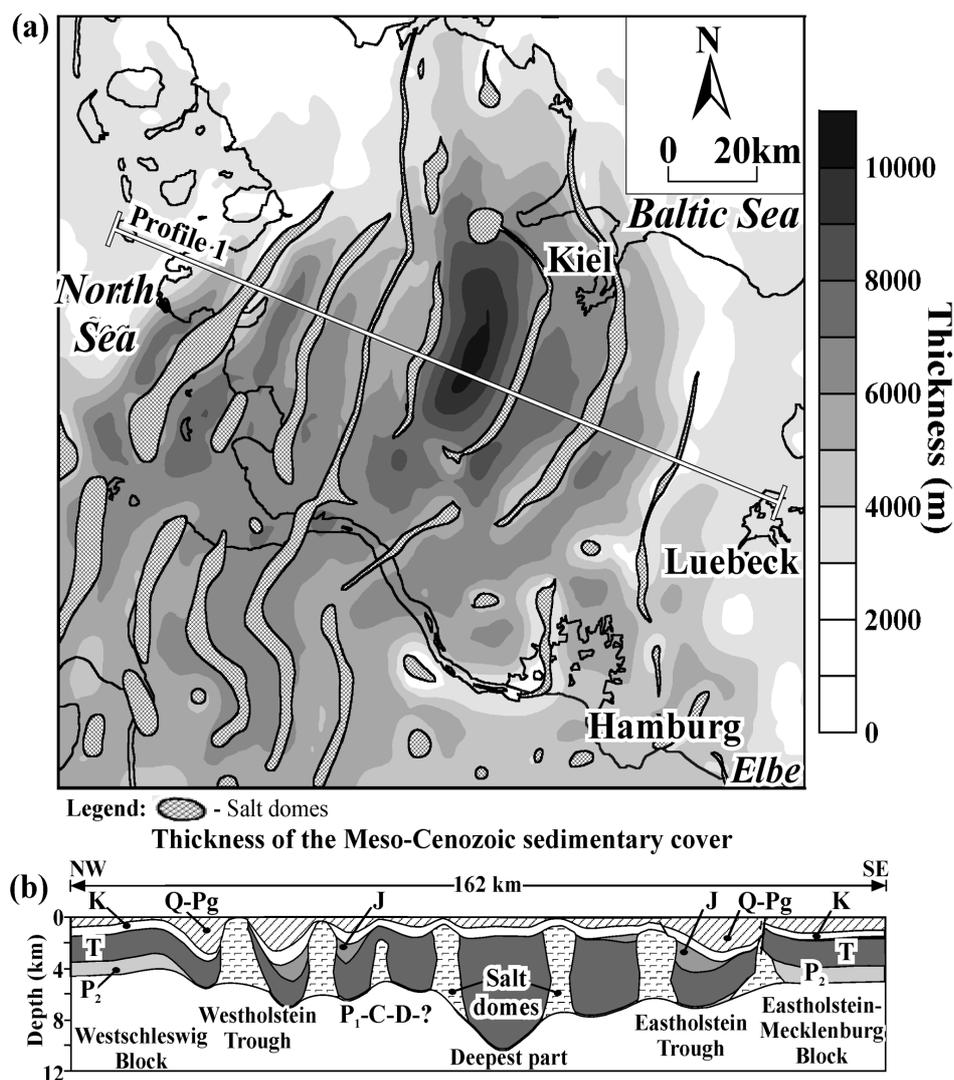
Figure 1.4. (a) Present thickness of the sedimentary cover down to top Upper Permian (Zechstein) in the Glueckstadt Graben and its surrounding area (based on Baldschuhn et al., 1996). (b) Regional NW–SE cross-section across the Glueckstadt Graben, showing main structural features (vertical slice from the 3D model of the Glueckstadt Graben). Stratigraphic key: P_1 -C-D = Undivided Lower Permian (Rotliegend), Carboniferous and Devonian deposits; P_2 = Upper Permian (Zechstein); T = Triassic; J = Jurassic; K = Cretaceous; Q-Pg = Paleogene-Quaternary (including Neogene).

The generalised northwest–southeast cross-section of Fig. 1.4b runs through the main structural zones described above. It is oriented approximately perpendicular to the central Triassic depocentre where the thickness of the Triassic reaches more than 8500 m. The cross

- 7 -

section has been extracted from the 3D model discussed later, in order to illustrate the key features of salt tectonics on the regional scale. The cross section shows that the formation of three centers of maximum subsidence (in Triassic, Jurassic and Cenozoic) was strongly controlled by salt movements through time: the centre of sedimentation was moving away from the central part of the original Central Triassic Trough towards its margins due to gradual withdrawal of Permian salt (Sannemann, 1968). In this sense, the GG was formed at least partially as a "basin-scale rim syncline" during post-Permian times.

1.1.2. Tectono-stratigraphic sequence

The sedimentary succession of the GG reflects the major stages in the tectonic development of the basin. Fig. 1.5 shows the post-Carboniferous lithostratigraphy of the GG, together with some major tectonic events. The post-Carboniferous basin fill may be divided into three major sedimentary sequences: Prepermian deposits, Permian salt and Meso-Cenozoic overburden. Unfortunately, the oldest known sedimentary strata, Upper Devonian and Lower Carboniferous (Tournasian and Visean), have been penetrated only in one deep well within the limits of the GG. The Precambrian crystalline rocks have only been reached within the Westschleswig block in the Nordsee Q-1 deep well (Best et al., 1983). Late Carboniferous-Early Permian rifting is reflected in the lithology of Lower Permian deposits by the presence of conglomerate series and volcanics. The known total thickness of the Lower Permian succession, including up to 450 m thick salt-rich layers, varies along the basin's flanks from 1500 meters to more than 2200 m. The Upper Permian (Zechtein) is characterized by carbonate-evaporite successions, dominated by rock salt. The Lower Triassic (Buntsandstein) consists mainly of clastics and thin layers of evaporites, whereas the Middle Triassic (Muschelkalk) contains carbonates and evaporites. It was postulated that the GG could have been affected by rifting towards the end of the Early Triassic (late Buntsandstein; Brink et al., 1992; Kockel, 2002), when a very narrow trough was formed within the central part of the basin. However, the main extension occurred during the latest Middle Triassic and Late Triassic (Keuper) when thick sediments (up to 5800 m in the basin depocenter) were deposited (Brink et al., 1992; Baldschuhn et al., 1996; Baldschuhn et al., 2001). The Keuper succession has a very complicated structure due to rapid subsidence and due to the presence of thick salt-rich layers (Bayer et al., 2003). It is important to note, that there is no direct evidence of Late Triassic volcanism, which could have accompanied the deposition of thick Keuper sediments within the GG.

	Age			Lithology	Tectonic events
Cenozoic	Q			Glacial deposits	Extension ?, strong salt tectonics at the flanks
	Neogene			Clastics: clays and sandstones	
	Paleogene			Clays, clay- and calcareous marls	
Mesozoic	Cretaceous	Upper		Chalky limestones	regional unconformity
		Lower		Claystones and marls	
	Jurassic			Claystones and sandstones	salt tectonics
	Triassic	Upper	Keuper	Claystones, clay marls, alternation of claystones (sometimes clay marls) and evaporites (mainly halite)	Main phase of extension, strong salt tectonics
		Middle	Muschel-kalk	Marlstones, limestones and layers of claystones and evaporites	
		Lower	Buntsand-stein	Claystones, clay marls, sandstones and layers of evaporites	extension ?
Paleozoic	Permian	Upper	Zechstein	Evaporites (salt and anhydrite) and carbonates (mainly dolomite and limestone)	Postrift sag stage
		Lower	Rotliegend	Alternation of shales and evaporites (salt and anhydrite). Shales, sandstones and conglomerates. Igneous rocks are in base.	Strong rifting

Legend:
- Sandstones
- Gravels
- Clays, mudstones and shales
- Marls and marlstones
- Rock salt / Halite
- Carbonates
- Anhydrite
- Volcanics
- Conglomerates

Figure 1.5. Lithostratigraphic chart and main tectonic events of the Glueckstadt Graben. Lithologies are taken from well data.

The Jurassic sequence includes clastics consisting of claystones and sandstones. Its thickness is significantly controlled by salt tectonics. The area around the GG was uplifted in Late Jurassic-Early Cretaceous times, indicated by a regional erosional unconformity.

Sedimentation resumed in the Cretaceous, a time of tectonic quiescence and rising sea level. Lower Cretaceous strata unconformably overlie the Triassic and Jurassic sequences and consist of marine and continental sediments. During the Late Cretaceous, the sediments were deposited in a gentle platform-type depression that extended far beyond the boundaries of the GG. The Upper Cretaceous succession comprises mainly chalky limestones.

Finally, the collision between Africa-Arabia and Eurasia caused the formation of the Alpine orogen during the Late Cretaceous-Tertiary. The collision-induced compression affected whole Europe, with some basins undergoing compression and inversion. Nevertheless, in contrast to other basins of the CEBS, such as the Polish Trough, Lower Saxony Basin, or North-East German Basin, the GG was not essentially inverted. At the same time, it can be infered from structural data that the area around the Glueckstadt Trough has been affected by an accelerated tectonic subsidence rate within the marginal Westholstein, Eastholstein and the Hamburger troughs. Interestingly, a regional Upper Cretaceous unconformity is not obvious from the seismic data, although it is a prominent feature in other parts of the North German Basin.

The Cenozoic succession consists mainly of clastics with some marls and reaches a maximum thickness of more than 5000 m. During the Paleogene-Neogene, the basin was tectonically reactivated with rapid subsidence along the northwestern and southeastern margins of the Triassic trough (Sannemann, 1968; Baldschuhn et al., 1996; Maystrenko et al., in press). This event coincides with rapid subsidence in the central North Sea (Kockel, 1988; Ziegler, 1990b; Evans et al., 2003) and most likely is related to almost E-W directed extension. Quaternary glacial deposits cover all older strata regionally.

1.2. Database

The available database consists of reflection seismic profiles supplemented by deep well data (Fig. 1.6). This database has been provided by the German oil and gas industry through the German Society for Petroleum and Coal Science and Technology (DGMK) in the frame of the research project "Dynamics of sedimentary systems under varying stress conditions by example of the Central European Basin system" (DFG-SPP 1135, DGMK
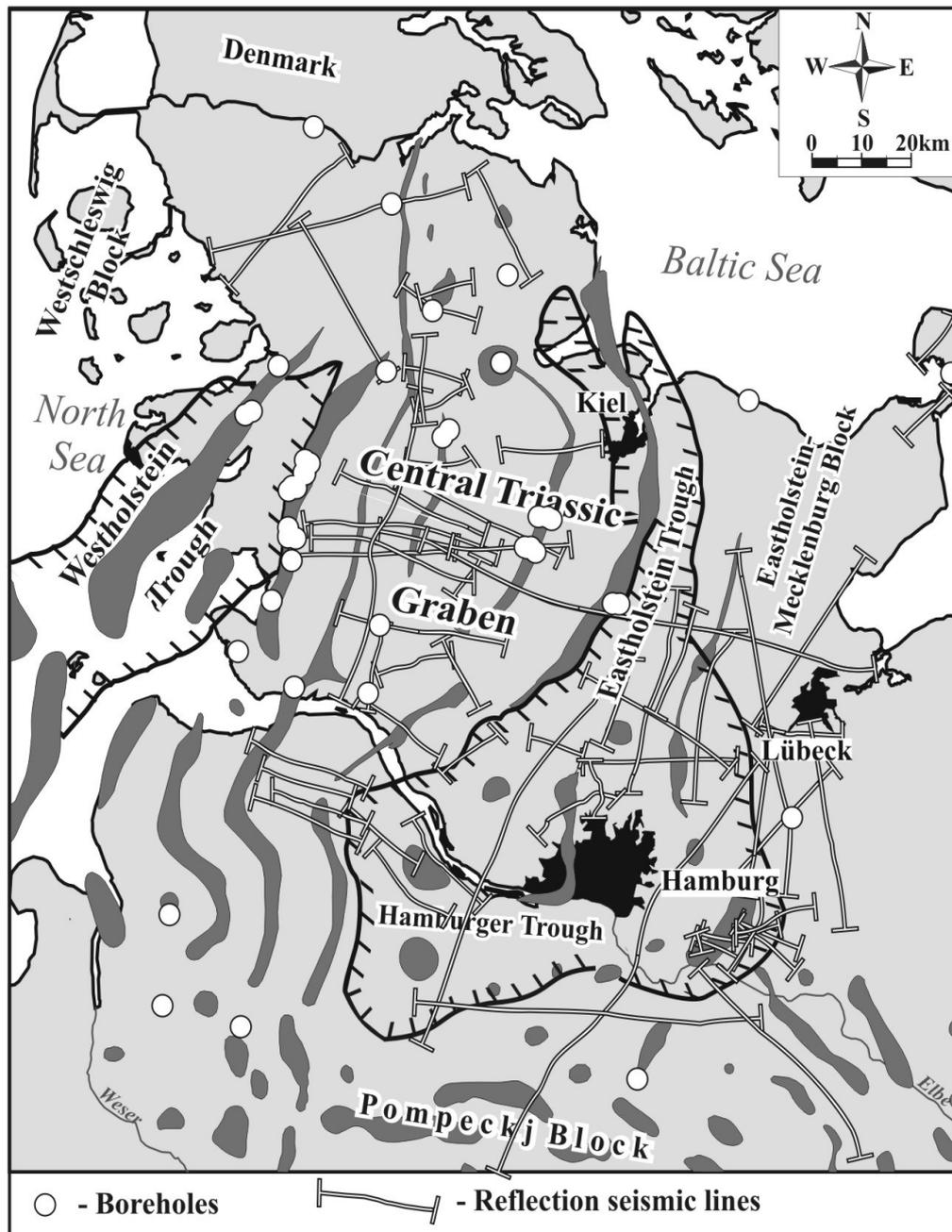
Figure 1.6. Available seismic data coverage of the study
area and the location of available wells.

Project 577). The quality of the seismic data varies within the study area, but in general the data are of high to medium quality. The medium data quality seems to be at least partly related to the complex structural style of the GG. Generally, the resolution of seismic images decreases beneath the salt structures because the salt dissipates much of the seismic energy.

- 11 -

In some places, the deep reflections may be represented by Devonian or Carboniferous rocks but it is very difficult to correlate them due to missing deep well data in the GG. This study highlights mainly nine sequences which have been correlated using the seismic profiles and available well data, these being:

(1) $P_1(s)$ = upper part of the Lower Permian (salt-rich Rotliegend);

(2) P_2 = Upper Permian (Zechstein);

(3) T_1 = Lower Triassic (Buntsandstein);

(4) T_2 = Middle Triassic without uppermost part (Muschelkalk);

(5) T_{2-3} = uppermost part of Middle Triassic and Upper Triassic (Keuper);

(6) J = Jurassic;

(7) K_1 = Lower Cretaceous;

(8) K_2 = Upper Cretaceous;

(9) Q-Pg = Paleogene-Quaternary.

The seismic lines have been interpreted in terms of seismic stratigraphy and some of them were migrated in the frequency domain by using a software for digital processing of 2D and 3D seismic data (SPS-PC: the software package developed for Windows-based PCs and was provided by the Russian company Nord-Express). Migration in the frequency domain has been chosen because it allows to migrate seismic lines with steeply dipping reflections without loosing important dynamic characteristics of the reflections compared with the finite-difference scheme or Kirchhoff. Moreover, additional seismic processing procedures have been applied to selected lines and some seismic reflectors have been flattened. The additional processing includes f-k filtering in order to amplify the seismic image of strongest reflections by removing low-amplitude reflections in the frequency domain, automatic gain control (AGC) and finally band-pass filtering.

In addition to well and seismic data, structural maps were provided by the Federal Department of Geosciences and Mineral Resources (BGR; Baldschuhn et al., 1996) which cover the area under consideration. The digital versions of depth maps from the Geotectonic Atlas of NW Germany (Baldschuhn et al., 2001) was integrated into a three-dimensional structural model after calculation of thickness maps. This 3D model was finally adjusted by using the results from seismic interpretation.
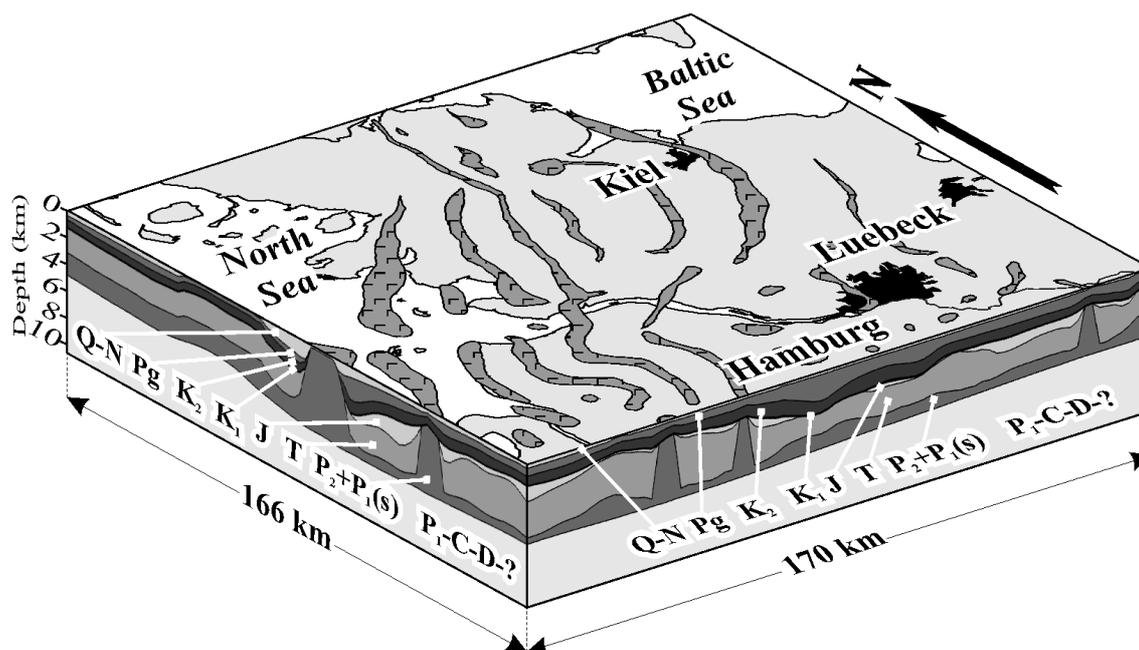
Figure 1.7. 3D structural model of the area under consideration.
For stratigraphic key see Figure 1.4.

The constructed three-dimensional model covers an area which is 170 km long and 166 km wide (Fig. 1.7) and has a 2x2 km grid spacing. It includes seven layers from the Rotliegend to the Quaternary:

(1) $P_1(s) + P_2 =$ salt-rich Rotliegend plus Zechstein;

(2) T = Triassic;

(3) J = Jurassic;

(4) K_1 = Lower Cretaceous;

(5) K_2 = Upper Cretaceous;

(6) Pg = Paleogene;

(7) Q-N = Quaternary-Neogene.

The 3D structural model has been used to calculate the initial Permian salt thickness within the limits of the GG by using software developed at the GeoForschungsZentrum Potsdam by Ulf Bayer, Magdalena Scheck-Wenderoth and Björn Lewerenz. In addition, the 3D modelling approach has been used to determine salt distribution at certain paleo-levels in response to unloading during sequential removing of the stratigraphic layers. The salt flow

- 13 -

has been determined by a finite-element method, depending mainly on the sedimentary load and the shape of the isostatically-balanced base of the salt. A basic assumption in this approach is that the behaviour of salt is similar to a viscous fluid that is usually in hydrostatic equilibrium with the overburden and that its volume is conserved. This modelling was already successfully applied within the NE German Basin by Scheck et al. (2003).

- 14 -

Chapter II

MAIN SALT DEPOSITS WITHIN THE GLUECKSTADT GRABEN

2.1. Regional overview

The CEBS contains a thick sedimentary fill, which was deposited over a wide area within Central Europe and the North Sea. Since the Late Palaeozoic, this region evolved into a number of different tectonic settings. Initially, this basin system was part of Pangea in Paleozoic times and included the Southern and Northern Permian Basins. A system of more or less N-S oriented Mesozoic graben structures was superimposed on the CEBS in Mesozoic times, and finally it became partially inverted during Late Cretaceous-Cenozoic times. The resulting lithological column of Upper Palaeozoic and Mesozoic sediments contains salt deposits at different stratigraphic levels in different parts of the CEBS. Permian salt deposits were the main viscous decollements during post Permian evolution within the CEBS. The Lower Permian (Rotliegend) salt is the oldest salt with regional extent, and the Upper Permian (Zechstein) salt is the thickest and most wide-spread evaporitic unit within the region. The paleogeographical map of the Rotliegend deposits indicates that the Upper Rotliegend salt was deposited in a narrow (about 130 km wide) and elongated basin (almost 650 km long), extending from the Sole Pit Basin to the North German Basin (Ziegler, 1990b). The Rotliegend salt-rich strata overlie a sequence of shales which have been deposited in semi-desert areas or continental deserts (Ziegler, 1990b). The salt-rich Rotliegend represents sabkha and desert-lake evaporites (Plein, 1990; George and Berry, 1997; Evans et al., 2003). At the beginning of the Zechstein, a marine environment developed during the initial transgression of the Zechstein Sea (Ziegler, 1990b). Zechstein salt was deposited in two giant evaporite basins, the Northern and Southern Permian Basins. The Zechstein halite precipitation was separated by the Mid North Sea High and the Ringkoebing-Fyn High. During the Zechstein, carbonates and thick evaporite rocks accumulated under arid climatic conditions. The marine Zechstein evaporites are characterised by the presence of chloride–sulphate evaporites and potassium salt, reflecting full cycles of evaporite precipitation. A third salt sequence of the CEBS consists of Triassic salt beds.

The basin infill of the GG contains all three major salt sequences (salt-rich Rotliegend, Zechstein salt and Triassic salt beds), mentioned above. The Rotliegend and Zechstein

evaporites formed the majority of the huge salt structures within the GG (Fig. 1.3). A 3D view on the modelled top Permian salt surface (Fig. 2.1) demonstrates that the high amplitude salt walls are located mainly within the Central Triassic Graben and the
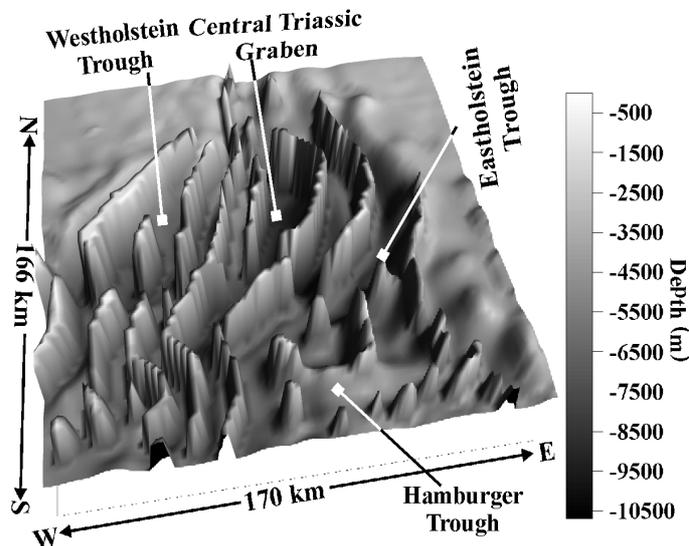
Figure 2.1. 3D view of the present-day top of the Permian salt in the Glueckstadt Graben and adjacent areas.

Westholstein Trough with decreasing amplitudes towards the marginal Eastholstein and Hamburger Troughs. Accordingly, the salt deformation is less intense at the north-western and south-eastern flanks of the basin (Fig. 2.1). The salt-rich Rotliegend mainly consists of an alternation of salt and shales which are concordantly overlain by the Zechstein evaporites. During the Late Triassic (Keuper) times, the thickest Triassic salt layers were deposited in the GG. Salt-rich Keuper is widespread within the GG and has a maximum thickness of up to 2000 m within the Central Triassic Graben. In terms of depositional environment, the Keuper is characterized by arid or semi-arid intracontinental conditions (Ziegler, 1990b).

2.2. Detailed lithology of the Rotliegend, Zechstein and Keuper salt-rich deposits within the GG

Rotliegend, Zechstein and Keuper salt successions have been distinguished because they played an important role during the evolution of the GG due to their great thicknesses and broad occurrence. In addition, solitary salt beds are present in the Bundsandstein and

Muschelkalk strata but they are rather thin (known thickness is up to 100 m) and they were not able to form significant salt structures during the post-depositional period. Several wells have been evaluated to characterize and correlate the different salt-rich intervals.

2.2.1. Rotliegend sequence
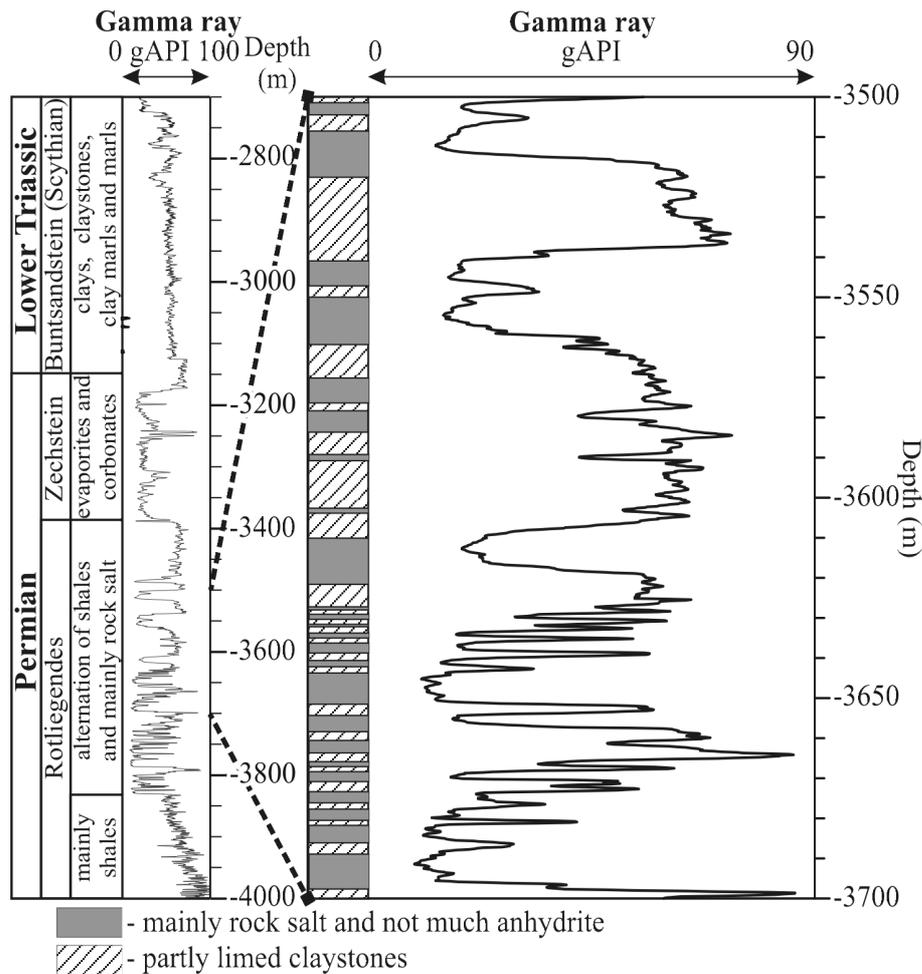
Figure 2.2. Detailed Rotliegend (Lower Permian) salt-rich section, gamma-ray log of Well 1.

The salt-rich Rotliegend is present in all boreholes of the GG, which penetrated the deposits of Lower Permian age. The typical sequence of the salt-rich Rotliegend is shown in Fig. 2.2, the interpreted gamma-ray log of Well 1 (for its location see Fig. 1.6.). The true composition of the Rotliegend is unknown within the deep part of the basin because these sediments have only been drilled in the crest of salt diapirs where they consist of displaced

carbonates, clastics and salt. The beginning of the salt-rich sequence is marked by a distinct fall in gamma-ray values (Fig. 2.2), lithologically corresponding to the presence of evaporites. The detailed structure of this argillaceous-evaporite sequence is shown in Fig. 2.2 by the enlarged interval of the gamma log. The rock salt is placed where the gamma log shows the lowest response. It is seen that the salt-rich succession consists of shales with some radioactivity (up to 88 g API) and intercalated salt layers as well as some anhydrite. The thickest salt beds reach up to 80-85 m thickness and, together with other salt layers, form more than fifty percentages of this argillaceous-evaporite sequence.

2.2.2. Zechstein sequence
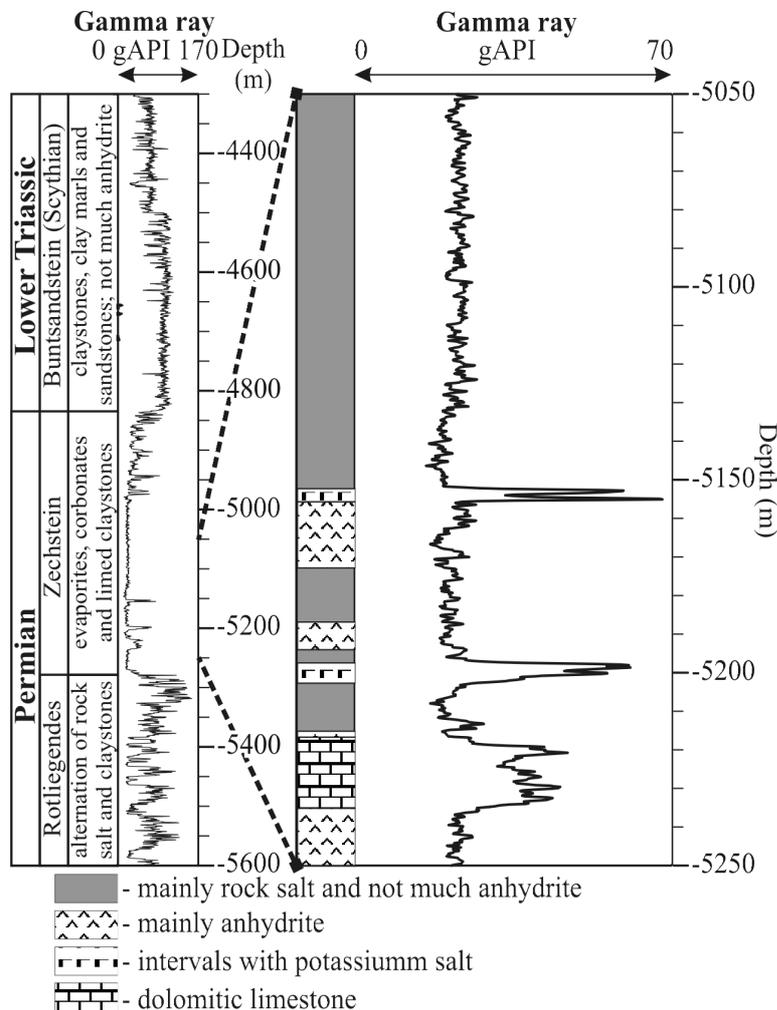
Figure 2.3. Detailed Zechstein (Upper Permian) salt section, gamma-ray log of Well 2.

The Zechstein sequence is shown by the example of the gamma log from Well 2 (Fig. 2.3; for location see Fig. 1.6). In the GG, the Zechstein is characterized by five cycles of evaporite deposition, reflecting increasing evaporation and salinity through time. One of these cycles is shown in Fig. 2.3 at the depth interval 5235 to 5198 m. It indicates the gradual precipitation from dolomitic limestone, anhydrite, halite to potassium salt. The enlarged interval of the data in Fig. 2.3 shows sharp spikes within the gamma-ray curve, related to the alternation of carbonates, anhydrites, halite and potassium. Radioactive potassium salt coincides with high gamma-ray peaks up to 68 gAPI. Carbonate beds are characterised by lower (up to 40 gAPI) gamma-ray values. The lowest gamma-ray values correspond to almost pure rock salt intervals. It is observable from the well-log data that rock salt predominates in the Zechstein section occupying more than seventy percent of it.

2.2.3. Keuper sequence
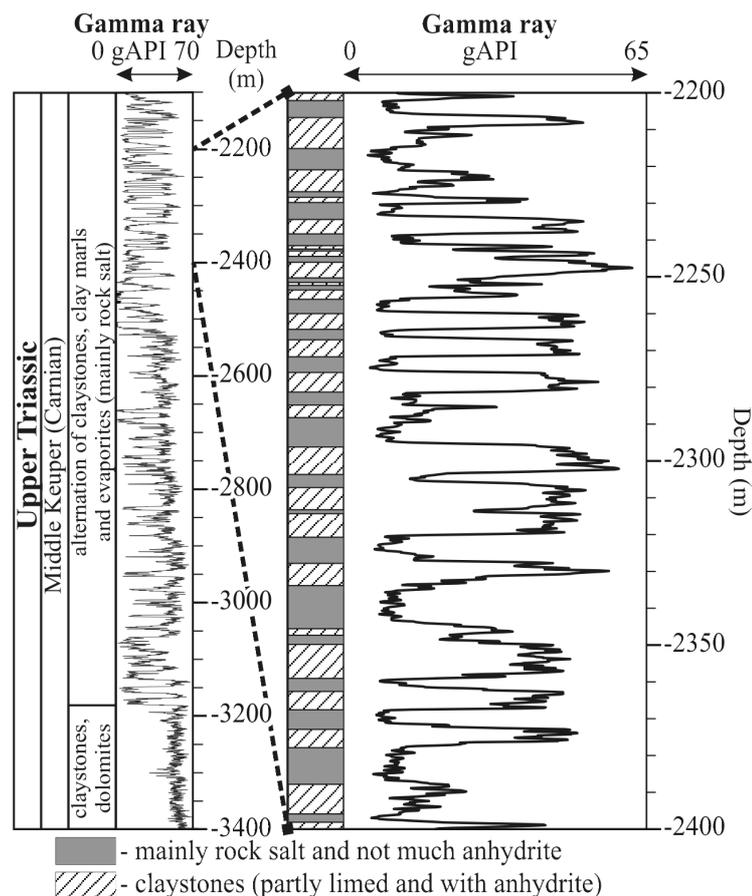
Figure 2.4. Detailed Keuper (Upper Triassic) salt-rich section, gamma-ray log of Well 3.

The Keuper succession consists of alternations of claystone, carbonate and evaporite series. The evaporite sequences are mainly represented by successions of interbedded halite, claystone, anhydrite and carbonates. The salt-rich Keuper is very thin within the flanks of the basin and is sometimes mainly represented by anhydrite or almost complete pinching-out of evaporite beds. It has been postulated that the Keuper was a syn-tectonic sediment deposited in SW-NE trending central trough of the GG (Brink et al., 1992; Baldschuhn et al., 1996; Baldschuhn et al., 2001; Kockel, 2002; Maystrenko et al., in press). It has also been suggested that a large proportion of the Keuper salt was reprecipitated from Permian salt that was dissolved from the many diapirs which were extruding on the paleosurface within the central part of the GG (Trusheim, 1960; Maystrenko et al., in press). The detailed section of the salt-rich Keuper is shown by the gamma-ray curve of Well 3 (Fig. 2.4). The well-log data highlighted in Fig. 2.4 illustrate that the gamma log has a serrate shape resulting from alternating beds of claystones and evaporites within the depth interval from 2400 to 2200 m. Higher gamma-ray values (up to 65 gAPI) are related to claystone layers, contrasting with the lower gamma-ray minima of salt seams. Salt beds are characterized by variable thickness within the limits of 5-18 meters and occupy about fifty percent of the salt-rich interval.

2.3. Summary

In summary, it can be stated that almost pure salt is prominent in the Zechstein and dominates in diapiric movements that have influenced the regional evolution of the GG. However, the presence of Rotliegend salt within the salt structures of the GG (Fig. 2.1) suggests that the initial thickness of Rotliegend salt was greater than is observed at the flanks of the basin today. The role of the Keuper salt is also important but mostly restricted to the area of the Central Triassic Graben where its thickness is significant.

Chapter III

SEISMIC PATTERNS WITHIN THE GLUECKSTADT GABEN

3.1. Introduction

Seismic stratigraphic interpretations of selected lines are given in this chapter. The discussed seismic lines are indicated in Fig. 3.1. Based on the reflection patterns, the main seismic sequences are identified in the multi-channel seismic data. Some sequence boundaries were precisely calibrated with borehole data. This combined data set (seismic lines and well data) was used to define the structure and evolution of the GG from Permian to Cenozoic. However, there are still open questions concerning the correlation of internal reflections of deep strata within the central part of the GG (Fig. 3.2). There are neither deep wells available which provide control, nor is a north-south running seismic line available which could connect the deeper parts with the well-controlled thinner sequence towards the Rinkoebing-Fyn High or the Pompeckij Block. In addition, there are no typical seismic patterns which could help to derive a probable interpretation. Although, Baldschuhn et al. (2001) provided a concise interpretation of the deep reflections, there is an ongoing discussion within the research project SPP-1135 concerning alternative models (Bayer et al., 2003). Furthermore, different interpretations have previously been published by Best et al. (1983) and Baldschuhn et al. (1996).

The crucial reflection seismic profile shown in Fig. 3.2 crosses the central and eastern part of the GG (see Fig. 3.1 for position). This line provides a regional overview of the area under consideration. The thickness differences shown in the profile provide the separation between the Central Triassic Graben and the Eastholstein-Mecklenburg block. Consequently, the cross section can be subdivided into two main structural zones, which represent the Central Triassic Graben with the superimposed Cenozoic Eastholstein Tough and the Eastholstein-Mecklenburg block. The presence of lengthy salt walls hampers seismic correlation between the different structural parts of the basin. The pre-Prepermium strata are only reached by very few wells within the GG. Consequently, the correlations of the pre-Permian reflections are not consistent due to the absence of the well data and due to the presence of huge salt structures (see line 1 in Fig. 3.2; see enlarged version in Appendix A). The base of the salt-rich Rotliegend is the oldest horizon which has been regionally dated
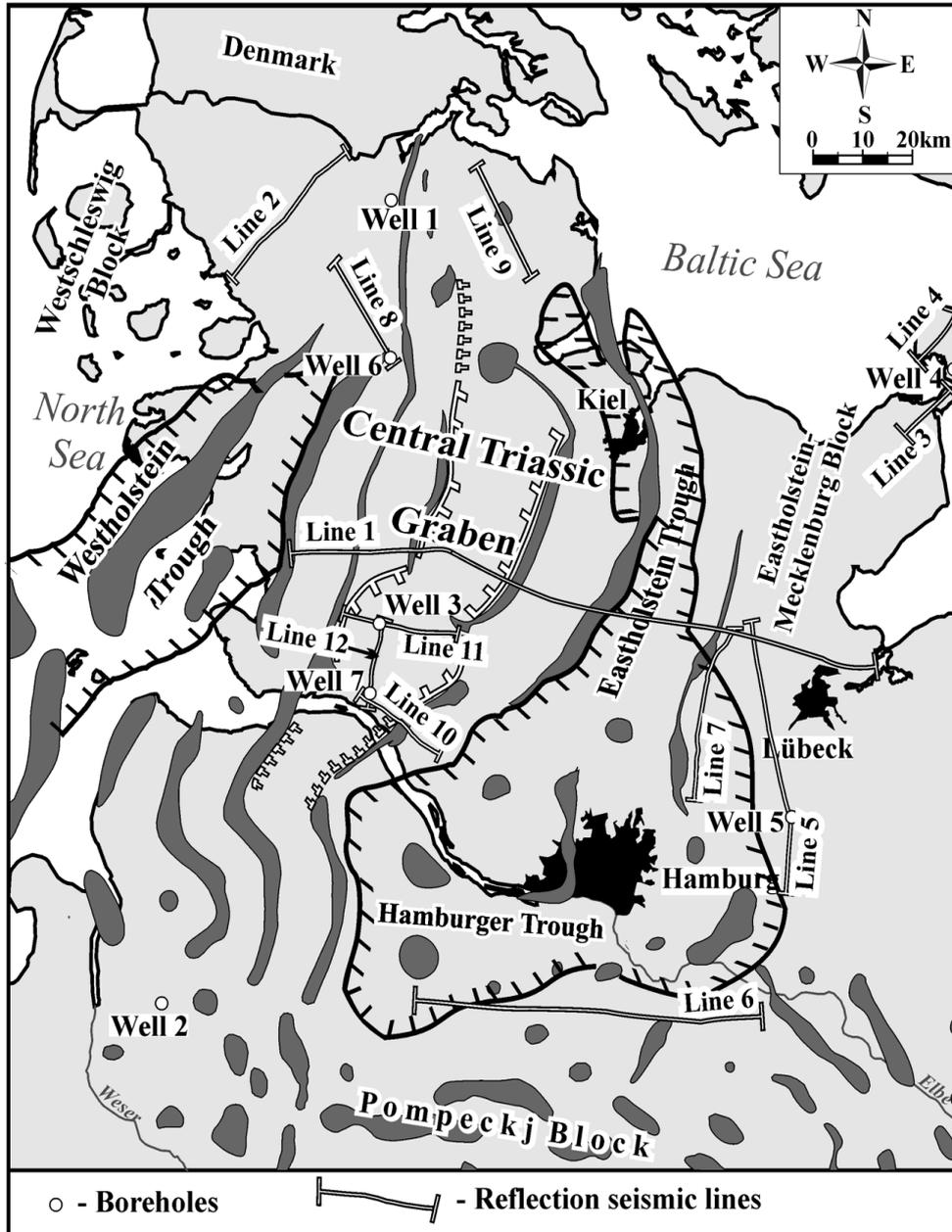
Figure 3.1. Simplified tectonic map of the Glueckstadt Graben (frame 1 in the Fig. 1) showing the location of seismic lines and boreholes mentioned in the text (position of salt domes after Baldschuhn et al., 1996).

within the GG. This horizon is quite well constrained by drilling and seismic images. The base of the salt-rich Rotliegend usually marks the deepest correlatable reflections beneath the high-amplitude reflections from the Zechstein base. The geologic identification of the Zechstein base is well established in the GG due to the presence of a strongly reflective

package consisting of two- or three-phases. The salt-rich Rotliegend has an almost constant thickness of 0.36-0.38 s TWT within the Eastholstein-Mecklenburg block. Structurally, the upper Rotliegend is characterized by a subhorizontall package of reflections, indicating undisturbed bedding of the salt-rich strata at the basin shoulder. Within the same structural zone, the slightly deformed Mesozoic-Cenozoic sequence and the almost flat base of the Upper Permian indicate the presence of displaced Zechstein salt (see SE part of the Fig. 3.2). Clear evidences of basement fault-controlled subsidence have been recognized at the SE boundary of the Eastholstein Through (Fig. 3.2). There, a steep westward-dipping normal fault is observed, separating the Eastholstein Through from the SE flank of the basin (Eastholstein-Mecklenburg block). Differential movements along the fault suggest a relatively young reactivation of this fault in Late Cenozoic times. Salt movements fold post-Permian strata around the fault. It is important to note that the base of the salt-rich Rotliegend is almost horizontal close to the fault. On the other hand, the Zechstein base is well traceable and folded within the hanging wall, indicating the dislocation of the Rotliegend salt. Thinning of both Zechtein and salt-rich Rotliegend strata further to the NW indicate a depletion of the salt-rich layers. As already pointed out, the presence of salt structures makes the interpretation of the seismic reflections rather difficult, particularly those located in the deepest part of the basin (Fig. 3.2). For the reasons given above, the base of the salt-rich Permian is not traced and the lower part of the Triassic is not subdivided within the deepest part of the Central Triassic Graben. The recognized Lower Triassic (Buntsandstein) strata are characterized by constant thickness with some evidences of postsedimentation erosion near its deepest part (Fig. 3.2). The Muschelkalk shows a constant thickness on the basin shoulder and variable thickness towards the central part of the line. The uppermost Middle-Upper Triassic (Keuper) is characterized by strong variations in thickness and complex reflectivity images (Figs. 3.2). This sequence represents the infill of the GG and shows increasing thickness towards the basin centre. In the SE part of the line, the Keuper interval shows a similar seismic pattern as the Buntsandstein and Muschelkalk sequences. Towards the Central Triassic Graben, the reflection patterns show evidence of strong syn-depositional thickening of the Keuper compare with the underlying strata. This structural difference between the Keuper and older Triassic strata indicates that significant changes of the tectonic setting occurred at the beginning of the latest Middle-Late Triassic

Fig. 3.13
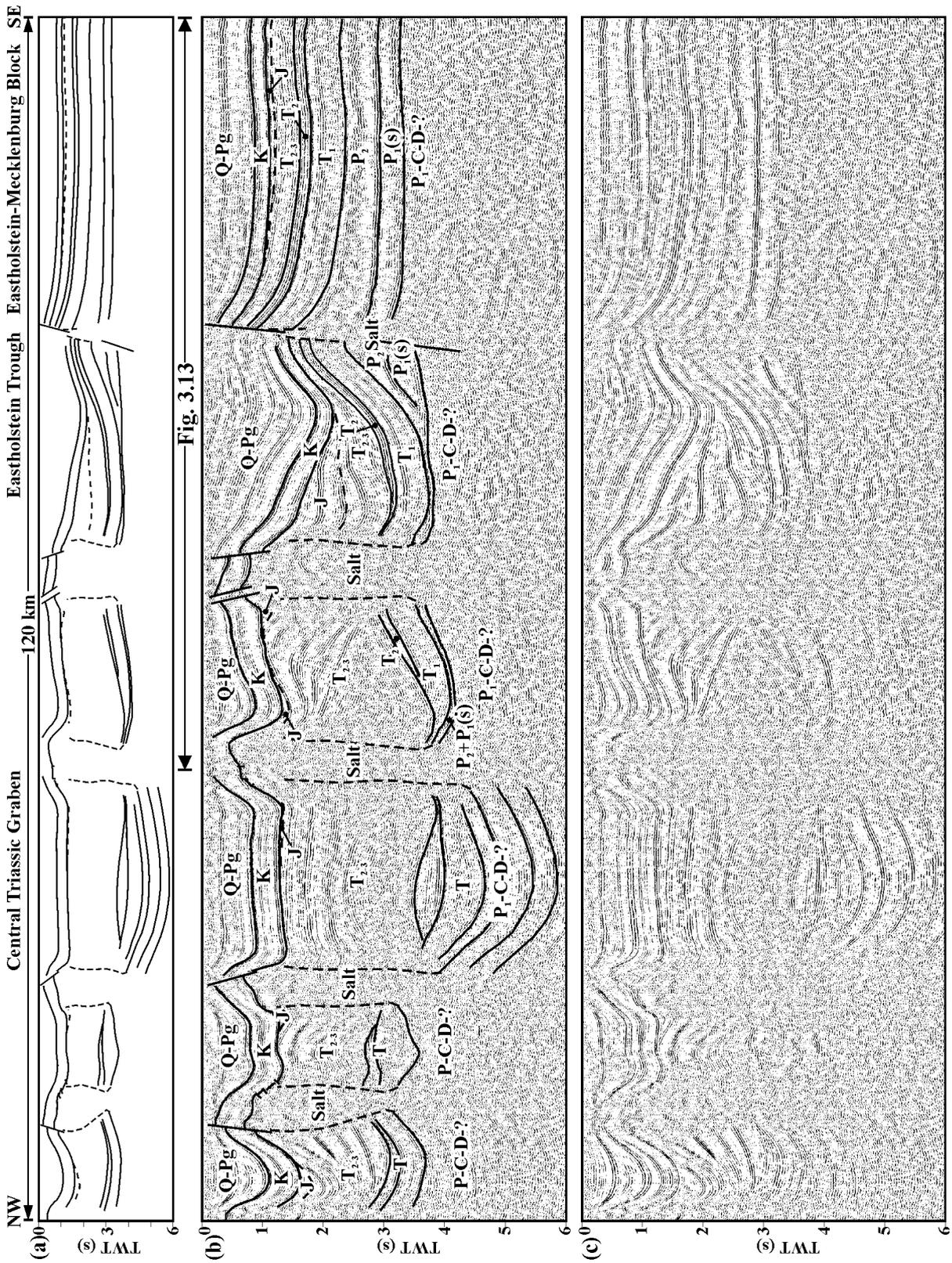
(Keuper) within the studied area. The Keuper has a subparallel reflective package at the basin flank. While, the presence of baselapping strata of the thick Keuper sequence indicates rapid subsidence, accompanied by dawnbuilding of the salt structures. Jurassic sediments are only present around the salt structures along the seismic line, indicating the development of rim synclines along the edges of elongated salt walls. The presence of Jurassic on the SE flank of the basin indicates that the original Jurassic infill likely covered a wider area before Late Jurassic-Early Cretaceous erosion. This erosional event is indicated by the angular unconformity beneath the base of the Cretaceous, which provides as a regional unconformity within the GG. The Cretaceous sequence shows an almost constant thickness along the line with thinning from the Eastholstein Through towards the SE flank. The deep Cenozoic Eastholstein Through is observed by thickening of the Cenozoic succession up to 2 s TWT on the eastern side of the line. Generally, the Cenozoic is characterized by thick sequences between the salt structures. Cenozoic rocks have been partially eroded from the crest of most of the salt structures (Fig. 3.2). The Cenozoic depressions between the salt walls indicate that the deposition of sediments occurred simultaneously with the growth of salt structures. In other words, the structure of the Cenozoic demonstrates the rim syncline character of deposition. By contrast, the Cenozoic strata have almost horizontal bedding within the axial part of the line and on the SE termination of the profile (Fig. 3.2). Such subhorizontal bedding indicates a rather weak effect of the salt movements on sedimentation.

Line 1 shows that the post-Permian sedimentary succession of the Central Triassic Graben and the Eastholstein Trough is deformed by salt movements. Thus, one of the main deformation mechanisms in the area of the GG is salt tectonics. Various structural styles in the GG are related to movements of Permian salt. Details of the evolution are expressed in a variety of salt structures representing different stages of growth such as salt rollers,

Figure 3.2. Interpreted northwest-southeast transect through Schleswig-Holstein (profile 1 in the Fig. 3.1). Stratigraphic key for this and other figures: C-D = Undivided Carboniferous and Devonian deposits; P1-C2 = Lower Rotliegend and uppermost Carboniferous; P1(s) = upper part of the Lower Permian (salt-rich Rotliegend); P2 = Upper Permian (Zechstein); P2+P1(s) = upper part of the Lower Permian and Upper Permian (undivided Zechstein and salt-rich Rotliegend); T1 = Lower Triassic (Buntsandstein); T2 = Middle Triassic without uppermost part (Muschelkalk); T2-3 = uppermost part of Middle Triassic and Upper Triassic (Keuper); J = Jurassic; K1 = Lower Cretaceous; K2 – Upper Cretaceous; Q-Pg = Paleogene-Quaternary.

anticlines, pillows, stocks, and most pronounced elongated salt walls. Based on the tectonic subdivision of the region, different salt structures and related structural features will be described below. The seismic architecture of the studied area are presented in terms of key regions: (1) the NW region, which extends along the NW boundary of the GG, named the Westschleswig block; (2) the central domain, which includes the Central Triassic Graben; (3) the marginal domains, that correspond to Eastholstein and Hamburger Throughs; and (4) the SE outer domain, the area of the Eastholstein-Mecklenburg block.

3.2. Flanks of the basin – Westschleswig and Eastholstein-Mecklenburg blocks
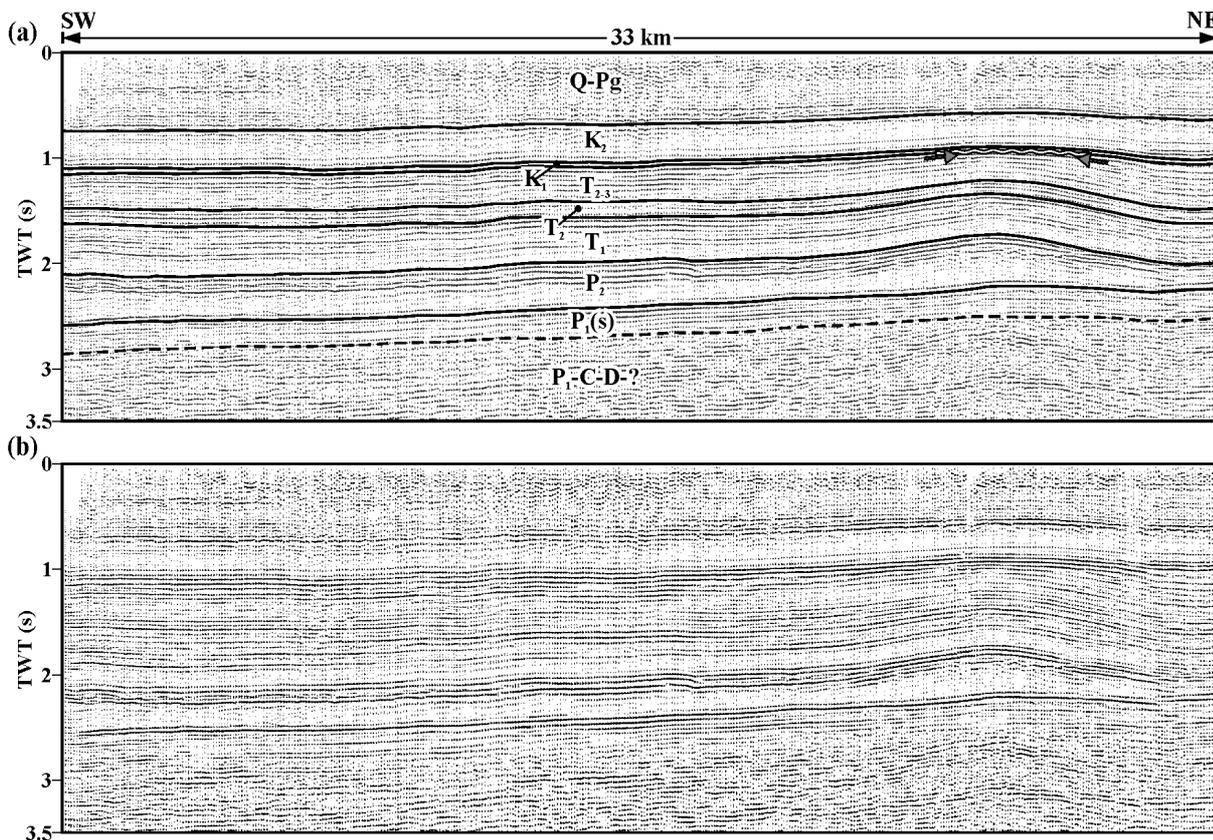
Figure 3.3. Interpreted seismic profile 2. A typical structure from the NW flank of the basin (Westschleswig block) is shown (visible erosinal unconformity is indicated by wavy line). See Fig. 3.1 for location. For stratigraphic key see Figure 3.2.

The Westschleswig and Eastholstein-Mecklenburg blocks represent the north-western and south-eastern flanks of the basin. Figure 3.3 shows the area of the north-western flank of the GG where the sedimentary cover is mainly characterized by almost horizontal bedding of post-Carboniferous strata with some solitary and low amplitude salt pillows. Bundles of subparallel reflections are dominating along the largest part of line 2 with exception of the NE part. There, a salt pillow complicates the subparallel seismic pattern (Fig. 3.3; see enlarged version in Appendix A). The Mesozoic to Cenozoic layers are subparallel to base Zechtein. The salt-rich Rotliegend below the salt structure and the constant thicknesses of the uplifted Buntsandstein and Muschelkalk indicate that the salt pillow developed during the Keuper by mobilisation of Zechstein salt. Insignificant reactivation of the Zechstein salt movements occurred in the Paleogene-Neogene, when a shallow anticline formed (see NE part of the Fig. 3.3). There is no visible structural unconformity at the base of the Cretaceous within the seismic image with exception of the crest of the salt pillow, where an inessential truncation can be observed prior to deposition of the thin Lower Cretaceous. However, the Jurassic sediments are missing along this line. This structural feature can be explained by reduced sedimentation in the Jurassic as well as by low degree Late Jurassic-Early Cretaceous uplift within the Westschleswig block.

Seismic lines 3 and 4 (Fig. 3.4; see enlarged version in Appendix A) show the structure within the outer NE part of the Eastholstein-Mecklenburg block. The interpretation of these lines is based on the geological information of the nearby situated Well 4 (see Fig. 3.1 for location). The salt-rich Rotliegend sequence has been interpreted only on line 3 (Fig. 3.4a). On the other hand, the salt-rich Rotliegend is not interpreted along line 4 (Fig. 3.4c) due to an almost chaotic seismic pattern beneath the base of the Zechtein. The salt-rich Rotliegend is characterized by a subparallel package of reflections with thickness up to 0.4 s TWT. The internal structure of the salt-rich Rotliegend does not indicate any salt movements of the upper Rotliegend salt in the area around the lines. In contrast, the variable thickness and the complex internal seismic pattern of the Zechstein clearly show that Zechstein salt was mobilized during post Permian times. Furthermore, the outflow of Zechstein salt created additional space for the deposition of Cenozoic deposits in the SW part of line 3 (Fig. 3.4). There, the thickness of the Cenozoic strata is more than doubled compared with the NE part of line 3 and line 4. The Jurassic sediments are only present on the SW limit of line 3 and the
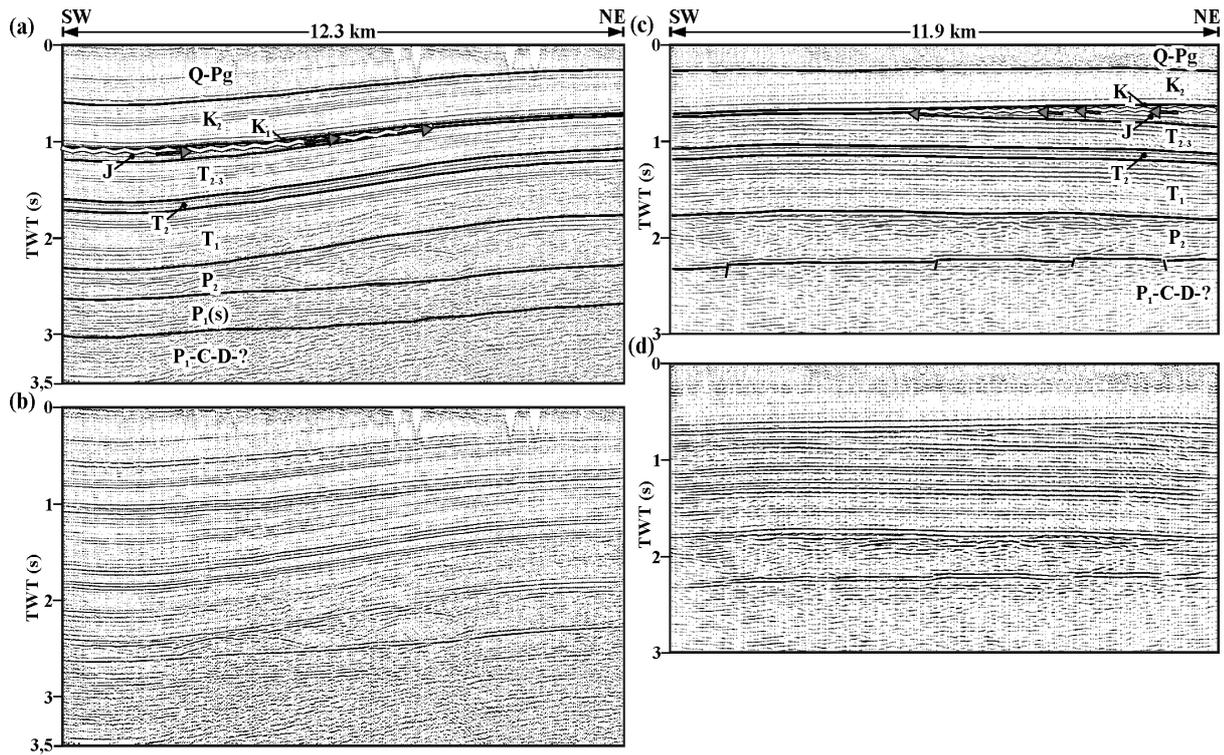
Figure 3.4. Interpreted seismic profiles 3 and 4. A typical structure from the NE part of the SE flank of the basin (Eastholstei-Mecklenburg block) is shown (visible erosinal unconformity is indicated by wavy lines). See Fig. 3.1 for location. For stratigraphic key see Figure 3.2.

NE limit of line 4. Possibly, they had a much broader distribution before the Late Jurassic – Early Cretaceous erosion. The visible truncation is indicated in terms of an angular unconformity by wavy lines along the lines. The borehole data (Well 4) indicate that the Keuper was also eroded but not so essentially. This can indicate a minor amplitude of erosion or the presence of thick Jurassic sediments before erosion. Triassic and Createceous sequences have an almost constant thickness along the lines, indicating minor or no movements of salt during the Triassic and Cretaceous times within this part of the basin (Fig. 3.4).

The geological interpretation of the various seismic events on line 5 (Fig. 3.5; see enlarged version in Appendix A) is supported by reliable borehole information (Well 5). The profile runs through the axial part of a salt pillow, demonstrating the structure of the western part of the south-eastern flank of the GG. The section intersects two faults at the base of the oldest

detectable reflections (near 4 s TWT). These reflections can be related to the lowest Permian or to uppermost Carboniferous sediments, possibly representing the rifting processes which occurred during the Late Carboniferous-Early Permian times within the studied area. The salt-rich Rotliegend shows an almost constant thickness which decreases to the south of the line, perhaps, due to Lower Permian salt withdrawal in the same direction. The base Zechstein reflection is relatively strong, and displays a tiny velocity pull-up underneath the massive salt pillow but is generally subhorizontal. This demonstrates the low "activity" of the underlying Lower Permian salt beds in this part of the basin. The Buntsandstein and Muschelkalk sediments have approximately constant thickness, indicating rather flat bedding during sedimentation. The Keuper sequence shows almost constant thickness along the line with slight thinning towards the southern termination of the profile. Thick Jurassic (about 0.5 s TWT) is interpreted within the southern limb of the salt anticline. The Jurassic infill pattern is characterized by onlap from below and truncated toplap from above in the southern anticline limb. This time section also highlights the unconformity at the base of the Lower Cretaceous (northern part of the line), where Jurassic sediments were partially eroded due to Late Jurassic-Early Cretaceous uplift or sea level fall at that time. The well data show that the Keuper sediments at the crest of the salt pillow have been also eroded. However, it is not obvious that Upper Triassic sediments were mainly eroded during the Late Jurassic-Early Cretaceous. Possibly, some part of the missing Triassic sediments was eroded during the formation of the relatively deep Jurassic depression on the southern termination of the profile. Furthermore, the presence of the Jurassic onlaps onto the top of the Keuper can indicate that northward lying Triassic strata were uplifted. Thus, there are no direct indications concerning the presence of thick Jurassic sediments at the crest of this salt anticline before Late Jurassic-Early Cretaceous erosion.

The Cretaceous strata have an almost constant thickness, indicating a rather stable period of sedimentation without strong tectonic activity or salt movements. The Cenozoic sedimentary succession forms three synclines, which are located above the reduced Upper Permian (Zechstein salt) section (Fig. 3.5). On the other hand, thinning of the Cenozoic strata occurs at the crest of salt pillows. Such structural features of the Cenozoic succession imply essential salt movements during the Cenozoic along the line 5. The culmination of the development occurred during the post-Miocene when the crest of the biggest salt anticline was affected by erosion with rapid subsidence of the southern and northern limbs.
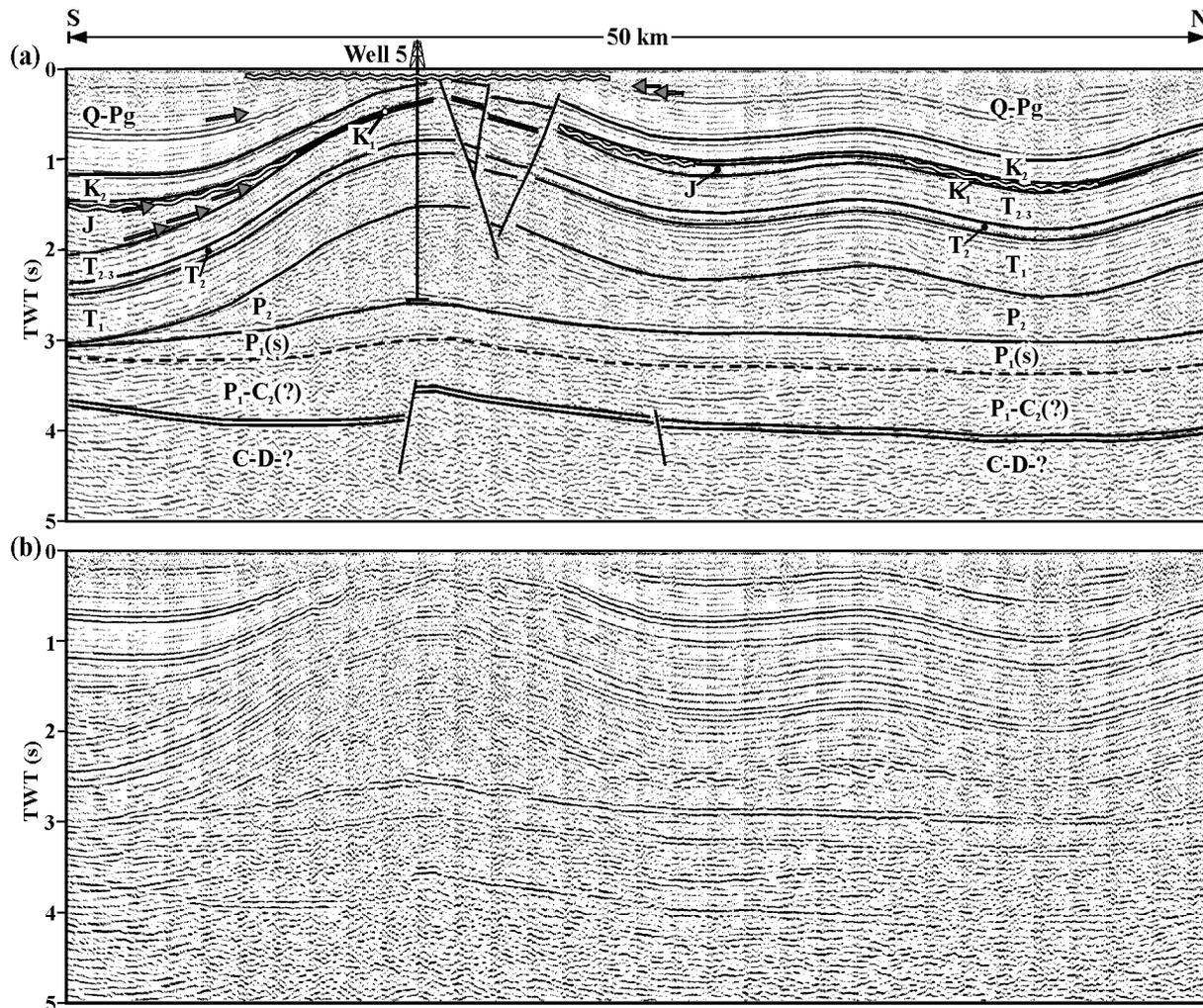
Figure 3.5. Interpretation of line 5 showing structural features along the Eastholstein-Mecklenburg block (visible erosinal unconformities are indicated by wavy lines; arrows show on- and toplap of the reflection terminations). Late Carboniferous-Early Permian extension tectonics is shown beneath Permian salt pillow. See Fig. 3.1 for location. For stratigraphic key see Figure 3.2.

In post-Miocene times, the overburden of the salt structure was faulted, possibly due to an extension. It is noteworthy that the southern limb of the salt anticline has steeper dipping layers at the Triassic level than at the Cretaceous level. This difference in dipping indicates two periods of anticline growth, suggesting the main phases of the salt activity during the Jurassic and during the Cenozoic, with interruption during the Cretaceous. A slight decrease in thickness of the Keuper towards the south indicates the initial stage of salt movements. On

the other hand, the deposition of the Buntsandstein and Muschelkalk sequences were not affected by salt movements but these strata were involved into the salt anticline during postdepositional times.

3.3. Marginal Hamburger Trough

The structure of the southern margin of the Hamburger Trough is shown by the west-east running seismic line 6 (Fig. 3.6; see enlarged version in Appendix A). The salt-rich Rotliegend sediments deposited as a huge flat blanket without prominent deformation in the western and eastern parts of the profile (Fig. 3.6). In the central part, the upper Rotliegend deposits are not correlated due to the presence of a salt diapir. The overall reflection pattern features high parallel and high coherency along the line, however beneath the salt diapir, the upper Rotliegend reflectors generally become chaotic and wormy. This can indicate that upper Rotliegend salt together with the Zechstein salt was involved in the formation of the salt stock. Zechstein deposits are geneally thinned. Thinning of the Zechstein occurred during the formation of salt structures such as three salt pillows and the mentioned salt diapir. The Buntsandstein-Muschelkalk deposits have constant thickness of about 0.6 s TWT with the exception of the salt anticline within the eastern part. There, the Buntsandstein and Muschelkalk have been truncated in the crest of this anticline. The western part of the line is characterized by the presence of the thin Keuper, which concordantly covers the underlying Middle-Lower Triassic strata. In contrast, the internal Keuper reflections are not in phase with the underlying bedding within the area around the salt diapir and towards the east. In the central part of the line, the Keuper sequence is extremely thickened up to 0,9 s TWT in comparison to 0,24 s TWT on the westward margin. The thickened Keuper sequence is characterized by the presence of clinoforms onlaping onto the top of Muschelkalk. These baselaps indicate a main phase of salt movements, which occurred at the beginning of the Keuper. In addition, the onlap of the Keuper onto the Muschelkalk demonstrates that structural highs were formed due to salt movements. Some of these structural highs were in existence until the Jurassic. Figure 3.2 shows one of these highs where thick Jurassic sediments discordantly cover eroded Buntsandstein and Mushelkalk sediments at the crest of the salt anticline. Jurassic strata are present within the seismic profile, forming three depocenters of sedimentation. The top of Jurassic is characterized by an angular
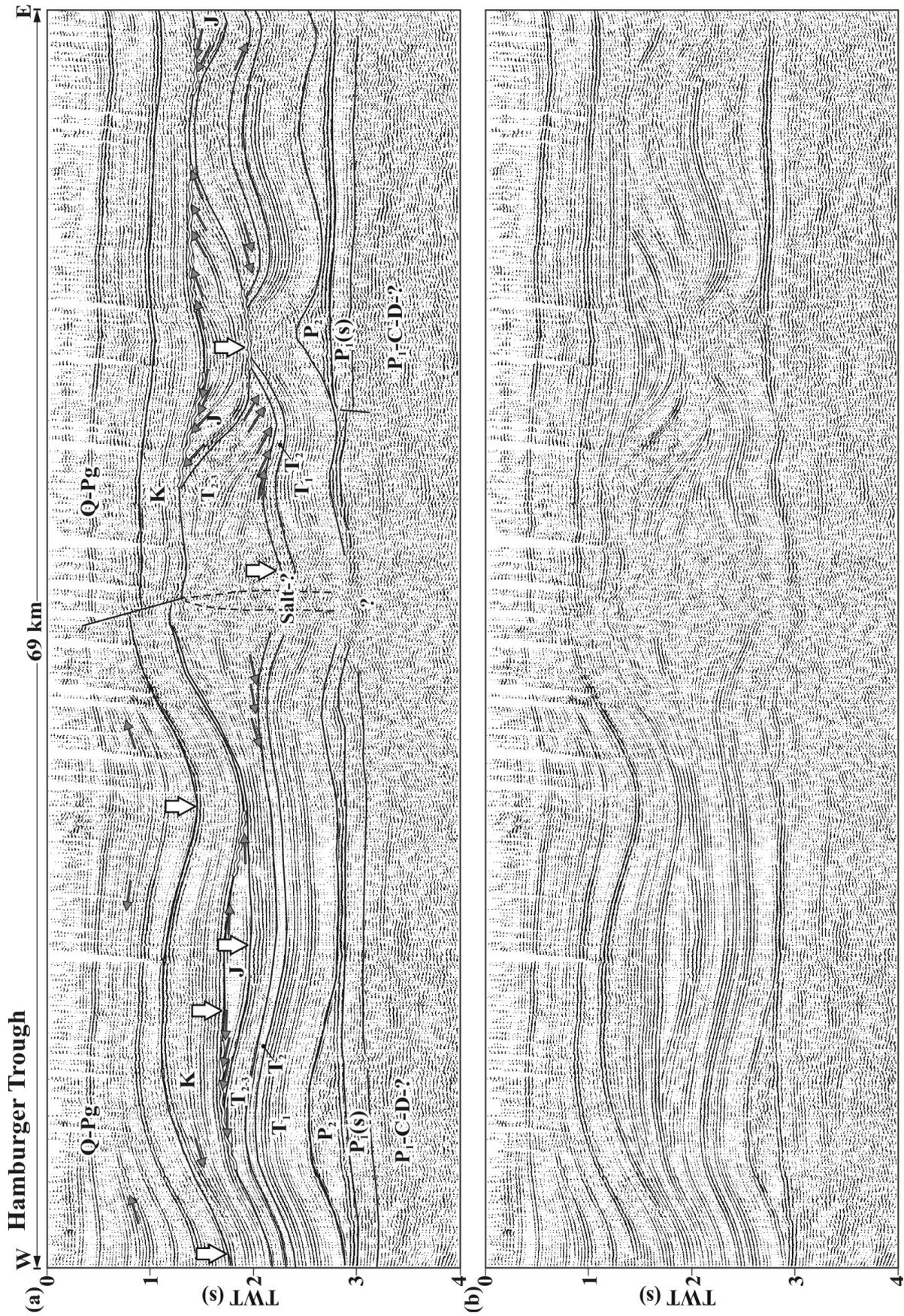
unconformity within these depocenters. Clearly, some parts of the Jurassic sediments have been eroded (Fig. 3.6), implying a major hiatus at the base of the Cretaceous. This major hiatus is traceable along the entire line, indicating a considerable long-term erosional process. On the other hand, thickening of the Jurassic sediments within the depositional centres does not necessarily indicate the distribution of equally thick Jurassic prior to the Late Jurassic – Early Cretaceous erosion along the entire profile. It is rather a consequence of progradation of clastic wedges following salt outflow. This is illustrated by the change from steeply-dipping seismic reflection pattern of the old Jurassic strata to an almost horizontal reflection pattern within the youngest Jurassic sediments, indicated by arrows within the Jurassic sequence in Fig. 3.2. The Cretaceous covers an erosionally leveled surface with thickness variation from 0.3 s up to 0.6 s TWT. Along line 6, the Cenozoic sequence reaches a thickness of 1-1.8 s TWT. A high angle normal fault cuts the Cretaceous and the Cenozoic through the anticline above the salt diapir, but stops within the Upper Cenozoic. This fault divides the line into two segments. The Eastern segment is characterized by approximately subparallel Cretaceous and Cenozoic reflections. There, a distinct angular unconformity separates folded Triassic and Jurassic deposits from subhorizontal Cretaceous-Cenozoic sediments. In contrast, the Cretaceous and Cenozoic successions are folded within the western segment of the line.

In addition, this seismic line demonstrates a prominent feature of the distribution of sediments thickening at the different stratigraphic levels. It is clearly seen, that the axial parts of the thickened sediments at the different stratigraphic layers never vertically aligned (see white arrows in Fig. 3.6a). For instance, two segments of the thick Keuper are separated by thick Jurassic sequence (Fig. 3.6a), and both thick successions are covered by ordinary Cretaceous and Cainozoic. Furthermore, an unusual extensive thickening of the Cretaceous strata is observed between two Cenozoic depressions on the western part of the line. These two Cenozoic depression are characterized by thickening of the strata, indicating rapid subsidence in comparison to other parts of the time section. The thickened Cretaceous is

Figure 3.6. Interpreted seismic profile 6. A typical structure along the southern margin of the Hamburger Trough is shown (visible erosinal unconformity is indicated by wavy line; grey arrows show on- and toplap of the reflection terminations; white arrows indicate the depocentres of sedimentation). See Fig. 3.1 for location. For stratigraphic key see Figure 3.2.

underlain by thick Jurassic but without vertical alignment of those axial parts. It is possible to conclude that thickening was strongly controlled by depletion of the Permian salt layer along the line. Thus, the seismic data reveal that thickening of the sediments was associated with simultaneous salt movements.

3.4. Marginal Eastholstein Trough
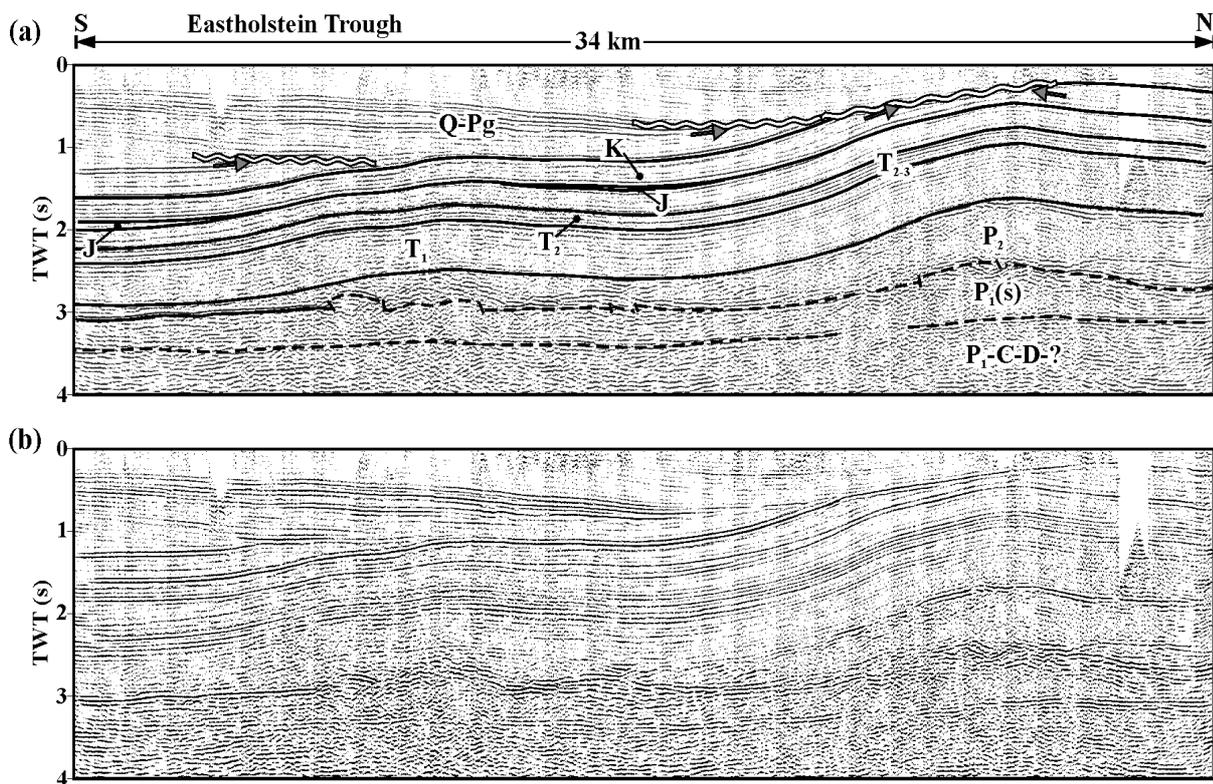
Figure 3.7. Interpreted seismic reflection line 7 from the Eastholstein Trough. Two Cenozoic unconformities are shown by wavy lines. See Fig. 3.1 for location. For stratigraphic key see Figure 3.2.

The Eastholstein Trough is characterized by increased thicknesses of both the Jurassic and the Paleogene-Neogene (Figs. 1.4b and 3.2). Line 7 (Fig. 3.7; see enlarged version in Appendix A) runs through the eastern part of this trough along the marginal salt wall, representing an area of extremely thick Paleogene-Neogene succession. The high-amplitude reflections at the base of the Zechstein are continuous and subhorizontal along the southern

part of the line. Northward from the Eastholstein Trough, reflections at the Zechstein base are transformed from a strong coherent seismic phases into a number of discontinuous and sporadic phases which are commonly folded and even faulted. Internally, the Permian salt interval shows high- to low-amplitude and sometimes almost disorganized reflections representing a high degree of salt dislocation along this line (Fig. 3.7). Thus, the presence of almost horizontal reflections at the base of the salt-rich Rotliegend and continuous reflection package of Triassic strata indicate the presence of a ductile layer between. Partially, this ductile layer is obviously represented by Zechstein salt. On the other hand, the structural features of the Zechstein base imply the presence of an additional ductile layer below. According to the litho-stratigraphic column of the GG, this lower part of the ductile layer can be only be the salt-rich Rotliegend. Consequently, the salt beds of the salt-rich Rotliegend together with Zechstein salt were involved in the formation of the two observed salt anticlines along the seismic profile (Fig. 3.7). The Buntsandstein, Muschelkalk and Keuper sequences have approximately constant thicknesses, demonstrating the absence of strong salt movements during this time. Jurassic sediments are found along the profile within the southernmost and central parts of the line where thin Jurassic strata were interpreted. The Cretaceous is the youngest interval with almost constant thickness along the entire line but it is truncated at the crest of the salt anticline within the northern part of the line. This erosional truncation occurred during the postsedimentation period in the Cenozoic. South of the line, an another erosional unconformity is observed during the Cenozoic. These two distinct erosinal unconformities indicate two main pulses of salt movements with migration of the crest of the salt anticline from south to north during the Paleogene-Neogene. It is a great pity, that these unconformities cannot be precisely dated due to missing well data. The thickness of the Paleogene-Neogene succession varies from less than 250 to 1680 ms two-way travel time. The thickest package of the Paleogene-Neogene sequence corresponds to the thinnest Permian salt beds and vice versa (Fig. 3.7). This structural feature demonstrates that the deposition of Paleogene-Neogene sediments was strongly controlled by gradual salt outflow towards the salt pillow in the northern part of the profile (Fig. 3.7) as well as parallel to the salt wall towards the west (Fig. 3.1). Thus, the syn-kinematic stratigraphic thickening of the Paleogene-Neogene interval indicates mainly Cenozoic salt movements along the entire line. In contrast, the whole Mesozoic interval is only deformed without considerable thickness variations related to salt-cored anticlines and synclines.

3.5. Transition zone from the NW flank to the Triassic graben

The NW-SE running line 8 (Fig. 3.8; see enlarged version in Appendix A) intersects the collapsed termination of a salt wall (Fig. 3.8) which continues towards the south (Fig. 3.1). This line commences in the north-western flank of the basin and further to the east
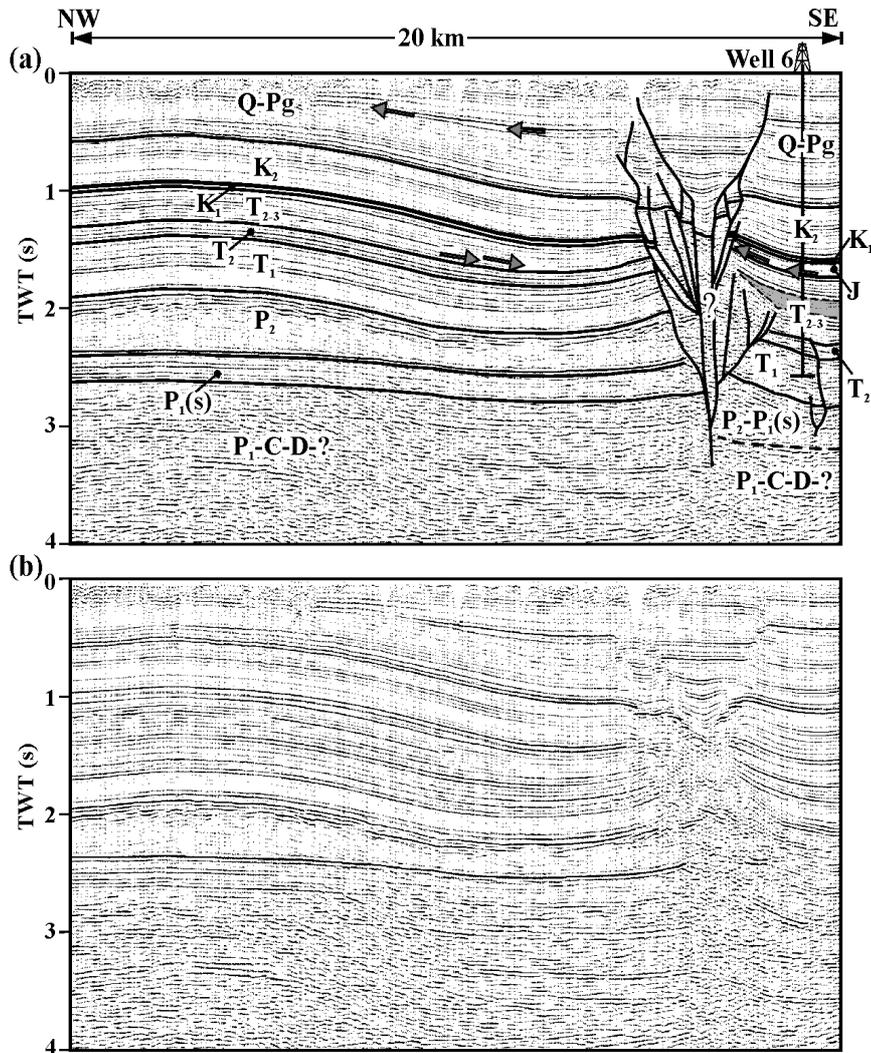
Figure 3.8. Interpreted seismic profile 8 showing a salt structure which collapsed during Paleogene-Neogene. The section shows the transition from the NW flank towards the center of the GG (arrows show onlap of the reflection terminations). The gray wedge corresponds to the salt-rich Keuper sequence. See Fig. 3.1 for location. For stratigraphic key see Figure 3.2.

crossing a major vertical normal fault, visible at the base of the salt-rich Rotliegend (offset is about the 0.5 s TWT). The thickness of the Keuper increases significantly, almost doubling within the footwall block, in comparison with the hanging wall, indicating activity of the fault during the Keuper. This normal fault can be related to the Triassic graben border-faults which extend along the basin margin beneath the salt wall. The interpretation of this line supports the concept that NNE-SSW-trending salt structures controlling abrupt changes of sediment thicknesses may have formed along basement faults (Sanemann, 1968; Maystrenko et al., in press). The onlapping Keuper reflections along the flank of the basin indicate that a salt wall was formed above the fault during Triassic extension. On the hanging wall, the thick Keuper is characterized by the presence of a salt-rich layer with a thickness up to 450 m as known from well 6. Moreover, this seismic line across the western boundary of the GG (cf. Fig. 3.1) shows clear evidence of syntectonic salt movements in response to normal faulting in the Keuper. However, taking into account the lack of Jurassic sediments on the NW flank of the basin and their presence south-eastward from the fault (Fig. 3.8), it is suggested that the fault experienced more than one phase with reactivation in the Jurassic. Onlap at the base Jurassic (SE part of the profile) points toward further salt flow and continued fault movements in this area. During the Paleogene-Neogene, this part of the salt wall (cf. Fig. 3.1) collapsed probably due to salt outflow towards its southern continuation, causing the formation of a complicated fault system above the former salt structure (Fig. 3.8). This complex fault system has the features of a flower structure, pointing toward a horizontal strain component in Paleogene-Neogene times. Similar structures have been described by Brink et al. (1992) within other marginal salt structure of the GG. Therefore, the trigger of post-Createceous salt movements in the study area was most likely the reactivation of former boundary faults of the Central Triassic Graben under a possible strike-slip regime in the Paleogene-Neogene. The thickness of the Paleogene-Quaternary varies from more than 1200 to 600 ms. Internally, the unit shows moderate- to high-amplitude clinoforms onlaping onto the underlying strata within the central part of the profile. These clinoforms could be due to salt outflow in the direction of the salt pillow imaged on the western part of this profile. Based on these data, south-eastward thickening of the Paleogene-Quaternary can be, at least partially, explained by salt movements. Due to strong salt tectonics, the tectonic development cannot be investigated in as much detail as in other parts

of the basin, but it is unlikely that the central segment of the GG behaved significantly different during the Meso-Cenozoic tectonic history.

3.6. Central Triassic graben

The central Triassic deep trough is the most complicated part of the basin, however, it is the most remarkable in terms of salt tectonics. This part of the basin is illustrated by two seismic lines (9 and 10) represented in Figs. 3.9 and 3.10.

A NNW–SSE oriented profile running through a salt diapir is presented in Fig. 3.9 (see enlarged version in Appendix A). The diapir rises from the base salt level and reaches a height of more than 4000 m. The diapir displayed in Fig. 3.9 is slightly asymmetric (north-westwards leaning). The reflectors from the Buntsandstein to the Jurassic terminate against the diapir, while the base Cretaceous reflector is continuous and covers the structure. Minor half graben structures are observed both in the north-western and south-eastern part of the profile at the base of the Permian salt. This normal faulting can be related to the Keuper extension which caused strong salt movements around the diapir. The Lower Triassic (Buntsandstein) is characterized by various thicknesses at both sides of the salt diapir (Fig. 12), indicating initial salt movements already in the Buntsandstein. Within the SSE part of the profile, the Buntsandstein has been truncated near to the salt stock during Middle-Late Triassic times. The observed truncation of the Buntsandstein implies that the overburden might have been penetrated during the Keuper. The Keuper sequence shows clinoforms onlaping onto the top of Buntsandstein and Muschelkalk. In addition, onnlaps are interpreted at the base of the Muschelkalk, indicating the initial pillow stage of this salt diapir. On the NNW wing of the salt structure, the Buntsandstein strata are tilted to NNW. The structural character indicates the formation of rim synclines in the Jurassic at the SSE wing of the salt stock. In contrast, the NNW wing is characterized by the absence of Jurassic sediments, possibly due to erosion. However, the structural features at the NNW part of the line (sub-horizontal Keuper strata underlay the Lower Cretaceous) do not allow us to suppose the existence of thick Jurassic sediments as observed at the SSE part of the line. The Late Jurassic-Lower Cretaceous unconformity is well imaged on both sides of the diapir by an angular erosinal unconformity underneath the base of the Lower Cretaceous. In spite of the angular erosional unconformity, toplapping Jurassic strata are still recognizable within the
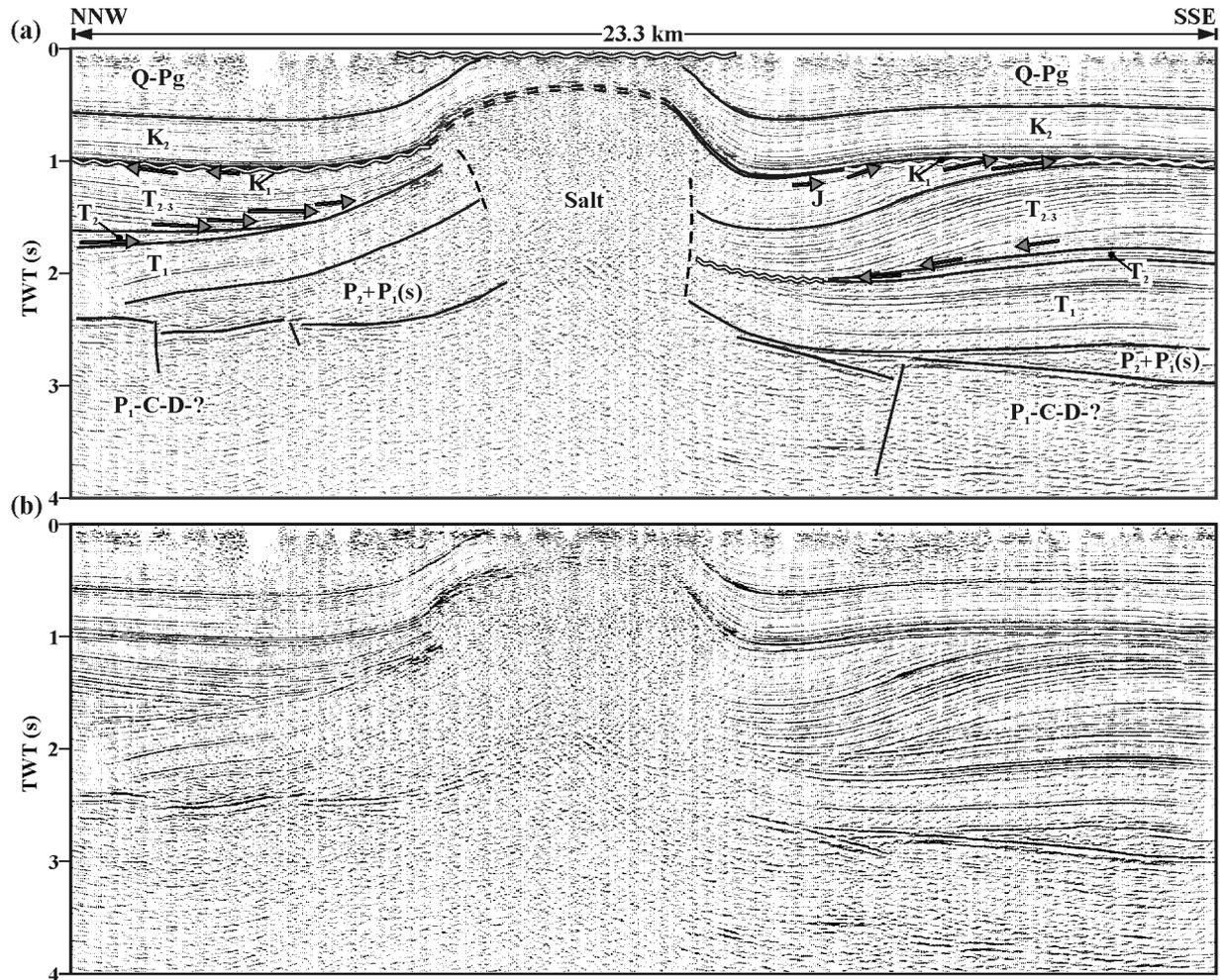
Figure 3.9. Interpreted seismic profile 9 showing the structure of a salt diapir within the northern part of the Central Triassic Graben (visible erosinal unconformities are indicated by wavy lines; arrows show on- and toplap of the reflection terminations). See Fig. 3.1 for location. For stratigraphic key see Figure 3.2.

SSE rim syncline, representing the proximal depositional limit of the Jurassic in some distance of the salt structure. The last stage of diapir growth occurred in Paleogene-Neogene when the crest of the salt structure was uplifted and partially truncated in comparison with the subsided NNW and SSE wings.

A typical salt structure within the deep part of the GG is displayed by line 10 crossing one of the salt walls (Fig. 3.10; see enlarged version in Appendix A). This seismic
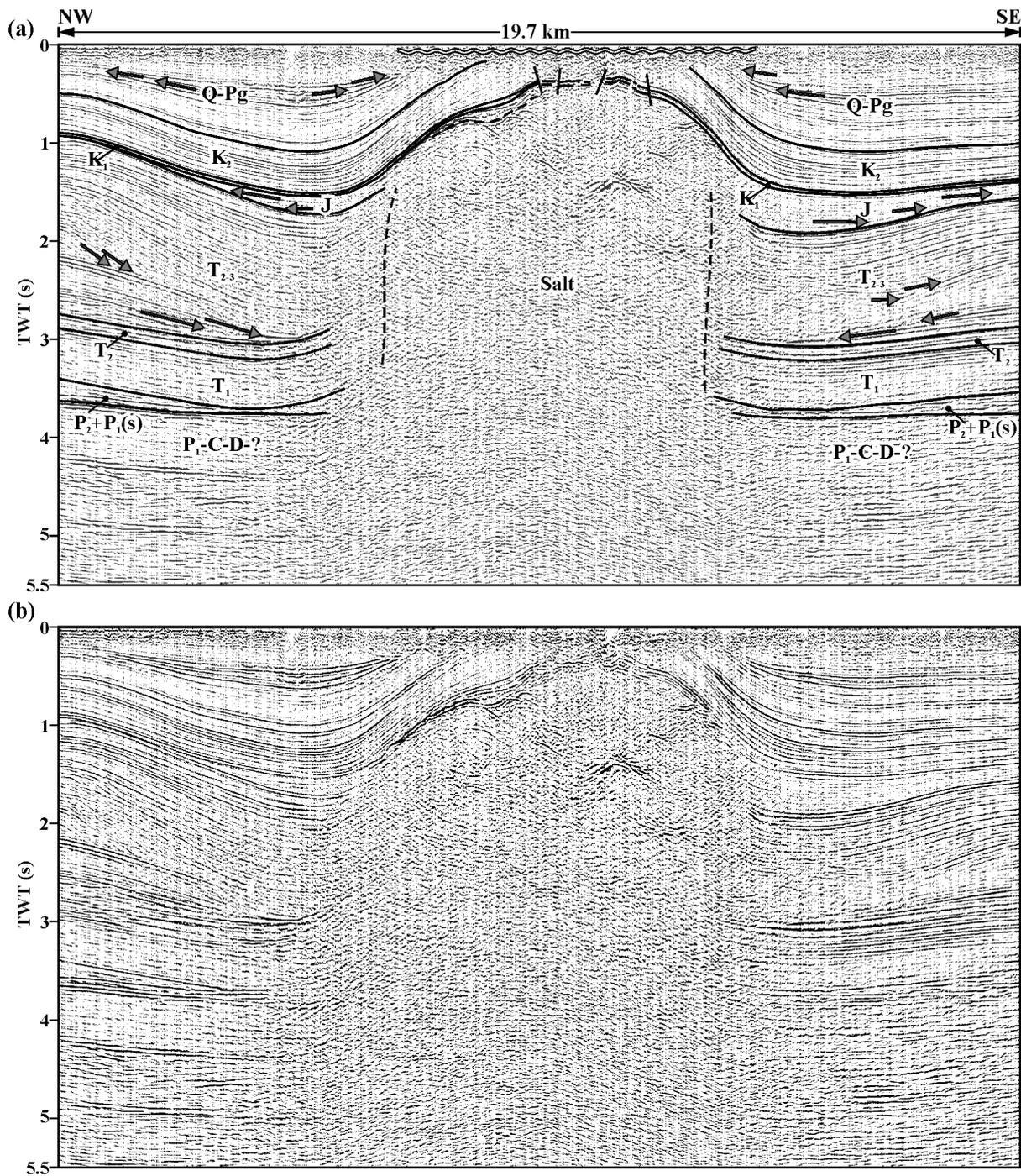
Figure 3.10. Interpreted seismic profile 10 across the central part of the Glueckstadt Graben, showing onlapping strata due to salt diapir formation within the Keuper, Jurassic and Paleogene-Neogene (onlapping strata are indicated by arrows; visible erosinal unconformity are shown by wavy line). See Fig. 3.1 for location. For stratigraphic key see Figure 3.2.

line demonstrates a vertical slice through an almost symmetrical salt wall, which reaches more than 5000 m height (Fig. 3.10). Like in the diapir described above, the salt has penetrated its cover layer up to the Lower Cretaceous succession. Strong reflectivity in the upper part of the salt diapir corresponds to the caprock. Usually, caprocks consist of displaced clastic rocks of Lower Permian age which were moved together with the salt-rich Rotliegend according to well information. The Buntsandstein and Muschelalk show constant thicknesses on both sides of the salt structure. The Keuper is the thickest sequence (up to 3400 m) along the line, indicating the main phase of subsidence within the central Triassic graben. An analysis of the seismic data shows that the Keuper clinoforms onnlap onto the top of the Muschelkalk, highlighting the character of basin-fill associated with the initial growth of the salt structure during the Keuper. Onlaps in the interior of the Keuper succession point toward subsequent extrusions of Permian salt which represent the next stage of the salt structure development – the penetration of the overburden. Considerable amount of Jurassic sediments are localized mainly around the salt structure with rim syncline character of sedimentation. Onlaps of the Jurassic reflections onto underlying Keuper demonstrate a progradation of the sedimentation away from the salt wall due to the gradual withdrawal of the Permian salt. The Late Jurassic-Early Cretaceous erosional unconformity is almost invisible in terms of seismic stratigraphy but it has been indicated by well data in this part of the basin. The Paleogene-Quaternary sequence shows thickening near the salt structure and is almost missing at the crest of the salt wall due to erosion. Internal onlaps within the Paleogene-Quaternary highlight the culmination of salt movements in the Oligocene-Neogene.

These two interpreted sections illustrate different intensities of salt tectonics in the limits of the central Triassic graben: Permian salt is almost completely extruded from the source layer along line 10, while great amounts of salt are still preserved along line 9.

3.6.1. Detailed structure of the internal Keuper sequence

The detailed image of the Keuper sedimentary infill is illustrated in Figs. 3.11 and 3.12 by NW-SE and N-S seismic lines at the depositional centre of the Glueckstadt Graben (seismic profiles 11 and 12; see enlarged version in Appendix A). The salt beds are very thin
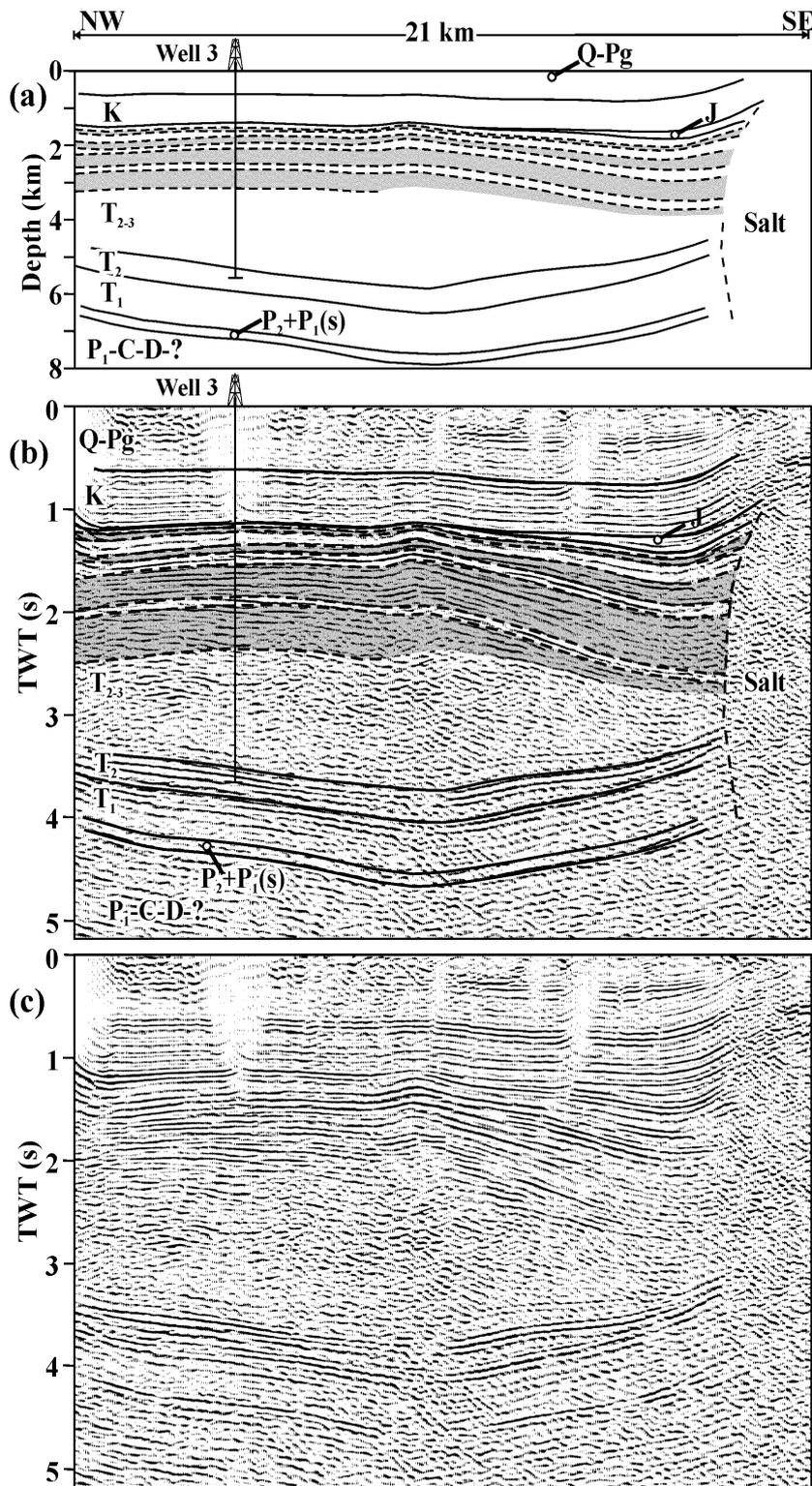
Figure 3.11. Structural features of the Keuper salt-rich layers across the Central Triassic Graben Depth. (a) Depth converted seismic section 11 (see Fig. 3.1 for location). (b) Interpreted time section 1. (c) Time section 11 without an interpretation. Grey areas correspond to salt rich layers. For stratigraphic key see Figure 3.2.

within the limits of 5-18 m except certain areas, where the Permian salt was extruded onto paleosurface. Therefore, it is not possible to show single salt beds in the seismic data, due to the limits of vertical resolution. The most prominent intervals of salt are shown by grey areas on the time sections. In general, the salt-rich layers within the Keuper are characterized by basinwide distribution within the Central Triassic Graben and by thinning towards the flanks of the basin. The internal seismic pattern of the salt-rich Keuper is dominated by concordant and subparallel clinoform beds (Figs. 3.11 and 3.12). The seismic profile 11 across the Central Triassic Graben of the GG shows the presence of four intervals where halite is interbedded with clastic sediments (Fig. 3.11). The deep part of the Keuper syncline was filled mainly by claystones (thickness up to 2000 m). This part of the line is characterized by non-regular reflectivity. The thickness of salt-rich layers is almost constant along the profile. However, the thickening of salt-rich layers is visible near the Permian salt diapir at the SE part of the line. Possibly, this increase of thickness occurred due to the presence of thicker salt beds, indicating an extrusion of Permian salt from the salt diapir. Therefore, some of the salt domes may have reached the surface providing a source for salt deposition within the Keuper sequence. Trusheim (1960) reported Permian spores within the Keuper salt rich layers somewhat south of the area under consideration. Thus, it is possible that the Permian salt partially extruded on the paleosurface during the Keuper and was redeposited due to superficial dissolution. This phenomenon of salt tectonics has also been observed in other basins of the world. In the Dniepr-Donets basin, the Lower Permian salt was partially deposited due to an extrusion and redeposition of the Devonian salt during Early Permian extension (Averiev, 1962; Stovba et al., 2003). In the Precaspian Basin – Permian salt extruded and was possibly redeposited within the Triassic and Jurassic (Ismail-Zadeh et al., 2004). Finally, present-day extrusions of salt are observed in the Zagros Mountains of Iran (Talbot et al., 2000).

The sedimentary infill in line 12 shows typical concave and sigmoidal reflections (base- and top-lapping) which can be identified as alternations of clay and salt layers by comparison with two wells (Wells 3 and 7) indicated in Figure 3.12. The seismic profile 12 is running from the south to the north along the strike of the axial part of the GG. In contrast to the cross section 11, the thickness of salt-rich layers strongly varies along line 12. Thinning of the salt-rich layers at the base of Keuper indicate a pinching-out of the
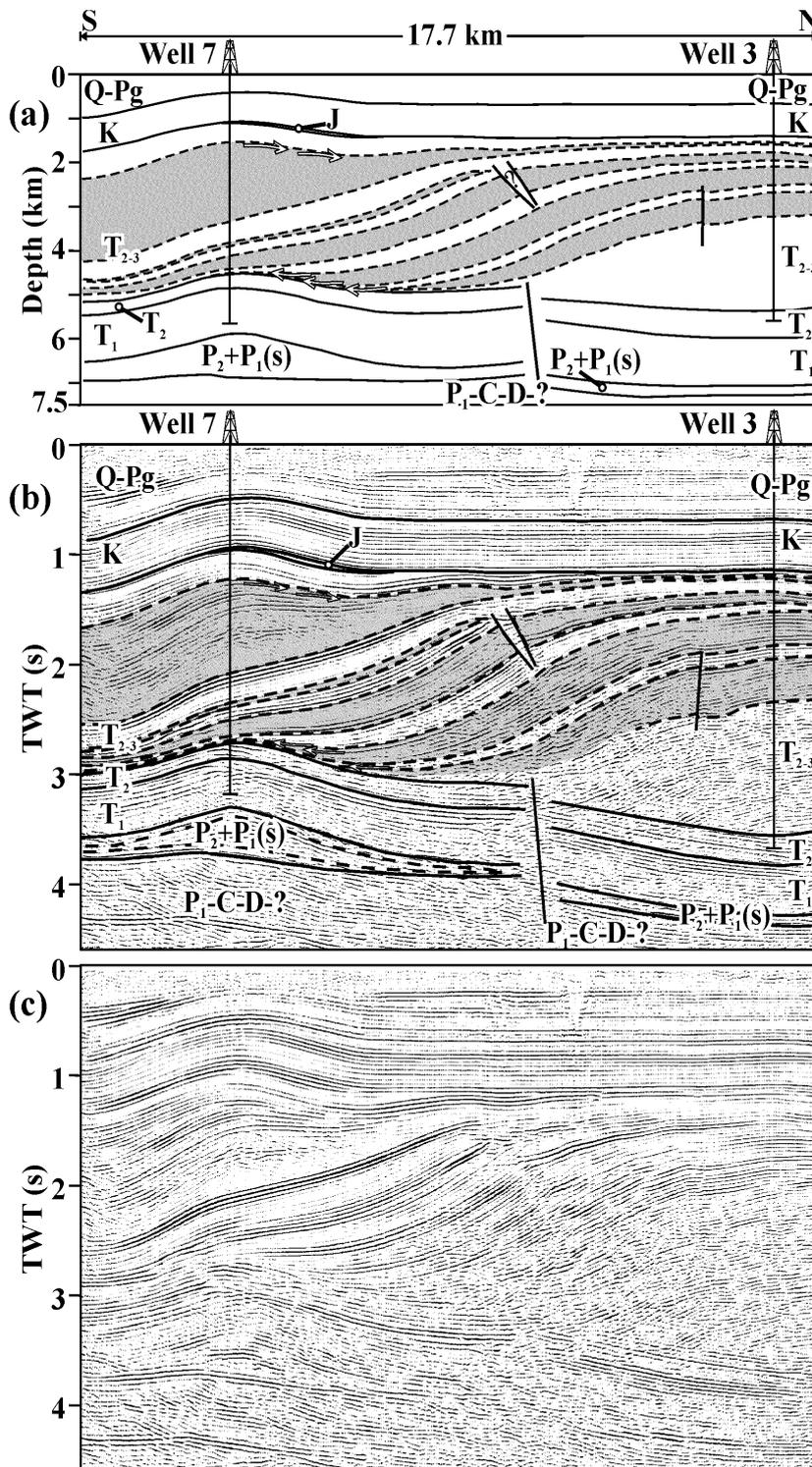
Figure 3.12. Structural features of the Keuper salt-rich layers along the Central Triassic Graben. (a) Depth converted seismic section 12 (see Fig. 3.1 for location). (b) Interpreted time section 2. (c) Time section 12 without an interpretation. Grey areas correspond to salt rich layers. For stratigraphic key see Figure 3.2.

sediments southward with exception of the youngest salt-rich interval. The sigmoidal layers indicate sediment progradation from north to south into a rapid subsided trough, which was subsequently filled from a source area in the north, perhaps the Ringkoebing-Fyn High. The present-day dips of the sigmoidal reflections are 18-25 degrees. Such steeper inclination of the reflections indicates a possible change after the deposition. Therefore, this values do not reflect true dipping at the time of sedimentation. It can indicate postsedimentation subsidence within the southern part of the profile. A possible reason for this subsidence can be salt movements during late Keuper times. Structural features of the salt-rich layers show that the salt movements created additional space, which was partially filled by extruded or redeposited Permian salt. The structural analysis indicates that polyphase movements of the Permian salt accompanied basin subsidence during the Keuper. Furthermore, the results of the interpretation show that the Permian salt was continuously near the paleosurface during the Keuper.

3.7. Summary

The evaluation of the diverse deformation patterns of the sedimentary cover and their relations to salt structures show that the strongest salt movements occurred at the beginning of the Keuper when the area under consideration was affected by extension. The NNE-SSW trending salt walls may have formed above normal faults within the pre Permian bedrock, implying a WNW-ESE directed Middle-Late Triassic extension. Minor primary salt-withdrawal synclines interpreted within the Buntsandstein and Muschelkalk deposits point toward earlier salt movements (Baldschuhn et al., 1996 and 2001). Some evidences of the initial salt movements in the Muschelkalk are illustrated in Fig. 3.9, where the Muschelkalk onlapps onto the Buntsandstein. The analysis of seismic data from the GG shows that the Middle-Late Triassic extension and associated normal faulting are the principle mechanisms for the tectonic subsidence during the Keuper. Basement faulting could have been a main trigger for the development of salt pillows and diapirs at that time. The possible syn-rift structure (apparent normal faulting) provides, therefore, the typical signature of a tectonically subsided graben while typical post-rift structures are missing as well as a typical subsequent thermal subsidence. Nevertheless, some faults at the margin of the subsidence

centre can be related to syn-rift erosion as indicated in Figure 3.13c by seismic flattening. Thereby, Figure 3.13 corresponds to the eastern part of Figure 3.2, an area where the correlation of the internal strata of the Triassic can be performed with some confidence. The palinspastic reconstruction of seismic reflections at the time before deposition of a particular layer was done by flattening its basal interface to the zero level of two-travel time. This kind of reconstruction provides structural snapshots for the time of deposition of each interface, and two of them are displayed in addition to the present-day image (Fig. 3.13a). The steeply dipping normal fault separates the Eastholstein Trough from the East-Mecklenburg Block on the present-day section (Fig. 3.13a). In contrast, the same fault is not observed on the sections flattened to the base of the Cretaceous and to the base of the Keuper (Figs. 3.13b, c), indicating rather young faulting in that place. The absence of fault can be inferred from the identical thicknesses of the Triassic sequences on both sides of the present position of the marginal salt dome. On the other hand, the Keuper section is characterized by the presence of mobile salt, which could have been deposited within the Eastholstein Trough during the Keuper. Subsequently, the Keuper salt could have beeen extruded from the section during post Triassic times, smoothing the thickness difference of the Keuper. This assumption is supported by the presence of the salt pillow within the Keuper sequence of the Eastholstein Trough to the south of the line 1 (Baldschuhn et al., 1996). Therefore, the probable displacements along this fault could have occured already in the Keuper times with following reactivation during the Cenozoic (Fig. 3.13a).

The internal seismic pattern of the Keuper, lithostratigraphic data and the results of pallinological investigations (Trusheim, 1960) indicate that Permian salt extruded on the paleosurface and was dissolved and redeposited within the Keuper strata. Krzywiec (2004) observed similar patterns in the Mid-Polish Trough, where the Permian salt also extruded on the paleosurface in the Keuper. The considerable superficial dissolution could also have occurred in the Jurassic and during the Late Jurassic – Early Cretaceous interruption of the sedimentation (Jaritz, 1980). The Lower Cretaceous sediments cover almost all salt diapirs and walls within the GG (Figs. 3.2, 3.9, 3.10 and 3.13a, b). This indicates that salt structures could be very close to the surface or even have reached the surface in the Jurassic with a main phase of superficial dissolution during the Late Jurassic – Early Cretaceous erosion. Sedimentation continued in the Early Cretaceous (mainly during Barremian-Hauterivian
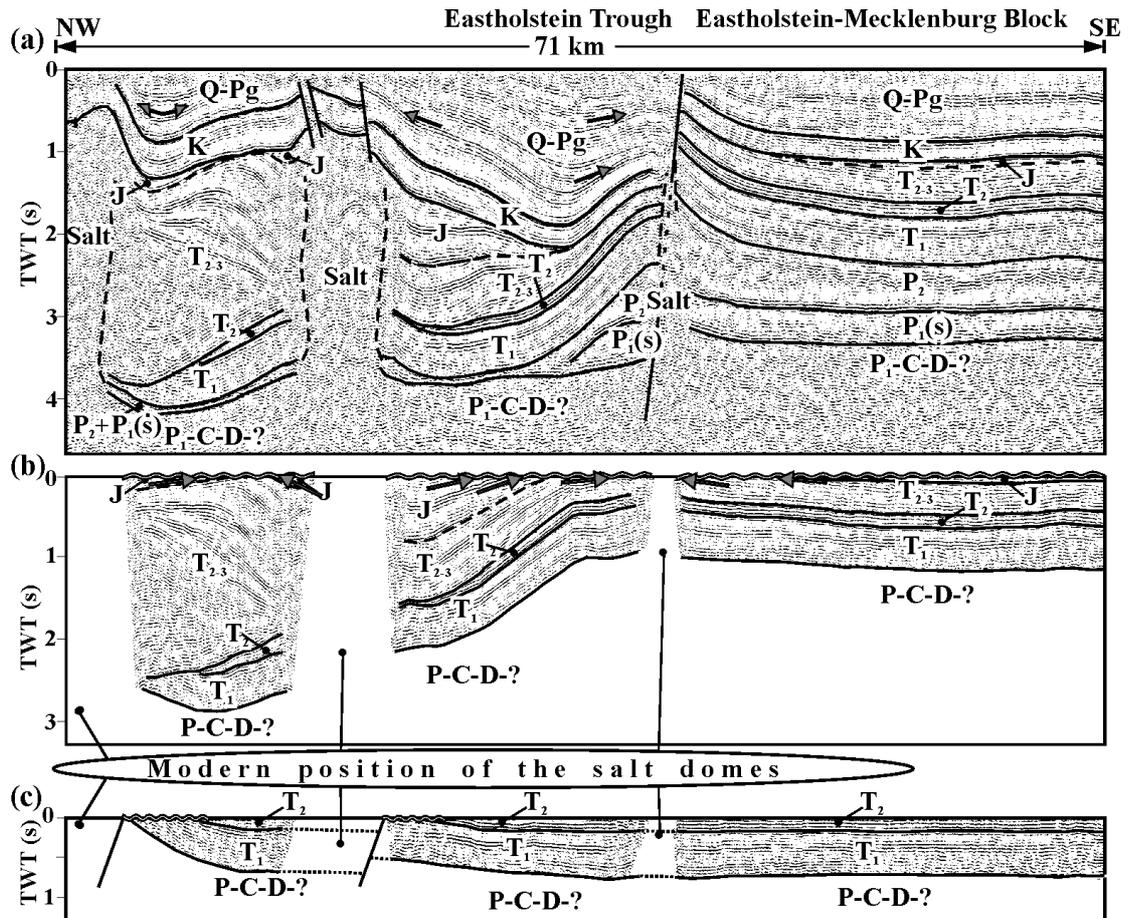
Figure 3.13. Structural evolution of the Glueckstadt Graben along south-eastern part of the seismic reflection profile 1 as visualized by flattening the SE part of line 1 to selected stratigraphic levels (for location see Figs. 3.1 and 3.2; visible erosinal unconformity is indicated by wavy line; arrows show on- and toplap of the reflection terminations). (a) Present-day structure; (b) Reconstruction to the base of Cretaceous. Late Jurassic – Early Cretatious regional erosional event is shown; (c) Reconstruction to the base of Keuper. Possible syn-rift faults and erosion are shown. For stratigraphic key see Fig. 3.2.

stages) when thin clays and marls (the prevalent thickness is about 70-80 m) have been deposited. The Upper Cretaceous strata have an approximately constant thickness and the parallel reflections pattern indicates a quiet tectonic setting with very minor salt movements in the Late Cretaceous within the area under consideration. In contrast to other parts of the

CEBS, the GG was not inverted during the Late Cretaceous and Tertiary, when up to 4,5 km of sediments were eroded during inversion of the Lower Saxony Basin (Petmecky et al, 1999) and along the southern margin of the NE German basin (Scheck et al., 2002). Renewed salt flow during the Paleogene-Neogene (mainly Eocene-Miocene) caused rapid subsidence along the marginal parts of the Central Triassic Graben in the Westholstein, the Eastholstein and the Hamburger troughs. Although many salt structures continued to rise within the centre of the GG. These movements were much less intense compared with the marginal troughs. Permian salt continued to intrude into existing salt domes at this time promoting the growth of large anticlines over salt structures, as seen in Figs. 3.5, 3.9 and 3.10. The continued rise of salt in almost N-S-striking salt walls indicates an E-W directed extension. This is consistent with the assumed regional stress field during Late Cretaceous-Early Tertiary inversion within the other parts of the CEBS. For this period, the stress field is characterized by N-S compression and E-W extension (Scheck and Lamarche, 2005) that is generally derived from the regional structural analysis within the Central Europe (Ziegler, 1990a, 1992). The GG was parallel to the principle strain direction and therefore was not prone to an inversion in Late Cretaceous/Early Tertiary. The data interpreted in this study also show that Paleogene-Neogene salt tectonics in the GG was most likely triggered by reactivation of Triassic structures due to horizontal movements (Fig. 3.8). The thick Paleogene-Neogene strata within the marginal troughs (Figs. 1.4b, 3.2 and 3.7) may also be related to a regional component of tectonic subsidence in the area, contemporary with the rapid subsidence in the North Sea (Sclater and Christie, 1980; Jordt et al., 1995; Garetsky et al., 2001).

Chapter IV

3D STRUCTURAL MODEL

4.1. Introduction

A 3D structural model has been constructed for the GG and adjacent areas from 53.4°N to 54.8°N latitude and 8.2°E to 10.8°E longitude (Fig. 4.1). This 3D structural model was derived from depth maps extracted from the digital version of the Geotectonic Atlas of NW Germany (Baldschuhn et al. 1996, 2001). The two-dimensional depth maps have been integrated into a three-dimensional structural model after calculation of thickness maps.
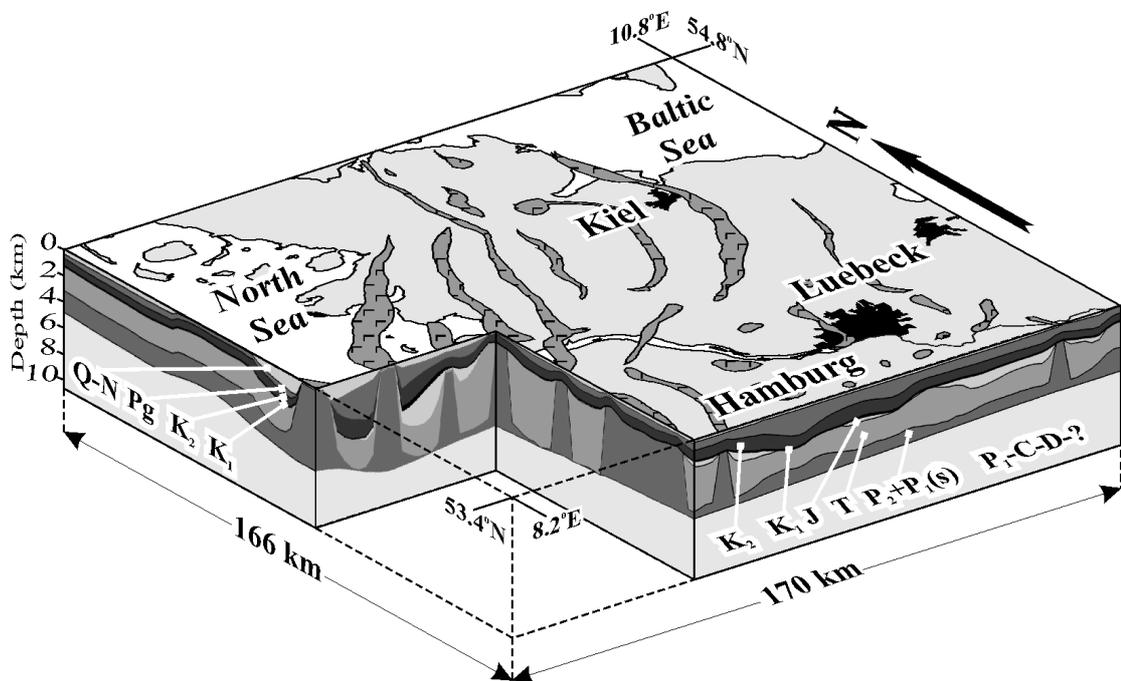
Figure 4.1. 3D structural model of the Glueckstadt Graben and adjacent areas. For stratigraphic key see Figure 1.4.

These data were gridded with a cell resolution of 2x2 km. In some areas, where stratigraphic levels intersected, corrections were necessary by the use of well and seismic information. The thickness data of the grids have been compared with the depth sections from the Geotectonic Atlas of the NW Germany (Baldschuhn et al. 1996, 2001), well data and interpreted depth converted seismic sections. In critical areas, additional control points have been added before interpolation, in order to ensure coincidence of contour lines with the

- 49 -

original data. The most problematic areas are in the vicinity of salt structures, where steeply dipping beds and strong thickness variations occur. These parts have been recontoured by hand. Finally, the corrected data were interpolated, gridded and merged into the 3D structural model of the GG. The model includes seven thickness maps from the Rotliegend to the Pliocene. The lowest one is the salt-rich Rotliegend plus the Zechstein, overlain by Triassic, Jurassic, Lower Cretaceous, Upper Cretaceous, Paleogene and Quanternary-Neogene.

The present-day structure and the evolution of the GG are discussed in this chapter, describing the Rotliegend to Quaternary in terms of thickness maps and three-dimensional views of the base of appropriate stratigraphic levels. The salt structures represent the present-day state, i.e. the thickness maps have not been corrected for post-sedimentary piercing by rising salt walls. The different areas of the GG have been described in Chapter III by 2D seismic lines. In contrast, plane views of the studied region are presented here for selected stratigraphic levels. In addition, 2D regional slices through the 3D model are analyzed in order to demonstrate the main regional structural features of the area under consideration.

4.2. Present-day structure

4.2.1. Permian salt

The present thickness of the Permian salt is shown in Fig. 4.2a. Only one layer in the 3D model represents the Permian salt, although, the Permian salt includes two independent layers: salt-rich Rotliegend and Zechstein. The salt-rich Rotliegend and the Zechstein have been merged in one layer because they cannot be distinguished within the Central Triassic Graben and the marginal troughs (West- , Eastholstein and Hamburger) where these layers are mixed in the limits of salt structures. The thickest Permian salt is localized within the salt structures (up to 8500 m). The north-western and eastern parts of the thickness map of the Permian salt (Fig. 4.2) are characterized by almost constant thickness of the Permian salt (about 1500-2000 m). Thus, the thickness of the Permian salt shows that the basin can be subdivided into two parts: (1) a central part where most of the Permian salt was

Thickness of the Permian salt

Top of the Permian salt

Base of the Permian salt
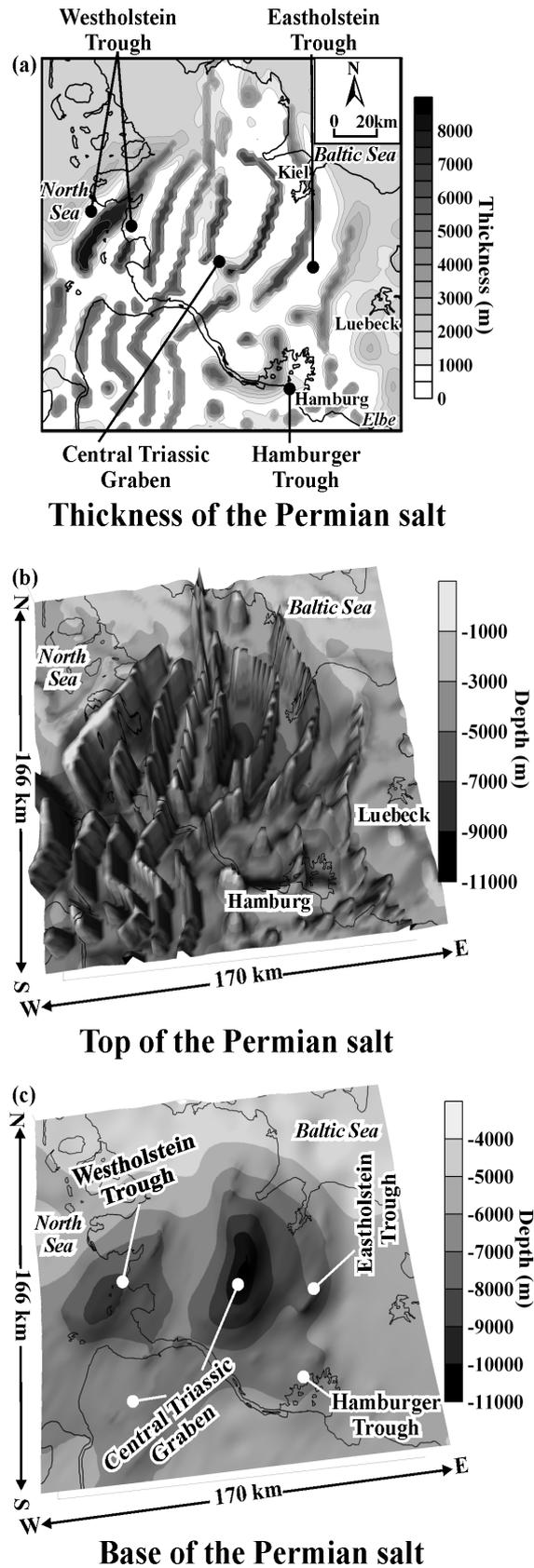
Figure 4.2. (a) Present-day thickness map of the Permian salt. 3D view on the present-day top (b) and base (c) of the Permian salt in the investigated area.

withdrawn, forming salt structures; and, (2) the north-western and south-eastern flanks where the salt formed salt pillows (Figs. 3.5 and 4.2a) or even is preserved in its original bedding (Figs. 3.3 and 4.2a). In addition, a 3D view of the modelled top of the Permian salt (Fig. 4.2b) demonstrates that the high amplitude salt walls are located mainly within the Central Triassic Graben and the Westholstein trough with decreasing amplitudes towards the Eastholstein and Hamburger marginal troughs. Accordingly, salt deformation is less intense at the north-western and south-eastern flanks of the basin (Fig. 4.2). There, the salt- rich Rotliegend is in an almost undisturbed, flat-lying position compared with the displaced Zechstein salt (Figs. 3.2-3.5), whereas both layers have been mobilized in the central part of the basin (Fig. 3.2, 3.9-3.12). The modelled base of the salt is smoothed due to the horizontal resolution of 2x2 km and does not image faults. The isolines of the salt base show merely an elongated trough with NNE-SSW orientation. However, it is known from seismic data that faults are present on this interface (e.g. Fig. 3.2). Actually, the modelled shape of the base of the Permian salt is more complex because of the lack of a unique phase correlation underneath the salt structures. This is due to low reflectivity within areas occupied by salt structures in the Central Triassic Graben and the marginal troughs (cf. Figs. 3.9 and 3.10). On the other hand, reflections from the base of the Permian salt are easily recognizable at the flanks of the basin (Figs. 3.2-3.4). The wave image is inconsistent within the salt diapirs and walls. Therefore, the base of salt cannot be determined from seismic data as there are no regular reflections. This provides a main source of uncertainty in estimating the base of the Permian salt under some salt structures. For that reason, the depth position below these salt structures was determined by interpolation of the well defined depth around salt walls and diapirs. The modelled base of the Permian salt is characterized by two deep minima which correspond to the Central Triassic Graben (depth up to -10900 m) and the Westholstein trough (depth about -8400 m; Fig. 4.2c). The huge salt walls attain a height of up to 8500 m and the deepest part of the salt base is located in the area where Triassic deposits reach the greatest thickness (Fig. 4.3a).

4.2.2. Triassic deposits

The Triassic is one of the thickest stratigraphic units of the 3D structural model (Fig. 4.3a). A broad area of the thick Triassic sediments occupies the whole Central Triassic Graben and is chracterized by a gradual increase of thickness from less than 3500 m at the

margins to more than 6500 m towards the basin centre. The thickness of the Triassic in the axial part of the GG is characterized by an intense oviform zone of high thickness with a predominant SW–NE trend. The thickness ranges from 6500 to 9300 m within this zone, which represents the thickest Triassic deposits within the GG. Salt walls bound this oviform zone from the NE and SE. Within the basin flanks and marginal troughs, the Triassic thickness varies between 1300 and 2300 m in general, which locally increases up to 3000 m. Some local decreases of Triassic thickness occur around some salt structures. These local decreases of Triassic thickness can be related to syndepositional salt movements in the Triassic or to post Triassic salt activity. Most isopachs of Triassic delineate the contours of salt structures in the horizontal plane, indicating a strong influence of salt movements on the distribution of the Triassic.

Triassic

Legend: ⬭ - Salt domes on the thickness maps; ⬭ - Salt domes on the 3D view of depth maps.
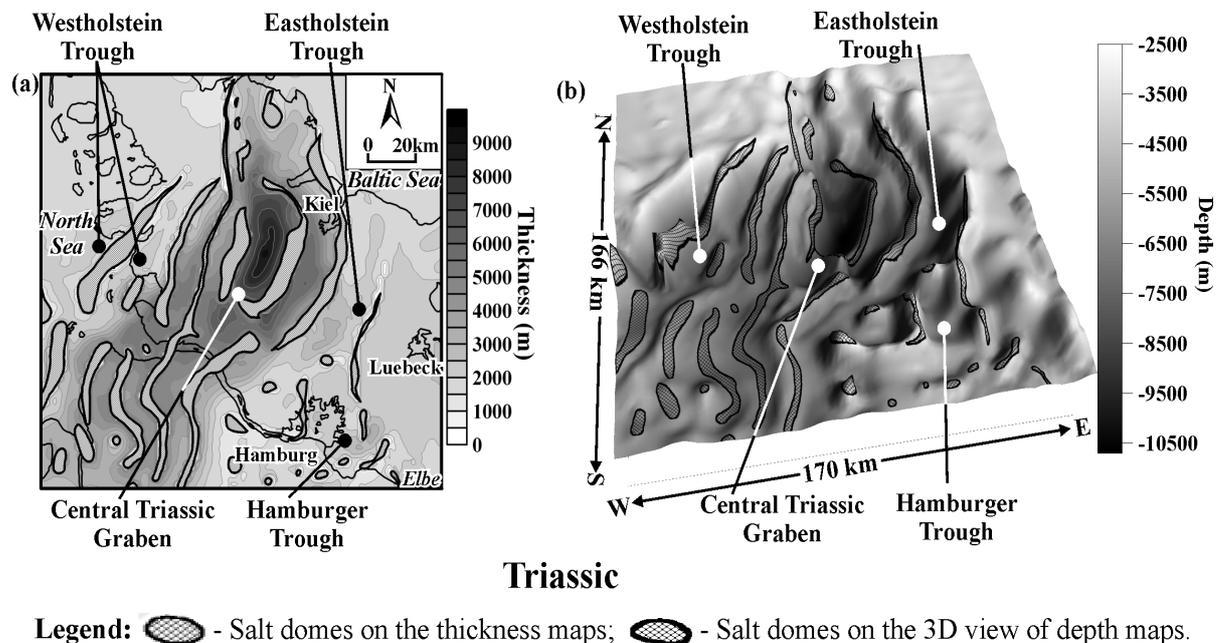
Figure 4.3. (a) Present-day thickness map of the Triassic. (b) Present-day depth position of the base of the Triassic, taken from the 3D structural model of the GG.

The base of the Triassic is located between 2500 and 4000 m depth, increasing to 7000-9000 m in the Central Triassic Graben. The base of the Triassic is complicated by many lows and rises (Fig. 4.3b), indicating salt induced deformation of the sedimentary cover. The base of the Triassic is strongly deformed within the central part of the GG where

elongated salt walls are present. On the other hand, the base topography within the flanks of the GG is more or less smooth, with local rises due to the presence of salt pillows (Fig. 4.3b). There is a visible relation between the isopach map and the Triassic base in Fig. 4.3. Relatively thin Triassic deposits occur at the almost flat north-western and north-eastern parts of the GG, where only some local irregularities are present. In contrast, thick Triassic corresponds to the area with high amplitude anticlines. It was inferred from the seismic data that salt movements created these anticlines mainly during the Keuper. Particularly, the thickest Triassic is underlain by a broad syncline, which reaches 10600 m depth. This syncline corresponds to the deepest area of the present-day Triassic base (Fig. 4.3b). However, the anticline and syncline structures of the present-day Triassic base are not obviously reflected in the thickness variation of the Triassic within the West-, Eastholstein and Hamburger Troughs. This indicates post Triassic deformation of the Triassic base within the marginal troughs.

4.2.2.1. Uppermost Middle Triassic plus Upper Triassic (Keuper)

The thickness map of the uppermost Middle Triassic plus Upper Triassic (Keuper) and the present-day depth position of the Keuper base are shown in Fig. 4.4. It is important to note that the depth position of the base of the Keuper can not be identified with confidence within the central part of the GG. The reason is a poor available seismic coverage of the central part of the GG and a complex seismic pattern within the Keuper. Meaning, that the localized thickening of Keuper, undoubtedly exists in the central part of the GG, is badly defined in the present map. For that reason, the Keuper was not separately included into the 3D structural model of the GG.

The first-order difference between the central part of the GG and the surrounding regions is evident on the thickness map. Two zones of relatively thin Triassic on the NW and SE are separated by the area of the very thick Triassic of the Central Triassic Graben. The thickness pattern within the Central Triassic Graben is complex, reflecting the main phase of the subsidence within the GG. On the other hand, simpler patterns dominate within the basin flanks and marginal troughs (Fig. 4.4a). An almost constant thickness of the Keuper suggests that the Westschleswig and the Eastholstein-Mecklenburg blocks were not strongly affected by Middle-Late Triassic extension (Fig. 4.4a). At these basin flanks, the thickness varies from 370-400 m up to about 600 m, reflecting a rather regional component of subsidence.
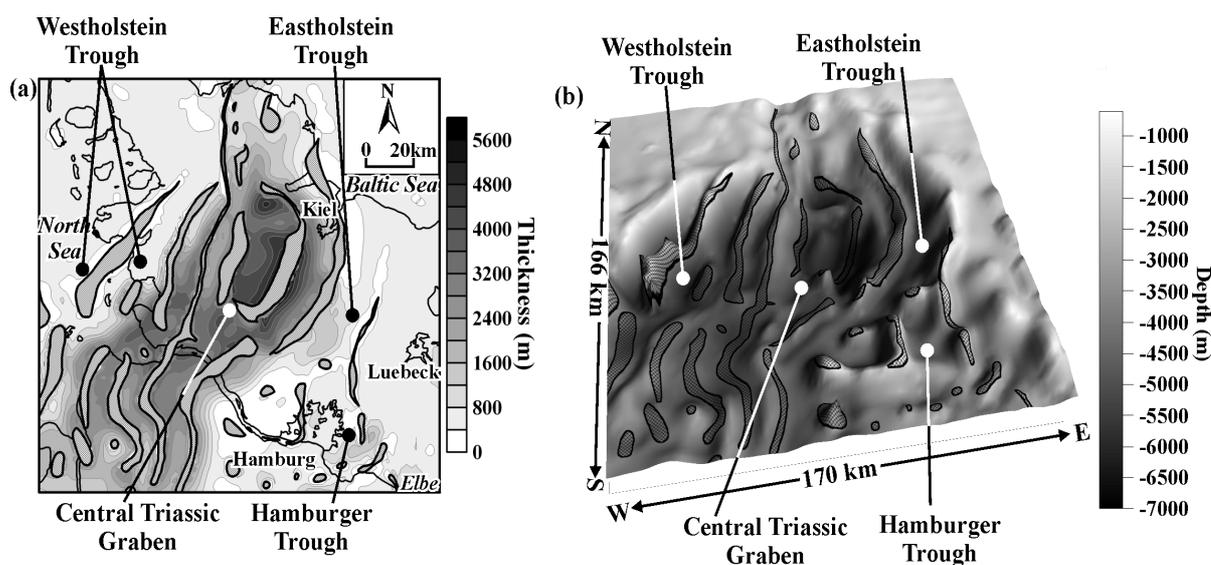
Uppermost Middle Triassic and Upper Triassic (Keuper)

Figure 4.4. (a) Present-day thickness map of the uppermost Middle Triassic and Upper Triassic (Keuper). (b) Present-day depth position of the base of the uppermost Middle Triassic and Upper Triassic (Keuper).

In the marginal troughs, the thickness is more variable. The area of increased Keuper thickness within the Central Triassic Graben is characterized by an almost SW-NE trend. This broadly curvilinear area is up to 65-km wide with thickness variations from 1500 m up to 5800 m. The total length of the Central Triassic Graben is approximately 220 km from the Ringkoebing Fyn High to the Pompeckj Block. In the northern part of the Central Triassic Graben, the thickness map (Fig. 4.4a) offers a good view of the rapid thinning of the Keuper towards the north where the Ryngkoebing Fyn High is located. A distinctive region of high thickness gradients is located within the central part of the GG. The reason for the localization of the highly increased Keuper thickness is salt movements during the Keuper within the central part of the Triassic Graben. This is supported by the thickness map in Fig. 4.4a, where the thickness gradient is always higher in the vicinity of salt walls. In addition, the increased Keuper thickness of the southern part of the Central Triassic Graben is running parallel to the curved salt walls. This structural feature indicates that the Keuper sedimentation was accompanied by strong salt movements and was even controlled by salt outflow.

The shape of the Keuper base is very similar to the base of the Triassic (cf. Figs. 4.3b and 4.4b). The differences are the absolute value of depths and local changes variations in shape. The central part is pierced by Rotliegend-Zechstein salt, forming anticline folds close to the salt structures. Within the basin flanks, the base of Keuper is mainly deformed by Zechstein salt pillows. The Keuper base reaches 7000 m depth in the Central Triassic Graben. The depth position of the Keuper base shallows towards the north-western and the south-eastern flanks of basin where it is located at 1200-2000 m depth.

4.2.3. Preserved Jurassic sediments
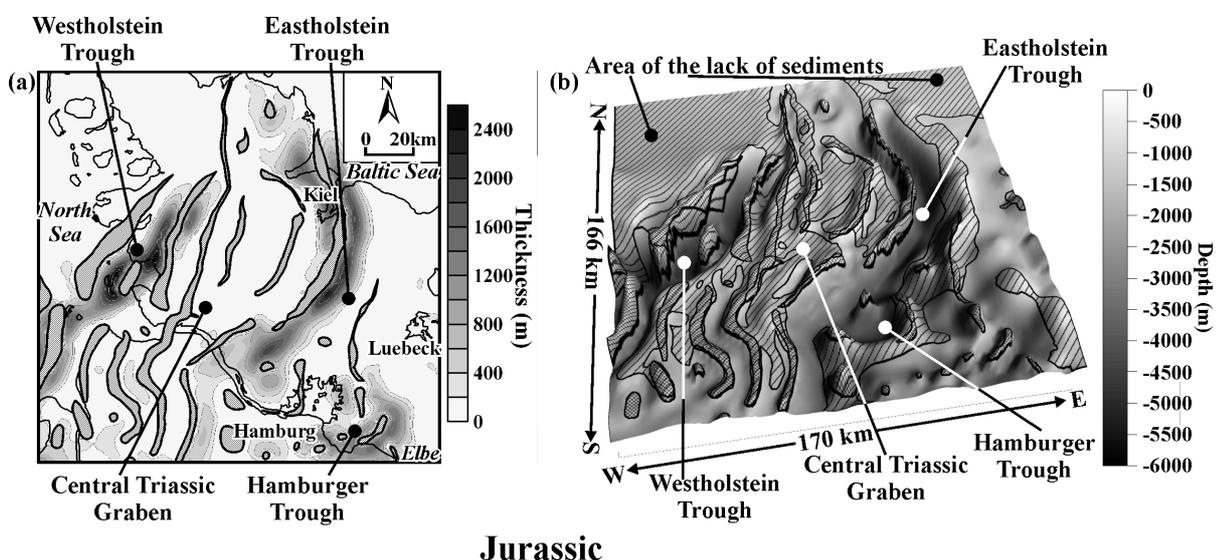
Figure 4.5. (a) Present-day thickness map of the Jurassic. (b) Present-day depth position of the base of the Jurassic, taken from the 3D structural model of the GG.

The thickness and structural maps of the Jurassic show only the present-day distribution of the sediments which remained after the Pre-Cretaceous erosion (Fig. 4.5). Therefore, the distribution of the preserved thicknesses of Jurassic strata can be explained by Late Jurassic-Early Cretaceous erosion or alternativly by variable syndepositional subsidence due to salt tectonics. From the seismic data discussed in Chapter III it is inferred that the remaining sediments represent areas where sedimentation and subsidence were most intensive. Fig. 4.5 illustrates that the centre of sedimentation is shifted from the central part

towards adjoining areas compared with the Triassic, forming two centres in the north-west and south-east. The Central Triassic Graben area is characterized by a lack of Jurassic sediments or by relatively thin deposits reaching 400 m thickness (Fig. 4.5). The Westholstein Through delineates the NW margin of the Central Triassic Graben (Fig. 4.5a). It has an estimated width of about 20 km and is associated with relative thick Jurassic sediments. The maximum thickness of the Jurassic is about 2500 m in the Westholstein Through. The Hamburger and Eastholstein Troughs were formed at the SE margin of the Triassic Graben (cf. Figs. 4.3a, 4.4a and 4.5a). The Eastholstein syncline is characterized by a SW-NE elongated band of sediments along the marginal salt walls. The Jurassic is locally 1800-2200 m thick with an average thickness between 1000 and 1200 m in the Eastholstein Trough. The distribution pattern of sediments is very similar to the West- and Eastholstein Troughs where thickening of the Jurassic is observed along salt walls, implying a strong influence of the salt movements on deposition. The complex Jurassic thickness pattern with almost circular and elongated zones near Hamburg defines the extent of the Hamburger Trough. This trough is filled by Jurassic sediments, reaching a thickness up to 1600 m. In contrast to the West- and Eastholstein troughs, the thickness distribution of the Hamburger Trough is not clearly SW-NE elongated, probably due to the presence of differently shaped salt diapirs. The thickness distribution of the Jurassic strongly coincides with salt structures, displaying a rim syncline character of sedimentation.

The deep synclines of the Jurassic base coincide with the areas of the thick Jurassic strata in the West-, Eastholstein and Hamburger Troughs (cf. Figs. 4.5a and 4.5b). Areas without Jurassic sediments are associated with an elevated Jurassic base in comparison to the deep synclines (Fig. 4.5b). Jurassic sediments are not observed within the NW and NE parts of the map in Fig. 4.5. Generally the distribution patterns of the Jurassic match well with the areas where complex relief prevails (see Fig. 4.5b).

4.2.4. Lower Cretaceous

The Lower Cretaceous sediments are wider distributed than the Jurassic sediments, because they cover most salt structures which already existed at the beginning of the Cretaceous (Fig. 4.6a). The Lower Cretaceous thickness does not strongly vary (about 90 m) within the basin with the exception of the areas near salt diapirs in the north-west and south-east (Fig. 4.6a). Therefore, the regional trend shows very slow subsidence after the Late

Jurassic-Early Cretaceous erosion (Fig. 4.6a). As a result, the present-day thickness of the Lower Cretaceous is considered to be partly controlled by predepositional regional erosion and/or interruption of the sedimentation during Late Jurassic- Early Cretaceous times.

Lower Cretaceous

Figure 4.6. (a) Present-day thickness map of the Lower Cretaceous. (b) Present-day depth position of the base of the Lower Cretaceous, taken from the 3D structural model of the GG.

However, prominent thick Lower Cretaceous deposits are observed around the salt structures within the Westholstein and Hamburger Troughs (Fig. 4.6a). The thickness of the Lower Cretaceous sequence increases from less than 90 m to more than 500 m within the Westholstein and Hamburger Troughs (Fig. 4.6a). A large zone of Lower Createceous thickening of the Westholstein Trough stretches in the SW-NE direction between two elongated salt walls. It is likely that the reason for this thickening is the simultaneous growth of the salt walls. In contrast, the Lower Cretaceous thickening zone is almost circular within the Hamburger Trough, reflecting sedimentation in the vicinity of the circularly shaped salt diapir. In addition, the described two areas of thick Lower Cretaceous have increasing thickness gradients towards the salt structures, reflecting salt induced sedimentation (Fig. 4.6a). Such thickening occurs in areas where German "Wealden" sediments are present, which represent the Berriasian and the lower Valanginian intervals of the lowest part of the Cretaceous (Boigt, 1981). The Berriasian and the lower Valanginian are not observed in the

other parts of the area under consideration, but they occur in the south, in the Lower Saxony Basin (Baldschuhn et al., 1996 and 2001). Thus, these two pronounced areas of the Westholstein and Hamburger Troughs indicate the continuation of salt movements during the Early Cretaceous, following the strong Jurassic salt activity in the same areas.

The Lower Cretaceous sediments of the marginal troughs are all characterized by deep burial depth (Fig. 4.6b). The base is locally below -6000 m within the Westholstein Trough and -4000 m within the Eastholstein and Hamburger Troughs. Such deep burial indicates strong post Cretaceous subsidence during the Tertiary. The position of the salt walls is easily recognizable from the presence of the elongated highs within the Central Triassic Graben (Fig. 4.6b), demonstrating postdepositional salt flow. A similar situation is observed within the marginal troughs and the basin flanks where the development of most synclines and anticlines took place in the Tertiary with the exception of a few salt structures which were also active in the Early Cretaceous. This means that the present-day base topography of the Lower Cretaceous does not reflect the correct relationship between thickness distribution and the shape of the base.

4.2.5. Upper Cretaceous

The thickness of the Upper Cretaceous indicates regional subsidence with local disturbance due to salt tectonics (Fig. 4.7a). The Cretaceous succession slightly varies between 500 and 700 m thickness within the Central Triassic Graben and the basin flanks. However, pronounced thickening occurs within the Westholstein and Hamburger Troughs. A slight thickening is also observed within the Eastholstein Trough but it has less intensity. The thickness of the Upper Cretaceous is characterized by a narrow band of thick sediments in the Westholstein Trough. In the Hamburger Trough, the relatively thick Upper Cretaceous forms two synclines, which are almost symmetrically situated towards the west and the east of a salt diapir (Fig. 4.7a). The structural features of the isochors indicate that the deposition of the thick Upper Cretaceous occurred simultaneously with salt movements within the relatively shallow rim synclines. The maximum thickness of Upper Cretaceous deposits ranges from 1400 to 1600 m within the Westholstein Trough and from 1200 to 1300 m within the Hamburger Trough. The thick Upper Cretaceous in the Westholstein Trough coincides with the Jurassic and Lower Cretaceous areas of thickenning (cf. Figs. 4.5a, 4.6a and 4.7a). However, the thick Upper Cretaceous covers a wider area towards the northwest

within the NW marginal trough. In the Hamburger Trough, the thick Upper Cretaceous sediments have a similar setting but the thickness maximum is shifted to the south in comparison with the Jurassic and Lower Cretaceous thickness maxima (cf. Figs. 4.5a, 4.6a and 4.7a). These features point to a long-term salt activity since the Jurassic within the north-west and the south-east marginal troughs.
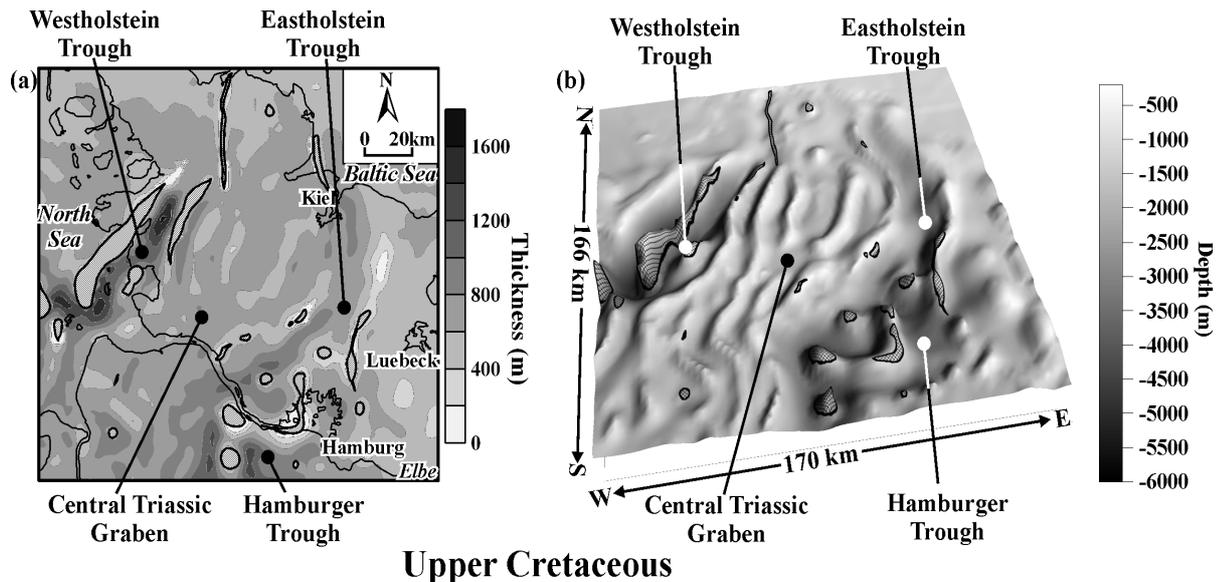
Figure 4.7. (a) Present-day thickness map of the Upper Cretaceous. (b) Present-day depth position of the base of the Upper Cretaceous, taken from the 3D structural model of the GG.

The comparison of the isochore map of the Upper Cretaceous and depth position of the base of the Upper Cretaceous shows good agreement. Where the Upper Cretaceous is relatively thick, synclinal structures are present at the base topography. Where the Upper Cretaceous is relatively thin, anticlinal structures are observed. It is obvious that the anticlines of the present-day depth position of the Upper Cretaceous base represent the location of salt structures within the study area. Therefore, the narrow areas of present-day reduced thickness reflect the position of the salt walls within the GG. Therefore, the present-day thickness distribution is considered to be partly controlled by later erosion of the crest of some salt structures (cf. Figs. 4.7a and 4.7b).

4.2.6. Paleogene
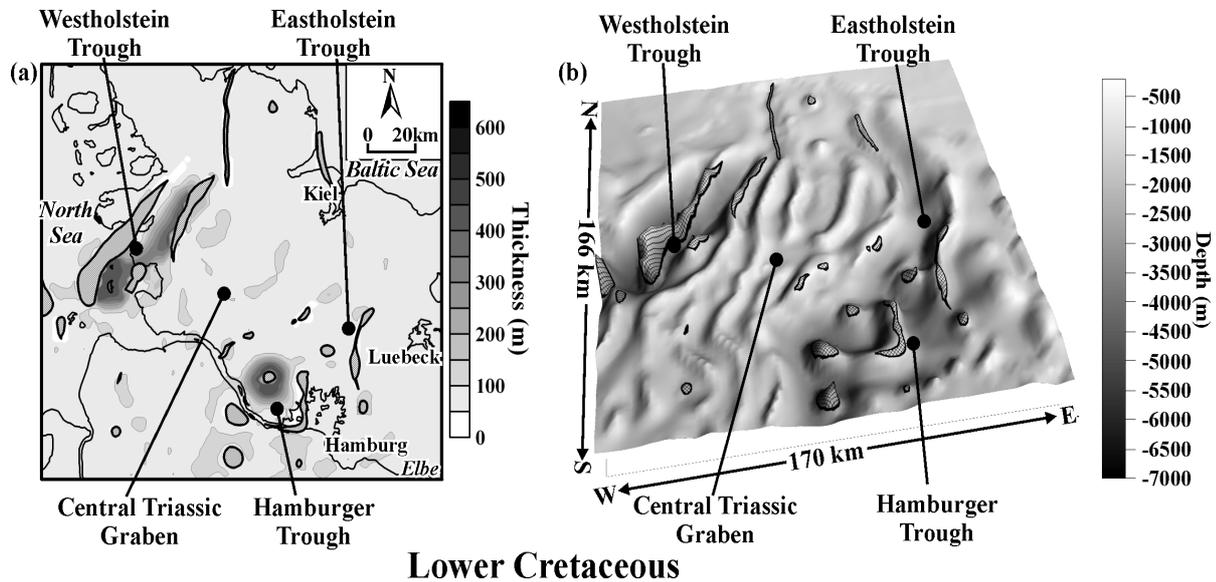

Figure 4.8. (a) Present-day thickness map of the Paleogene. (b) Present-day depth position of the base of the Paleogene, taken from the 3D structural model of the GG.

The isochore map of the Paleogene (Fig. 4.8.a) shows two thickness maxima in the West-, Eastholstein and Hamburger Troughs. This indicates that Paleogene subsidence occurred mainly within the marginal sub-basins, while, sedimentation was much less in the axial part of the GG and on the basin flanks. The zones of Paleogene thickening are in the same areas as the highest thickness values of the Jurassic, Lower Cretaceous and Upper Cretaceous, indicating further increased sedimentation rates in the marginal troughs. However, the thick Paleogene extends further to the west within the Westholstein sub-basin compared with the Jurassic and Cretaceous, where the zone of thickening is located only around the eastern margin of the salt wall. According to the map in Fig. 4.8., the Paleogene reaches locally 2500-3000 m thickness with a strong isochore gradient from the salt wall towards the centres of the rim synclines. The thickness varies between 200 and 2000 m within the 10 km wide synclines. In the Eastholstein and the Hamburger Troughs, the entire area of the former Jurassic and Cretaceous troughs was affected by increased rates of subsidence with the strongest thickness gradient in the south-western part of the Hamburger Trough. The Eastholstein Trough is a pronounced NW striking zone of thick Paleogene with

a maximum thickness between 1300 and 1700 m. Two circular thickening zones are visible within the western part of the Hamburger Trough, where the highest isochore values vary between 2300 and 2900 m. The area of the Central Triassic Graben is characterized by narrow bands of reduced Paleogene thickness (Fig. 4.8a). These areas of low Paleogene thickness within the axial part of the GG coincide with highs of the base, which correspond to the crests of salt walls and diapirs. A similar coincidence can be recognized at the basin flanks, where the areas of thinned sediments are located above the locally elevated base topography (cf. Figs. 4.8a and 4.8b). Thinning of the Paleogene occurs mainly above the salt structures in the area under consideration. The coincidence is in agreement with the seismic lines (e.g. see Figs. 3.2, 3.9 and 3.10), indicating growth of the salt structures during the Paleogene and a post-Paleogene erosion of the crests. In the Central Triassic Graben and on the basin flanks, the Paleogene thickness varies from 0-200 m above the crest of salt structures, and reaches 400-900 m between the salt structures (Fig. 4.8a).

The base topography of the Paleogene is characterized by the presence of two deep synclines surrounding the Central Triassic Graben from the NW and SE. The Paleogene base reaches locally depth greater than 5200 m in the Westholstein Trough and greater than 3300 m in the Hamburger Trough. The north-western and north-eastern parts of the map in Fig. 4.8b demonstrate an almost flat base of the Paleogene with depth values vary between 300 and 600 m. In contrast to the Cretaceous, the present-day thickness distribution and depth position of the Paleogene base are in a good agreement. The position of the relativly thick Paleogene correlates with the low base topography and thinning of this stratigraphic unit occurs above elevated areas (cf. Figs. 4.8a and 4.8b).

4.2.7. Quaternary -Neogene

The thickness map and a 3D view of the base of the Quaternary-Neogene are shown in Fig. 4.9. The structural map of the base Quaternary-Neogene (Fig. 4.9b) is the "negative" of the thickness of the Quaternary-Neogene sediments (Fig. 4.9a) within the German lowlands. This means that the present-day thickness distribution and 3D view on the depth position of the Quaternary-Neogene base are in an excellent agreement with each other. The areas of the elevated base precisely correspond to the minima of Quaternary-Neogene thickness and vice versa (cf. Figs. 4.9a and 4.9b). The uplifted SW-NW elongated highs on
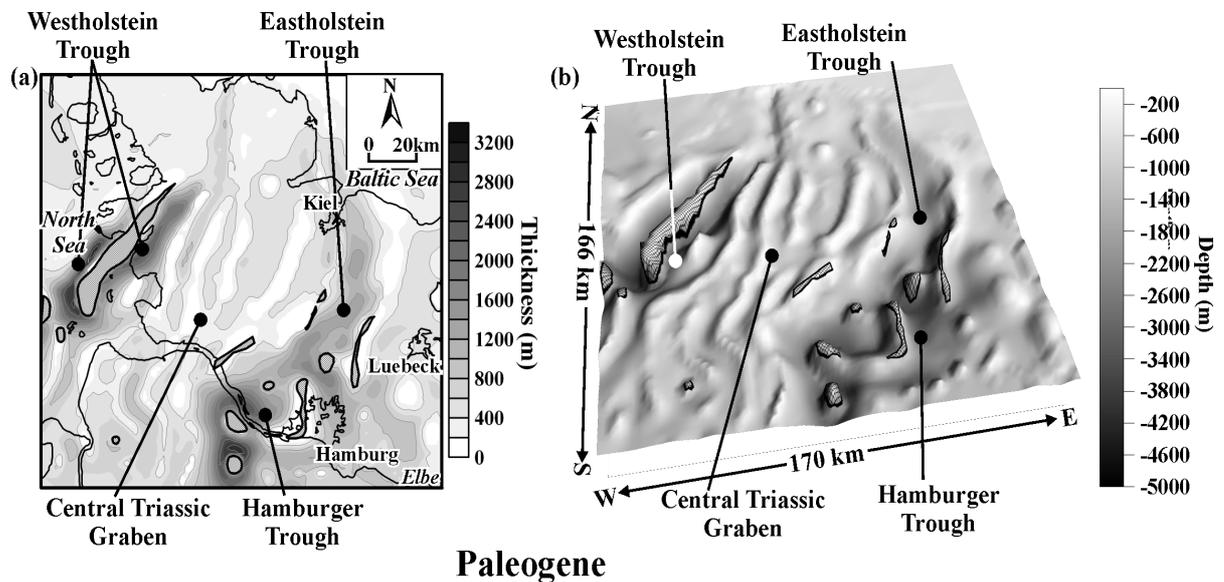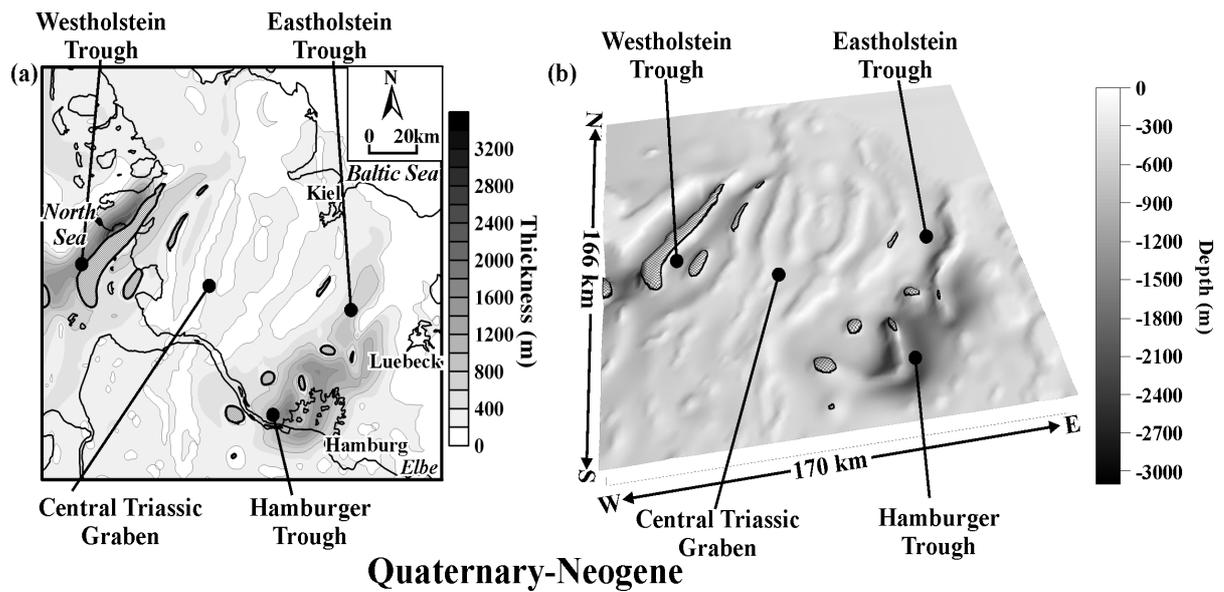
Figure 4.9. (a) Present-day thickness map of the Quaternary-Neogene.
(b) Present-day depth position of the base of the Quaternary-Neogene, taken from
the 3D structural model of the GG.

the base in Fig. 4.9b indicate growth of salt walls within the Central Triassic Graben during the Neogene. On the basin flanks, the roundish highs reflect the formation of the salt pillows. SW–NE-oriented deep synclines are visible within the north-western and south-eastern parts of the map in Fig. 4.9b. The location of the zones of Quaternary-Neogene thickness maxima overlaps with the areas of the Paleogene maximum within the marginal troughs (cf. Figs. 4.8a and 4.9a). The thick Quaternary-Neogene occupies only a restricted area on the western wing of the most-marginal salt wall in the Westholstein Trough. This indicates a migration of the subsidence centre to the west in comparison to the Paleogene. This zone of high thickness values of the Westholstein sub-basin forms a 9 km wide syncline parallel to the salt wall with more than 3000 m of sediment fill. In the Hamburger Trough, the centre of subsidence is shifted to the east in comparison to the Paleogene. The thickness of the Quaternary-Neogene reaches 1500-1800 m. In the Central Triassic Graben and on the flanks of the basin, the thickness varies between 80-120 m above the salt structures and 280-350 m elsewhere (Fig. 4.9a). The thinning of the Quanternary-Neogene above salt structures reflects syndepositional growth of most of the salt-related anticlines.

4.3. Regional structural features of the GG

Here, the regional features of the basin structure are analyzed by use of a set of 2D vertical slices from the 3D structural model. The position of the vertical slices is shown in Fig. 4.10, also indicating their position relative to major tectonic units. The NW-SE cross-sections 1–4 show the large-scale structure across basin strike (Fig. 4.11). In contrast, the SW- NE profiles 5-9 demonstrate the structural features of the GG along basin strike (Fig. 4.12).
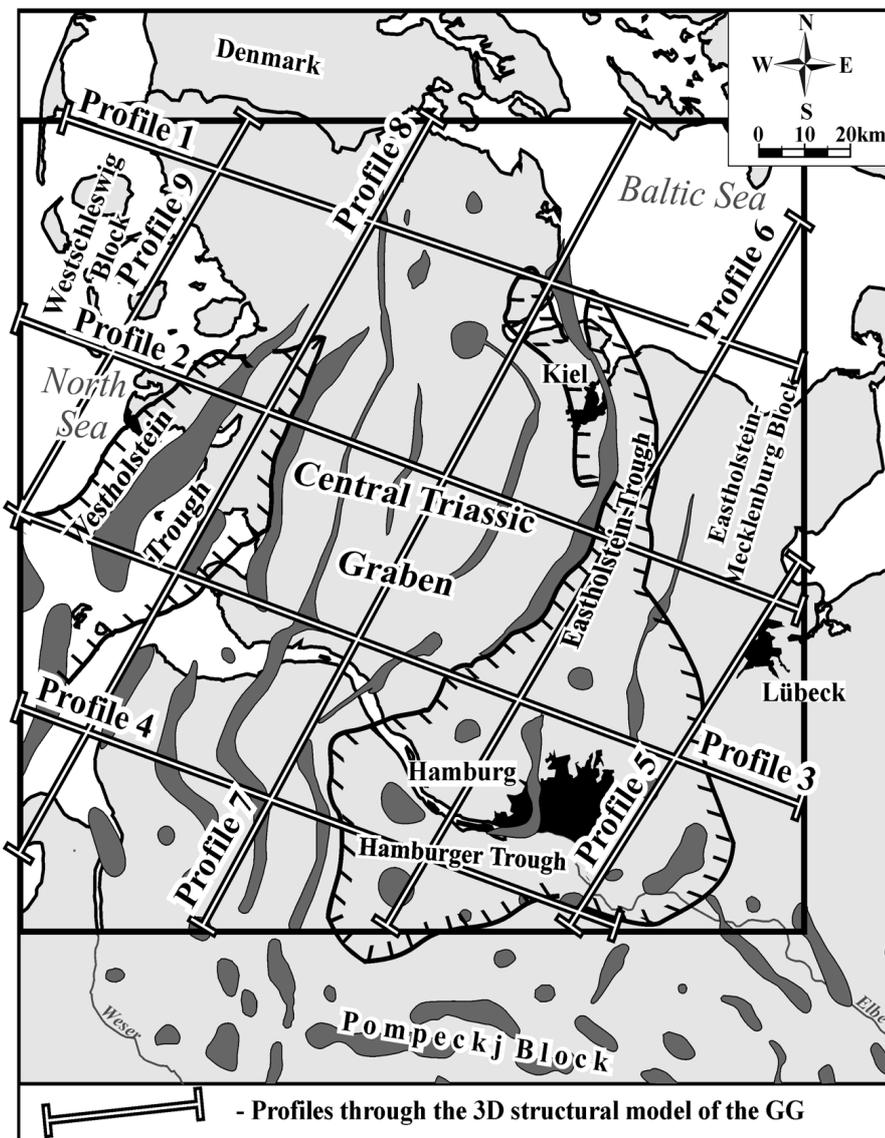
Figure 4.10. Location of the 2D large-scale regional slices projected onto the specified vertical planes through the 3D structural model of the GG (position of salt domes after Baldschuhn et al., 1996).

- 64 -

Figure 4.11 provides cross-sectional views, showing the structural relations between the Central Triassic Graben, the marginal troughs (the West-, Eastholstein and Hamburger troughs) and the basin flanks (Westschleswig and Eastholstein-Mecklenburg blocks) from the north-east to the south-west. Profile 1 in Fig. 4.11a shows the NE continuation of the GG where the Central Triassic Graben is narrow and strikes more southnortherly, but the zone of Triassic thickening can still be recognized. Along this profile (Fig. 4.11a), the Central Triassic Graben is characterized by a relatively thick Triassic within restricted zone between two salt walls. The Triassic sequence does not show obvious thickening in the Westschleswig and Eastholstein-Mecklenburg Blocks. The marginal Eastholstein Trough is evident at the south-eastern part of this section where it is mainly displayed by thickening of Jurassic strata around a salt wall.

The central segment of the 3D model (see Profile 2 in Fig. 4.11b) indicates close relations between the thick sequences of the Triassic, Jurassic and Tertiary across the GG. The thick Triassic succession of the central part overlying the Permian evaporites thins towards the West- and Eastholstein Troughs. Significant thinning broadly coincides with the axial parts of these marginal troughs. In contrast, the Jurassic deposits are cut by the Late Jurassic-Early Cretaceous erosion and are significantly thinning towards the Central Triassic Graben. Profile 2 demonstrates the deformation of post Triassic units due to the growth of the salt structures. Prominent thickening of the Paleogene and the Quaternary-Neogenere occurs in limits of the West- and Eastholstein Troughs along Profile 2 (Fig. 4.11b). Along Profile 3 (see Fig. 4.11c), marginal Jurassic-Cenozoic sub-basins at the north-western and the south-eastern edges of the Central Triassic Graben are most broadly extended in comparison to other parts of the GG. In addition, Profiles 2 and 3 show thick Upper Cretaceous within the SE syncline of the Westholstein Trough. This contrasts with the basin-wide thickness distribution of Upper Cretaceous sediments within other parts of the GG, e.g. they are a much thinner further to the southeast (Figs. 4.11 b, c). Profile 4 demonstrates the thickest part of the Hamburger Trough where only the Paleogene is thickened (Fig. 4.11c).

The location of profiles 5-9 was chosen to display an individual structure of each tectonic unit (for location see Fig. 4.10). This was done in order to show the structure of the tectonic zone parallel to strike of the GG (Fig. 4.12). Along the Profiles 5 and 9 (Figs. 4.12 a, e), the Mesozoic-Cainozoic sedimentary cover of the Westschleswig and Eastholstein-

- 65 -

Profile 1

Profile 2

Profile 3

Profile 4

Legend:

- Q-Ng = Neogene-Quaternary;
- Pg = Paleogene;
- K₂ = Upper Cretaceous;
- K₁ = Lower Cretaceous;
- J = Jurassic;
- T = Triassic;
- P₂+P₁(s) = upper part of the Lower Permian and Upper Permian (undivided Zechstein and salt-rich Rotliegend);
- P₁-C-D = Undivided Lower Permian, Carboniferous and Devonian deposits.
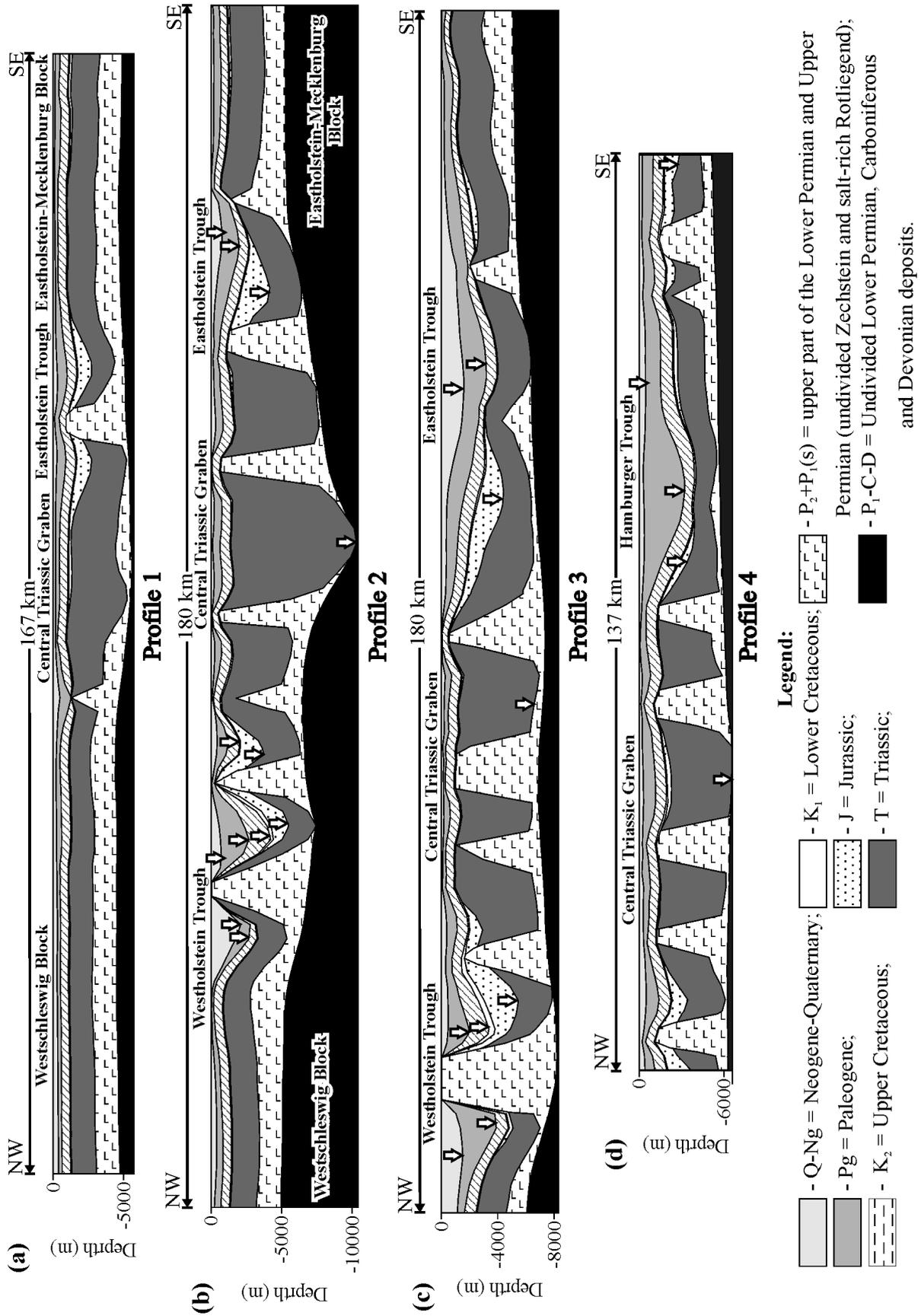
Mecklenburg blocks has an almost constant thickness (Figs. 4.12a, e), reflecting a regional component of subsidence with some solitary complications during post Permian times. Profile 7 in Fig. 4.12c shows the Triassic depocenter along the axial part of the GG, consisting of SW-NE trending thick Triassic sediments, which are underlain by extremely depleted Permian salt. The longitudinal view of Central Triassic Graben is characterized by thinning of the Triassic from the central part of the GG to the southwest and to the northeast (Fig. 4.12c). The thickness pattern along Profile 7 (see Fig. 4.12c) shows that the post Triassic succession thins significantly within the axial part of the Central Triassic Graben. Furthermore, Jurassic sediments are almost absent within the central part of the basin (Fig. 4.12c) but the deep Jurassic synclines overlap the thick Triassic within the West- and Eastholstein Troughs (Profiles 6 and 8 in Figs. 4.12 b, d). Extremely thick Quaternary-Neogene and Paleogene deposits notably extend into the area of the marginal synclines between the Central Triassic Graben and the basin flanks (Profiles 6 and 8 in Figs. 4.12b, d). Profiles 6 and 8 (Figs. 4.12b, d) show that thick Jurassic and Tertiary successions extends along the Central Triassic Graben, and that the deformation following the salt movements, resulted in the formation of the deep rim synclines within the marginal troughs. In addition, Profiles 6 and 8 run along the Eastholstein and Westholstein Troughs, providing evidence for a major discordance between the Jurassic and Cretaceous strata (Figs. 4.12b and d).

The cross-sections in Fig. 4.11 are not indicative of a clear boundary between the Central Triassic Graben towards the marginal troughs. Furthermore, the transition from the Central Triassic Graben towards the marginal troughs is smoothed. Additionally, the profiles displayed in Figs. 4.11 and 4.12 indicate a important relationship between the depocentres of sedimentation for different stratigraphic units of the Meso-Cenozoic sedimentary cover. The observation indicate that the axial parts of the thickened sediments are not vertically aligned, indicating displacement of the depoceneres of sedimentation in time and in space (see arrow's indications in Figs. 4.11 and 4.12). A similar observation was already discussed for individual lines in the Chapter III; but here, this regularity is described for the entire GG.

Figure 4.11. Cross-sectional views are taken through the 3D structural model of the GG. Regional profiles 1-4 demonstrate the main structural features across strike of the GG (white arrows indicate the depocentres of sedimentation). For stratigraphic key see Figure 1.4.

Profile 5

Profile 6
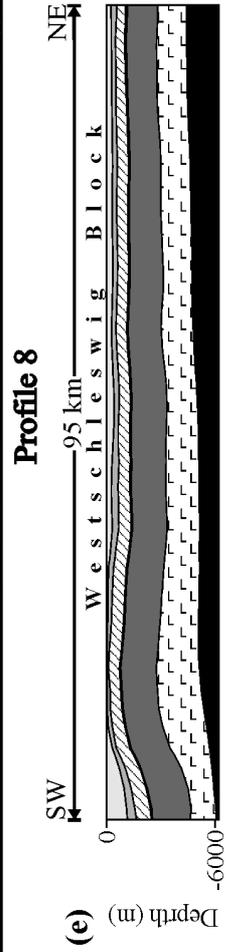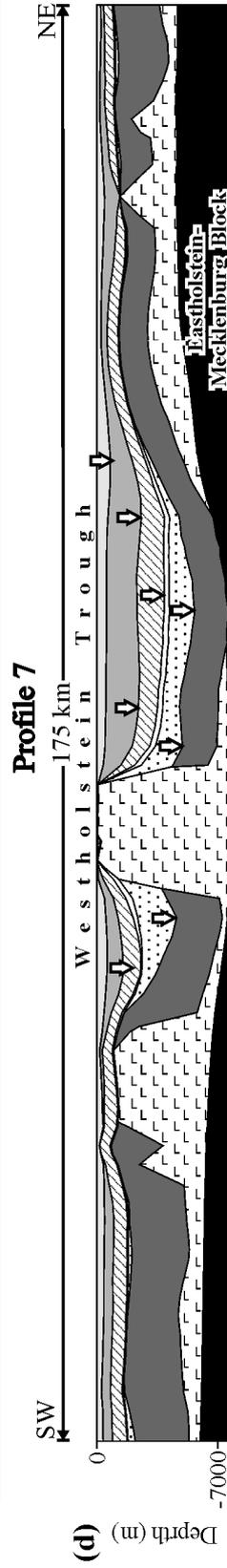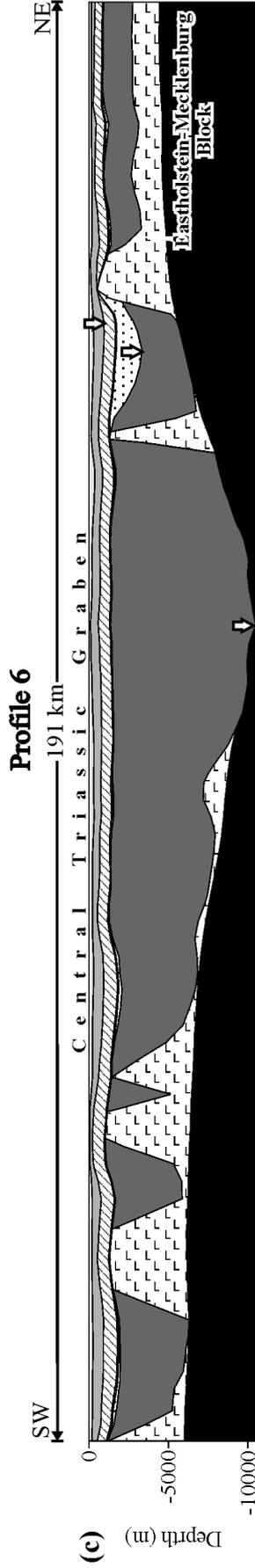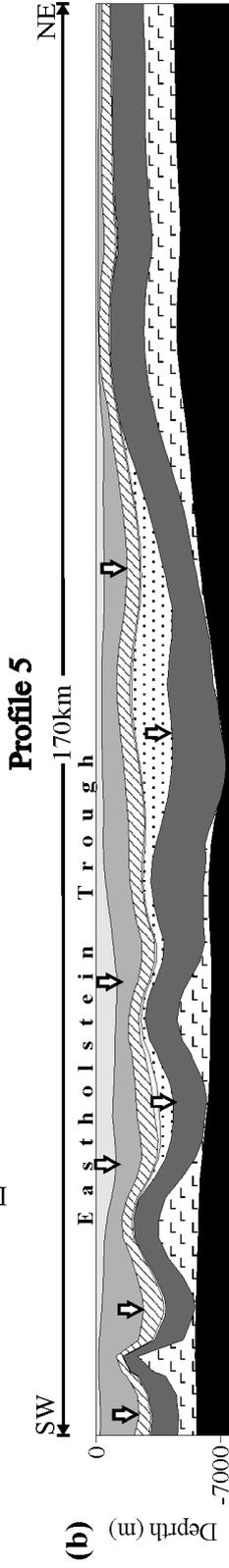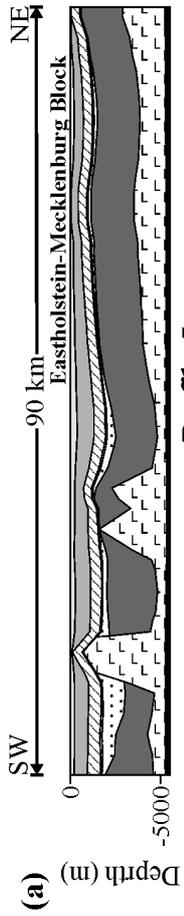
Profile 7

Profile 8

Profile 9

The West-, Eastholstein and Hamburger Trough are separated by thick Triassic (mainly Keuper) within the Central Triassic Graben and prominent thickening towards the axial part of the GG (e.g. Fig. 4.11b). On the other hand, the area of the Central Triassic Graben is characterized by relatively thin Cretaceous and Cainozoic sediments and partly by the absence of the Jurassic. Furthermore, the internal structure of the Westholstein Trough demonstrates that the thick Jurassic is covered by thickened Cretaceous, Paleogene and Neogene but without the vertical alignment of those axial parts (see arrows in Figs. 4.11 b, c and 4.12d). Along profile 6 (Fig. 4.12b), the thick Paleogene of the SW part generally thins to the northeast, where its thinned continuation is covered by thickened Qunternary-Neogene. Zone of Jurassic thickening is observed within the central part of this profile but without thickened younger strata above (Fig. 4.12b). It is possible to conclude, that these profiles document of the subsidence following reactivation of salt tectonics, and suggest that a greater amount of subsidence occurred close to the active salt structures, and may have resulted in gradual depletion of Permian salt from the source layer. Thus, this observation indicates that the source of the long-term subsidence is derived from gradual depletion of the Permian salt, which began within the axial part of the basin and further move away towards the basin flanks.

4.4. Summary

During the Triassic (mainly in the Keuper), rapid subsidence occurred within a central band (Figs. 4.3a, 4.4a, 4.11 and 4.12c) which provides the "core" of the GG. However, already in the Jurassic the subsidence pattern deviates strongly from typical post-rift thermal subsidence. Instead of a typical thermal subsidence, we observe the evolution of two subsidence centres at the former shoulders of the initial Graben (Figs. 4.5, 4.11 and 4.12b, d). These narrow secondary subsidence centres persisted until present, slowly departing outward from the initial subsidence centre, one to the west, the other to the east. Presently, these depocentres are located within the western Westholstein, the southern

Figure 4.12. Longitudinal views are taken through the 3D structural model of the GG. Regional profiles 5-9 demonstrate the main structural features along strike of the GG (white arrows indicate the depocentres of sedimentation). For stratigraphic key see Figure 1.4.

Eastholstein and the Hamburger Troughs (Figs. 4.9, 4.11b-d and 4.12b, d). In contrast, there is no post Triassic accelerated subsidence within the Keuper depocentre besides some minor salt reactivations as most of the salt was already consumed in the Keuper period. The post tectonic subsidence, therefore, does not show the typical thermal subsidence following a stretching event. The Jurassic subsidence and associated reactivation of the salt movements occurred simultaneously with extension in the Lower Saxony Basin and the Pompeckj Block (Kockel, 2002), but were interrupted by the Late Jurassic-Early Cretaceous erosinal event. This truncation is reflected by lack of the Jurassic sediments in some parts of the GG (Fig. 4.5). This development is especially surprising because the adjacent areas were affected by the development of the Lower Saxony Basin during the Late Jurassic (Betz et al., 1987), as well as by stretching events in the North Sea Central Graben (Nielsen et al., 2000), the Central and Western Netherland Basins (Wijhe, 1987) and the Polish Trough (Dadlez et al., 1995; Stephenson et al., 2003). Thus, the Late Jurassic extension mainly occurred along the margins of the CEBS, while its central part (North German Basin) was stable at that time. Since, the area was uplifted and strongly eroded, at the Jurassic-Cretaceous boundary; the remaining Jurassic sediments may represent the areas where sedimentation and salt tectonics were most intensive during that time. This assumption is in agreement with the results from seismic data in Chapter III. The Lower Cretaceous deposits are separated by a regional hiatus from Jurassic succession. The regional sedimentation was renovated in the Hauterivian when the relatively thin Lower Cretaceous covered the entire GG with very slight thickness variations. However, salt tectonics-controlled subsidence is recognized in the Westholstein and Hamburger Troughs. In these sub-basins, the accumulation of comparatively thick Lower Cretaceous seems to be concentrated in the Valanginian and Berriasian (Fig. 4.6). There is no evidences of fault tectonics during the Early Cretaceous in the GG. Thus, this time interval was tectonically quiet, while salt-induced deformation persisted within the Westholstein and Hamburger Troughs where rapid subsidence continued. Tectonic quiescence continued into the Late Cretaceous and deposition of carbonates and marls took place in the GG. In general, the thickness of the Upper Cretaceous does not strongly vary and reflects a regional component of subsidence through the wider region (Figs. 4.7, 4.11 and 4.12). On the other hand, thickened Upper Cretaceous is observed within the Westholstein and Hamburger Troughs just as in the Early Cretaceous. The structural data reveal that this thickening was associated with simultaneous local salt movements (Figs. 4.11b, c and 4.12d). The thickness of the Paleogene implies further

growth of salt structures with the formation of deep synclines near the flanks of the GG. These troughs formed around salt walls (Figs. 5a-d and 9). The Tertiary to recent development coincides with the formation of rifts of similar orientation in Central Europe like the Rhein Graben, Leine Graben, and Eger Graben.
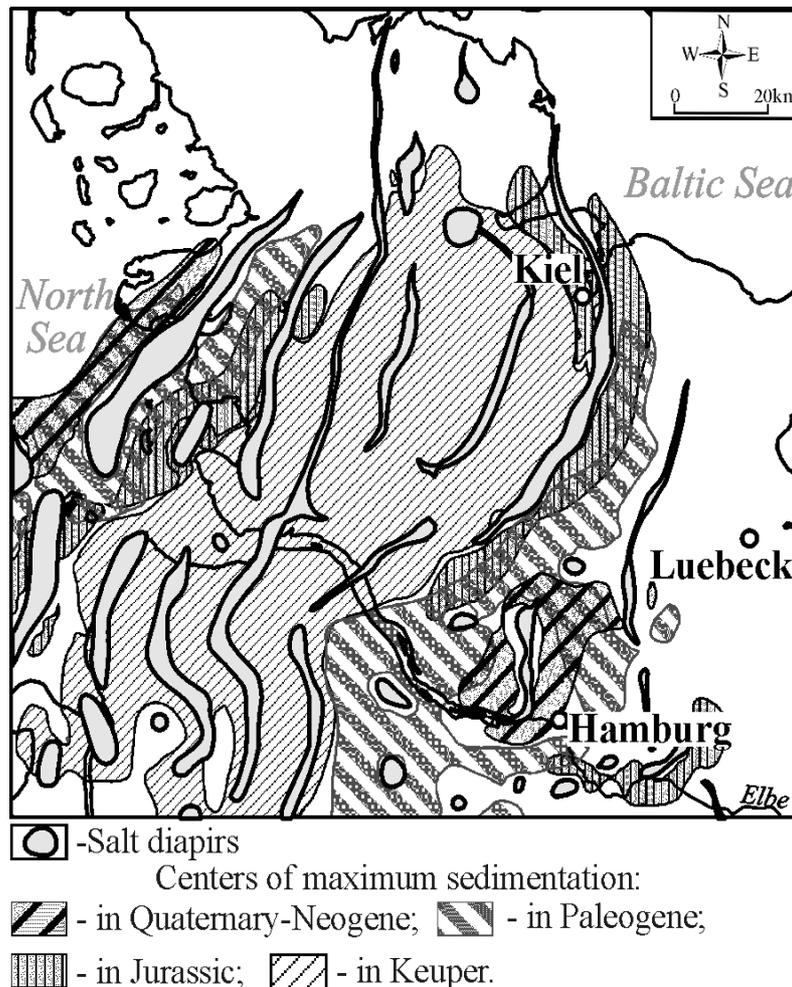
Figure 4.13. Summarized map of maximum sedimentation centres from the Keuper to Neogene-Quaternary within the Glueckstadt Graben.

In summary, it can be stated that the centre of the sedimentation was moving away from the central part of the original Graben structure towards its margins (Fig. 4.13). Starting with the Jurassic, the subsidence-centre was partitioned into two parts located adjacent to the Central Triassic Graben (Figs. 4.4, 4.11b, c and 4.12b, d). Later, the two centres of

- 71 -

sedimentation moved gradually towards the flanks of the Central Triassic Graben during Cretaceous and Paleogene (Figs. 4.5-4.9 and 4.11b, d). Such a pattern was already observed by Sannemann (1968, 1983) who called it "salt-stock families", meaning that salt stocks spread in time becoming gradually younger away from the axial part of the graben. Indeed, the data point to salt mobility as controlling factor for the post-Permian evolution, which was triggered by the initial removal of salt along the axis of the Keuper subsidence centre. In this sense, the Glueckstadt Graben was formed at least partially as a "basin-scale rim syncline" during post-Permian times. However, as indicated by the Tertiary acceleration of subsidence, large-scale changes in the stress field may have interacted with the local evolution. Within the Tertiary and Quaternary sequences, the general subsidence pattern remains stable, although, the total amount of subsidence increases in the Paleogene as well as in the Quaternary-Neogene (Figs. 4.8, 4.9 and 4.11). The Tertiary acceleration of subsidence in the GG coincided more or less with the development of a major subsidence centre in the North Sea during the Miocene-Oligocene (Kockel, 2002, 1988, Garetsky et al., 2001), which may have been active until today. Thus, the present-day Hamburger, East- and Westholstein Troughs are the actual state of the long term salt tectonics which still may continue and may play a role in terms of young processes and e.g. for costal protection within NW Germany.

Chapter V

3D MODELLING

5.1. Introduction

Many analogue and numerical models have been constructed in order to investigate the salt behaviour under different tectonic settings and load conditions. The modelling approaches of salt movements focussed on different aspects of salt tectonics. This includes a combination of two major effects on salt flow by: (1) fault tectonics at the base of the salt and/or overburden as a triggering mechanism; and (2) changing load distributions in time and space. The results of analogue experiments and numerical simulations demonstrate that the viscous salt is very responsive to variable sediment loading and fault tectonics (e.g. Woidt, 1978; Schmeling, 1987; Roemer and Neugebauer, 1991; Vendeville and Jackson, 1992; Koyi et al., 1993; Poliakov et al., 1993; Daudre, B., Cloetingh, S., 1994; Koyi, 1998; Kaus and Podladchikov, 2001). Most of these experiments were performed in terms of two-dimensional studies. However, three-dimensional modelling has to be used to investigate salt flow phenomena. Recently, only a few physical models have been implemented in full 3D (e.g. Guglielmo et al., 1999; Scheck et al. 2003; Ismail-Zadeh et al.; 2004). The advancement from the 2D to 3D modelling was illustrated by Guglielmo et al. (1999) who visualized the results of 2D analogue modelling into a 3D digital model, demonstrating changes of sedimentation, deformation, and underlying salt thickness through time. A full 3D numerical approach was applied by Scheck et al. (2003) for the NE German Basin, considering salt flow as a consequence of spatially changing overburden, isostatic response and sediment compaction. Ismail-Zadeh et al. (2004) investigated the evolution of salt structures both forward and backwards in time by means of 3D numerical finite-element models.

This chapter presents the results of three-dimensional modelling within the GG by using a software developed at the GeoForschungsZentrum Potsdam by Ulf Bayer, Magdalena Scheck-Wenderoth and Björn Lewerenz. The 3D reverse modelling approach has been used to determine salt distribution for selected stratigraphic levels in response to unloading due to sequential removing of the stratigraphic layers. In addition, 3D forward modelling has been applied to calculate the initial Permian salt thickness within the area covered by the 3D model. Salt flow has been determined by using a finite-element method,

- 73 -

depending mainly on the sedimentary load and the shape of the isostatically-balanced crust. Finite-element methods are ideal for problems with a complex geometry, which predominates among the salt structures. A basic assumption in this approach is that the behaviour of salt is similar to a viscous fluid that is usually in hydrostatic equilibrium with the overburden and that its volume is conserved. It is also assumed that all new load conditions generated by salt redistribution are isostatically compensated at the crustal level.

5.2. Analytical and numerical approaches

The 3D numerical modelling work presented here is based on some numerical approaches, which have been described in details by Scheck (1997), Scheck and Bayer (1999) and Scheck et al. (2003). Here, the conceptual definition of the salt redistribution is only elucidated.
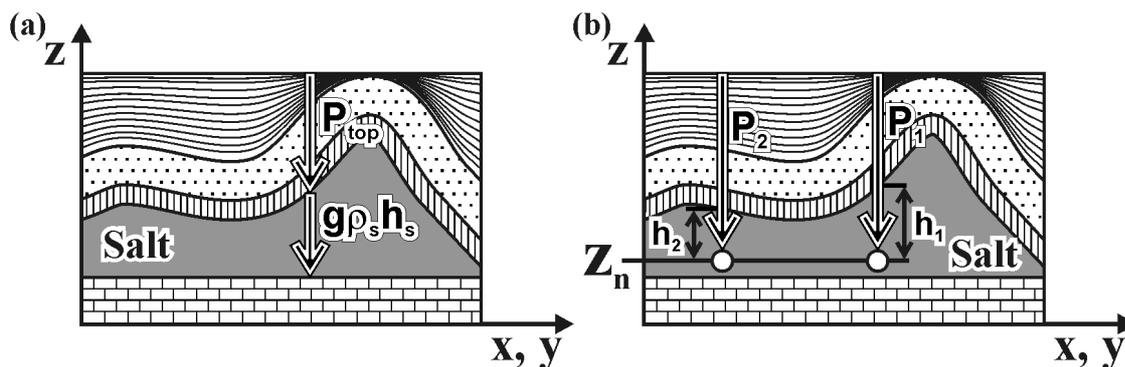
Figure 5.1. Schematic illustration of the pressure distribution in the viscous salt layer under isostatic balance (slightly modified after Scheck et al., 2003). (a) The pressure at the salt base is the sum of the load acting on the salt surface (P_{top}) and the load of the salt column ($g\rho_s h_s$). (b) The pressure difference between two points in the salt layer equals zero at the same depth (Z_n).

The model contains algorithms to simulate the changes of the salt thickness due to loading or unloading. Changes of salt thickness are calculated in response to these processes. Figs. 5.1 and 5.2 illustrate some of the parameters included in the model calculations. A typical starting condition for the modelling is shown in Fig. 5.1, demonstrating a schematic load pressure distribution in the viscous salt layer under isostatic balance. The modelled salt

layer is isostatically conditioned with an equilibrated pressure at the base of the salt P. P is the sum of the overburden load (P_{top}) and the load of the salt column $(g\rho_s h_s)$ (Fig. 5.1a).

$$P = P_{top} + g\rho_s h_s, \tag{1}$$

where g is the gravitational acceleration, ρ_s is the salt density and h_S is the salt thickness at a predefined time.
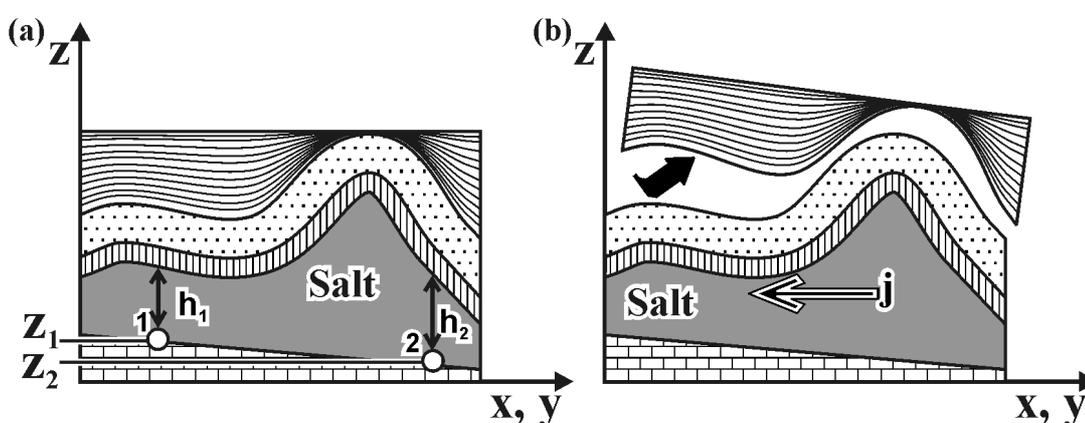
Figure 5.2. (a) Pressure balancing above the variable base topography of the salt layer. Calculation is performed by taking into account the pressure balancing for the interval between two points Z_1 and Z_2 as a reference depth. (b) Salt redistribution under new load conditions due to removing layer from top. Salt flow is characterized by the formal flux j which operates as a flow of salt towards areas of load deficit (modified after Scheck et al., 2003).

The pressure difference ΔP between two points 1 and 2 at the same depth z_n (Fig. 5.1b) can be derived according to follow equation:

$$\Delta P_{[1,2]} = P_1 - P_2 + g\rho_s(h_1 - h_2) \tag{2}$$

- 75 -

This pressure difference ΔP equals zero under hydrostatic equilibrium. In case of variable base topography of the salt layer (Fig. 5.2a), Eq. (2) becomes:

$$\Delta P_{[1,2]} = 0 = P_1 - P_2 + g\rho_s(h_1 - h_2) - g\rho_s(z_1 - z_2), \qquad (3)$$

where $g\rho_s(z_1 - z_2)$ is the pressure difference between two points z_1 and z_2 due to their absolute difference in depth, representing the reference depth $(z_1 - z_2)$, which has to be taken into account during isostatic balance calculation.

When overburden is unloaded or loaded, the system becomes hydrostatically unbalanced and $\Delta P_{[1,2]} = 0$ is not satisfied. The formal flux of salt (j) is introduced (Fig. 5.2b) in order to reestablish the hydrostatical equilibrium of the system by salt redistribution in response to the new load conditions:

$$j = \Delta(P_{top}(t) + g\rho_s h_s(t) - g\rho_s Z_{base}), \qquad (4)$$

where $Z_{base} = z_i - z_{i+1}$. The system becomes again hydrostatically balanced when the flux of salt equals zero ($j=0$).

5.3. Results of 3D reverse modelling

5.3.1. Modelling concept

Salt flow can cause local or regional thickening and thinning of sediments, which represent the most prominent manifestation of salt movements in salt-containing sedimentary basins. In other words, the tectonically induced thinning (depletion) of the salt layer generates an additional accommodation space for sedimentation. On the other hand, thickening of the salt layer (formation of salt structures) generates increased surface topography, causing a shortage of sedimentation space. In contrast, the 3D reverse modelling represents an inverse process when thinning and thickening of the salt layer occur due to unloading of the model by removing of layers (Fig. 5.3).
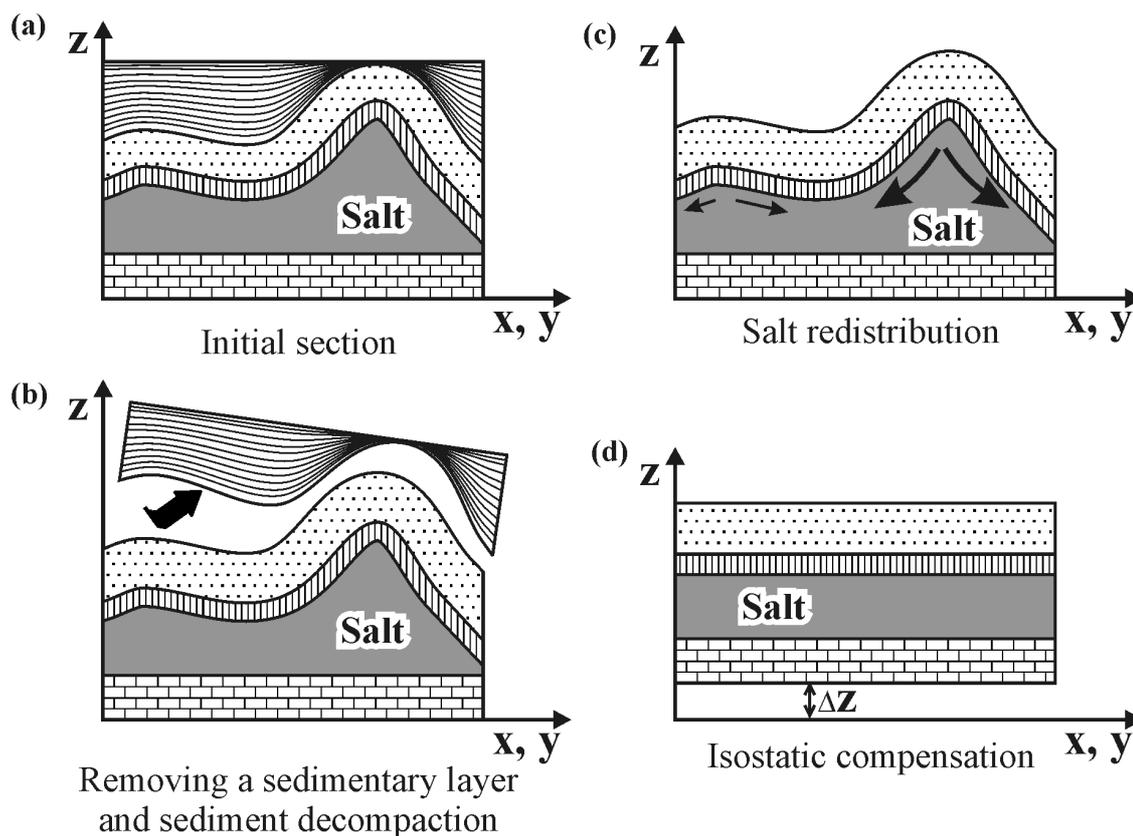
Figure 5.3. Schematic diagram showing steps of the reverse modelling from the initial state to the selected stratigraphic level (modified after Scheck et al., 2003).

A 3D reverse modelling of the development of salt structures consists of a number of steps which are illustrated by the schematic two-dimensional diagram in Fig. 5.3. The section in Fig. 5.3a corresponds to the present state of the model. The first step is to remove the sediments above the selected stratigraphic level (Fig. 5.3b). Sediment decompaction is the next culculated. An exponential decrease in porosity under loading for each lithology is used for decompaction according to decompaction parameters which are given in Table 5.1. Subsequently, the new distribution of the salt is calculated under reduced sediment load of the remained layers above the salt (Fig. 5.3c). Finally, an isostatic equilibrium of the model is recalculated according to the new mass distribution. The new mass distribution includes both the unloading of the model due to removing of sediments, and loading/unloading by the new thickness of salt (Fig. 5.3d). The described sequence of the modelling procedures was applied to every step of backstripping, which has been used to reconstruct a reasonable geometry of salt structures from present day to the end of the Triassic.

Stratigraphic layer	Matrix density ρ_m (kg/m³)	Initial porosity Φ_o (%)	Compaction depth constant c (1/km)
Quaternary-Neogene	2690	58	0,43
Paleogene	2710	65	0,57
Upper Cretaceous	2700	67	0,68
Lower Cretaceous	2715	65	0,59
Jurassic	2690	58	0,33
Triassic	2684	53	0,47
Permian salt	2300	0	0,00
Pre-Permian crust	2850	0	0,00
Mantle	3300	0	0,00

Porosity Φ is assumed to decrease under loading according to $\Phi = \Phi_{min} + (\Phi_o - \Phi_{min})e^{-\beta P}$, where Φ_{min} is the minimum porosity at the maximum depth (assumed to be 0 for all layers), Φ_o is the porosity on the surface (initial porosity), P is the effective load, and β is given as $\beta = c/g\rho_r$, where c is compaction depth constant, g is the gravitational acceleration and ρ_r is the matrix density.

Tabl. 5.1. Decompaction parameters of rocks for the different layers of the 3D model within the GG. These parameters were calculated according to lithological composition of rocks, which is shown in Fig. 1.5.

5.3.2. Reconstruction of the initial distribution of sediments

Modelling difficulties arise when input data contain layers, which were affected by postdepositional changes. Such changes occur as a result of several geological processes. One process is erosion due to salt tectonics, regional uplift or sea level fall. Simple removing of the upper layers above partially eroded stratigraphic interval does not produce proper load conditions, which existed before erosion. Therefore, salt redistribution will not provide a correct geometry for this stratigraphic interval. Scheck et al. (2003) solved this problem by

reestablishment of initial sediments distribution. The concept for a particular case is illustrated in Fig. 5.4 where two sedimentary layers are pierced by a salt diapir after deposition. At first, all pierced layers have to be removed before salt redistribution (Fig. 5.4b). The next step is the reestablishment of the restored distribution of sediments into the model in order to obtain a correct load distribution above the salt diapir (Fig. 5.4c). Only after that step, salt can be correctly redistributed.

(a) Initial section

(b) Removing all sedimentary layers up to top of salt

(c) (1) Restoration of the sediment distribution prior to piercing by salt; and (2) salt redistribution
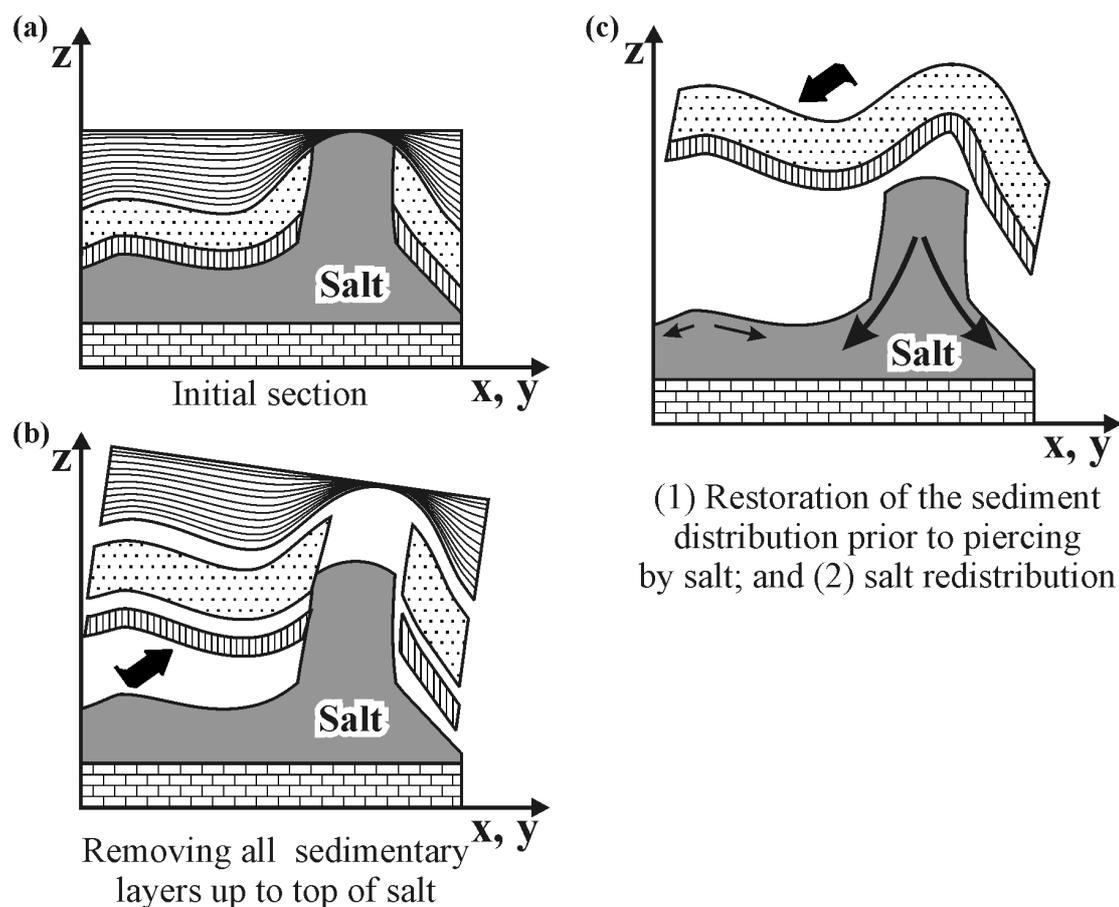
Figure 5.4. The schematic diagram shows a reconstruction of the sediment thickness prior to postdepositional erosion, allowing salt redistribution from the salt structure at the selected stratigraphic level (modified after Scheck et al., 2003).

Local postdepositional erosion of the sediments in the GG occurred during the main phases of salt tectonics which took place in the Triassic, Jurassic and during Tertiary. In addition, the area under consideration was affected by regional Late Jurassic-Early

Cretaceous erosion. Therefore, part of sediments is missing due to erosion and has to be re-established prior to salt redistribution for selected time steps. In order to solve this problem, the reconstructed sediment distributions were introduced as additional input data in terms of thickness maps. The reconstruction of the primary isochore maps was mainly based on the interpretation of seismic lines and published structural data from the GG (Baldschuhn et al., 1996; Baldschuhn et al., 2001; Kockel, 2003). The primary sediment distributions have been re-established for selected intervals, such as Triassic, Jurassic, Lower Cretaceous, Upper Cretaceous and Paleogene.

5.3.2.1. Triassic
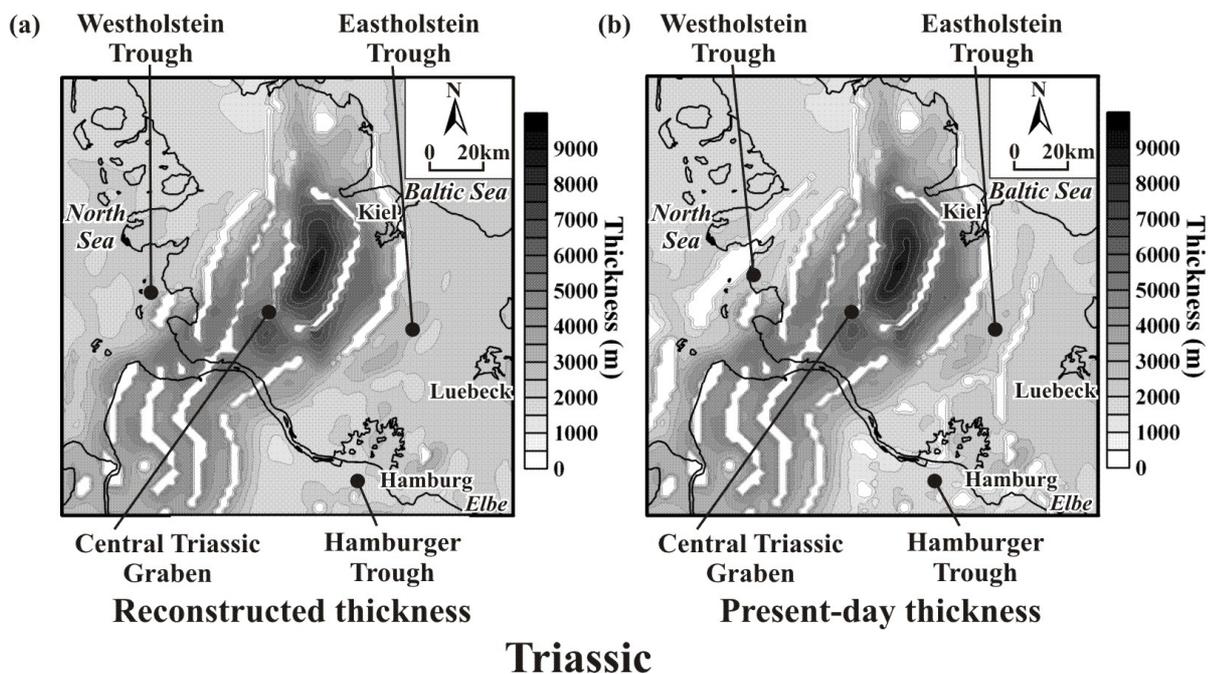
Figure 5.5. Thickness maps of the Triassic: (a) reconstructed to the end of the Triassic; and (b) present-day.

The reconstructed and present-day thickness maps of the Triassic are shown in Fig. 5.5. It is inferred from wells and seismic data that Triassic sediments were affected by Late Jurassic-Early Cretaceous regional erosion (e.g. Fig. 3.13b). The effect of the Late Jurassic-Early Cretaceous erosion was not strong because Triassic sediments were covered by

Jurassic prior to truncation. During this erosion, Triassic deposits were mainly eroded in the crests of salt structures where sediments were elevated higher than elsewhere by salt flow (e.g. Figs. 3.3a, 3.13b). In addition, post Triassic salt movements pierced Triassic sediments within the West-, Eastholstein and Hamburger Troughs. The effects of the postdepositional piercing and the Late Jurassic-Early Cretaceous erosion were taken into account for the reconstruction of the initial distribution of the Triassic sediments. In order to produce a reconstructed thickness map (5.5a), the present-day thickness map of the Triassic (Fig. 5.5b) has been corrected by re-interpolation of the areas where Triassic deposits are pierced and/or eroded. The greatest difference between the present-day and the reconstructed maps is visible within the marginal troughs. On the reconstructed map, the distribution of the Triassic sediments within the West-, Eastholstein and Hamburger Troughs has been re-established at the pre Jurassic state. Therefore, the position of the post Triassic salt structures is not shown as it is seen in Fig. 5.5b. On the other hand, salt walls and diapirs are still recognizable within the central part of the basin because their development occurred simultaneously with Triassic sedimentation. This is supported by seismic and borehole data which indicate that the Permian salt was extruded and even redeposited during latest Middle-Late Triassic (Keuper) time (see Chapter III). It is important to note, that the effect of post Triassic movements of the Keuper salt was not taken into account during the reestablishment of the initial distribution of sediments. In other words, Keuper salt movements have not been considered for the reason that it is impossible to separate the Keuper salt from the Permian salt within the salt structures. Therefore, the restoration of the initial thickness distribution of the Keuper salt has been neglected in the modelling process.

5.3.2.2. Jurassic

The restoration of Jurassic sediments prior to Late Jurassic-Early Cretaceous erosion is a more problematic task than the reestablishment of the Triassic thickness map. Figure 5.6 demonstrates the reconstructed and present-day thickness maps of the Jurassic. In the some parts of the GG, the entire Jurassic and lowermost Cretaceous sequences are missing (Fig. 5.6b). From the seismice data, it is not possible to decide whether the unconformity is erosive or non-depositional within the areas where sediments are lacking. Furthermore, many questions remain unresolved concerning the origin of the marginal troughs (Hamburger, West- and Eastholstein) where up to 1900-2400 m of Jurassic sediments were

- 81 -

accumulated (Fig. 5.6). Sanemann (1968) postulated that the formation of the marginal Jurassic rim-synclines occurred as a consequence of the Keuper extension by subsequent wave-front-like growth of salt stocks in post-Triassic times. In other words, the salt-induced deformation persisted in the Jurassic when rapid subsidence continued mainly around the former Triassic salt structures by gravity driven flow. This concept is not strictly consistent with the onlap patterns of the Jurassic sediments at the top of the Keuper succession (see Figs. 3.5, 3.8 and 3.10) indicating essential changes of the sedimentation style during the Jurassic. Kockel (2002) has documented the Early Jurassic extension and related normal faulting affecting the entire sedimentary succession within the Lower Saxony Basin and the Pompeckj Block. Although, there is no direct evidence of normal faults in the Jurassic of the
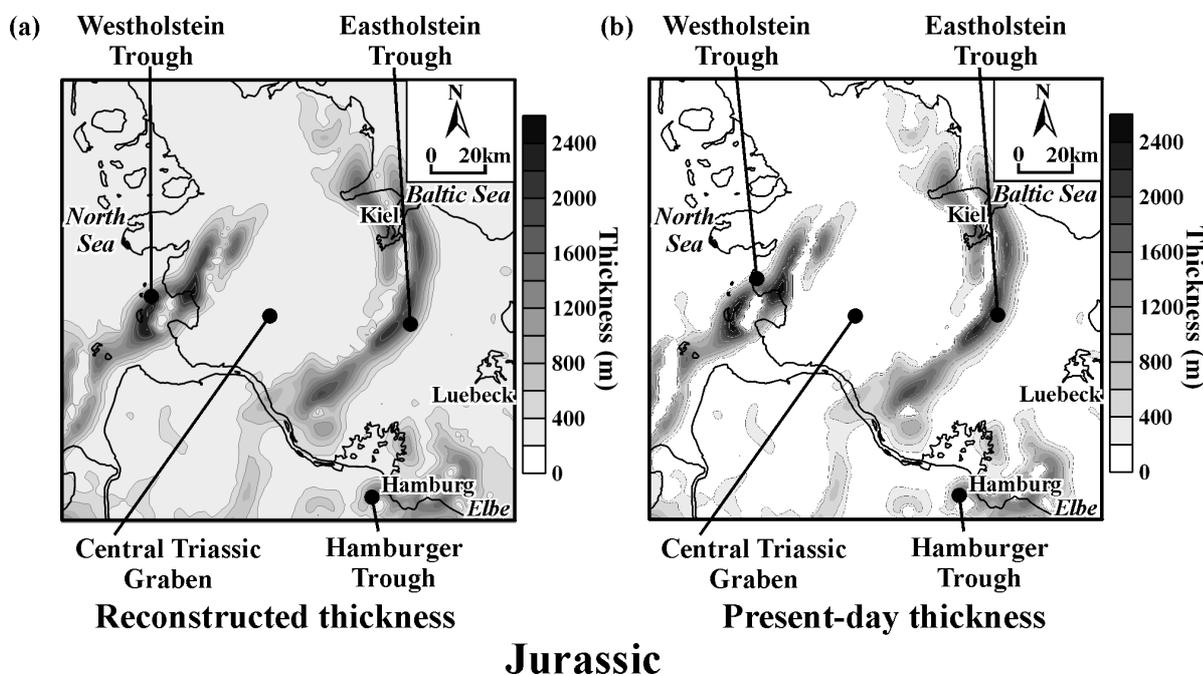
Figure 5.6. Thickness maps of the Jurassic: (a) reconstructed prior to the Late Jurassic-Early Cretaceous erosion; and (b) present-day.

GG, one of them can be inferred from structural features of the Jurassic strata in the Figure 3.8. Therefore, the Jurassic tectonic event documented in the Lower Saxony Basin and within the Pompeckj Block (Kockel, 2002) may have also affected the GG. However, post-Keuper salt tectonics occurred mainly along the north-western and the south-eastern margins of the GG (Figs. 1.4b and 3.2) where Permian salt was not depleted during the

Triassic. Thick Jurassic sediments are only observed around salt structures and are thinning away from salt walls or salt stocks (Figs. 3.2, 3.6, 3.9, 3.10, 3.13). Possibly, essential parts of the Jurassic might be missing due to erosional truncation in the Late Jurassic-Early Cretaceous. However, the Keuper strata were eroded mainly in the vicinity of salt structures (Figs. 3.3 and 3.9) or are transgressivlly covered by Lower Cretaceous sediments (for example see Fig. 3.3 and the NW part of the line 10 in the Fig. 3.10). The low degree of erosion of the Keuper (only up to the first hundred meters), the presence of truncated toplaps within the Jurassic strata (Figs. 3.5 and 3.9), and the absence of visible unconformities within the NW flank of the basin (Fig. 3.3), suggest a low degree of erosion rather than a strong uplift during Late Jurassic-Early Cretaceous times. In order to produce a reconstructed thickness map of the Jurassic (Fig. 5.6a), a constant value of 250 m was added to present-day thickness map. The constant value of 250 m was chosen in order to cover the entire region by sediments rather than to provide the true amount of the eroded sediments. This was done because the pattern of sediment distribution prior to erosion and postdepositional changes are unknown in detail. However, it is possible to suggest that the present-day thinning of the Jurassic sequence could reflect the proximal depositional limit with little Late Jurassic-Early Cretaceous erosion near rising salt structures. Thus, the erosional features did not extensively modify the ratio of thickness distribution of the depositional sequences in the Jurassic. Furthermore, the present-day remains of thick Jurassic still represents the areas of intensive subsidence, which was strongly controlled by withdrawal of the Permian salt from the source layer. Consequently, the reconstructed map in Fig. 5.6a can be taken as a qualitative approximation of the sediment distribution prior to erosion. On the other hand, it is obvious that the quantitative characteristic of the reconstructed thickness is poorly estimated due to an uncertainty of spatial and temporal changes in Late Jurassic-Early Cretaceous erosion rates and volumes.

5.3.2.3. Lower Cretaceous

The distribution of Lower Cretaceous deposits was only affected by post Cretaceous development of some salt structures, which pierced the sedimentary cover during the Tertiary. Therefore, the reestablishment of the Lower Cretaceous thickness map (Fig. 5.7a) was done by filling those areas, which have been pierced by post Cretaceous salt walls and diapirs (Fig. 5.7a). Consequently, the difference between reconstructed (Fig. 5.7a) and

present-day thickness maps (Fig. 5.7b) of the Lower Cretaceous is only the absence of pierced areas on the re-established sediments distribution.
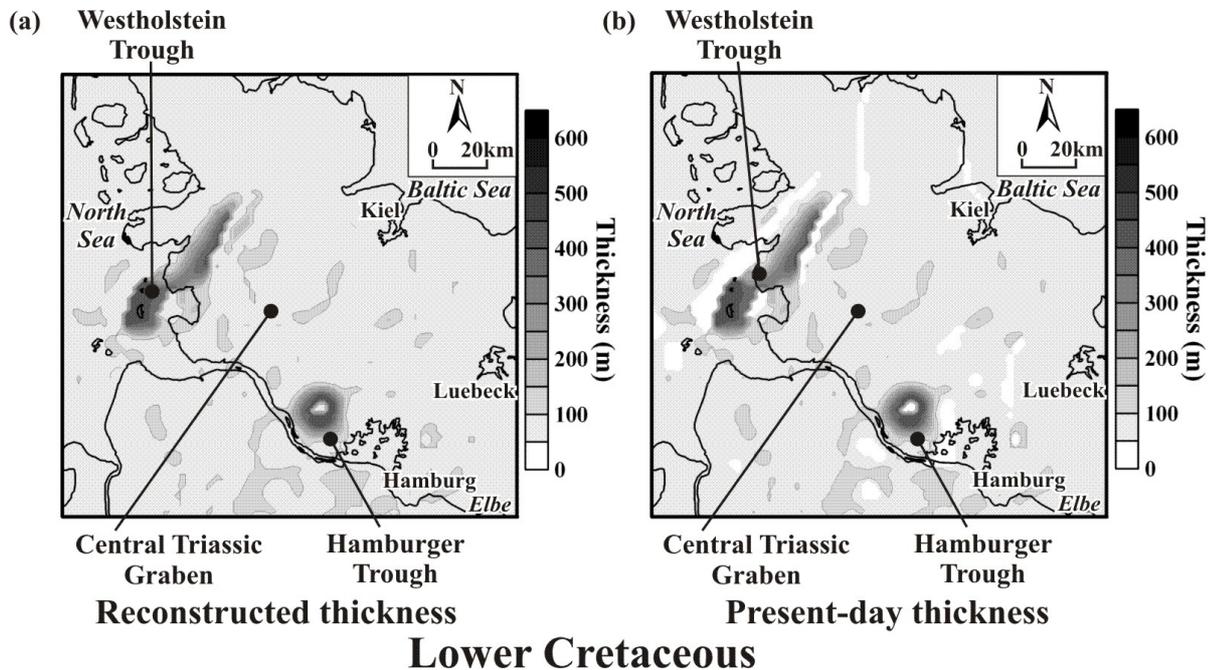
Figure 5.7. Thickness maps of the Lower Cretaceous: (a) reconstructed to the end of the Early Cretaceous; and (b) present-day.

5.3.2.4. Upper Cretaceous

The reconstructed and present-day thickness maps of the Upper Cretaceous are shown in Fig. 5.8. It was inferred from seismic data that the deposition of the Upper Cretaceous took place under tectonically quiescent conditions (see Chapter III). There are no indications of strong salt movements during the Late Cretaceous in the area under consideration. Therefore, the presence of holes due to piercing by salt walls and diapirs is a result of post Cretaceous salt movements. Like for the Lower Cretaceous, pierced regions were removed from the present-day thickness map (Fig. 5.8b) by reinterpolation of those areas which correspond to the present-day position of post Cretaceous salt walls and diapirs. In addition, Upper Cretaceous sediments were deformed, uplifted and partially eroded within the crest of some salt structures during postdepositional times (e.g. Figs. 3.2, 3.7-3.10). These features are easily seen on the present-day thickness map (Fig. 5.8b) due to the

presence of locally decreased thickness of the Upper Cretaceous. These areas were
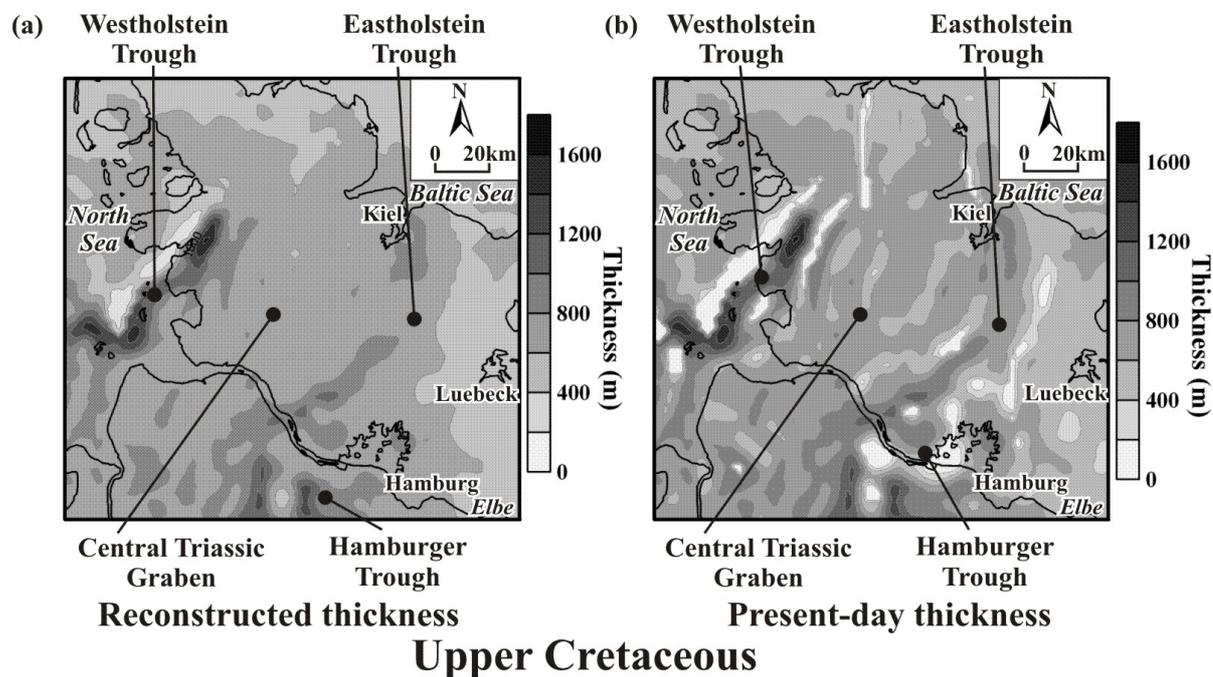
Figure 5.8. Thickness maps of the Upper Cretaceous: (a) reconstructed to the end of the Late Cretaceous; and (b) present-day.

reinterpolated in order to remove the effect of the salt induced postdepositional erosion above the salt structures. On the reconstructed map (Fig. 3.8a), the distribution pattern of the Upper Cretaceous is characterized by almost constant thickness with exception of two areas within the Westholstein and Hamburger Troughs (Fig. 5.8a). These two areas of the decreased thickness correspond to two salt structures, which were active during the Late Cretaceous. There, the structural features indicate that the deposition of the thick Upper Cretaceous took place simultaneously with salt movements within relatively shallow rim synclines (see Chapter IV for details). Therefore, the formation of the Upper Cretaceous rim synclines requires partly decreased thicknesses in the limit of the simultaneously growing salt structures.

- 85 -

5.3.2.5. Paleogene

It is inferred from seismic data (Chapter III) and published structural data (Baldschuhn et al., 1996; Baldschuhn et al., 2001; Kockel, 2003) that the deposition of the Paleogene was accompanied by simultaneous development of salt structures. Some salt structures pierced the sedimentary cover at that time within the West-, Eastholsein and Hamburger Troughs. The effect of syndepositional growth of salt structures is visible by the presence of locally increased thickness around salt structures (Fig. 5.9b). In addition, Neogene growth of salt structures caused partial erosion of the Paleogene sediments within the crest of the salt anticlines and walls. During the reconstruction of the Paleogene thickness, the main attempt focussed at the reestablishment the Paleogene thickness within the crest of salt structures prior to Neogene. The result of the reconstruction of the Paleogene sediment distribution is shown in Fig. 5.9a. The thinning of the Paleogene in the crests of salt structures is smoothed on the reconstructed thickness map (Fig. 5.9a) in comparison to the present-day thickness map (Fig. 5.9b).
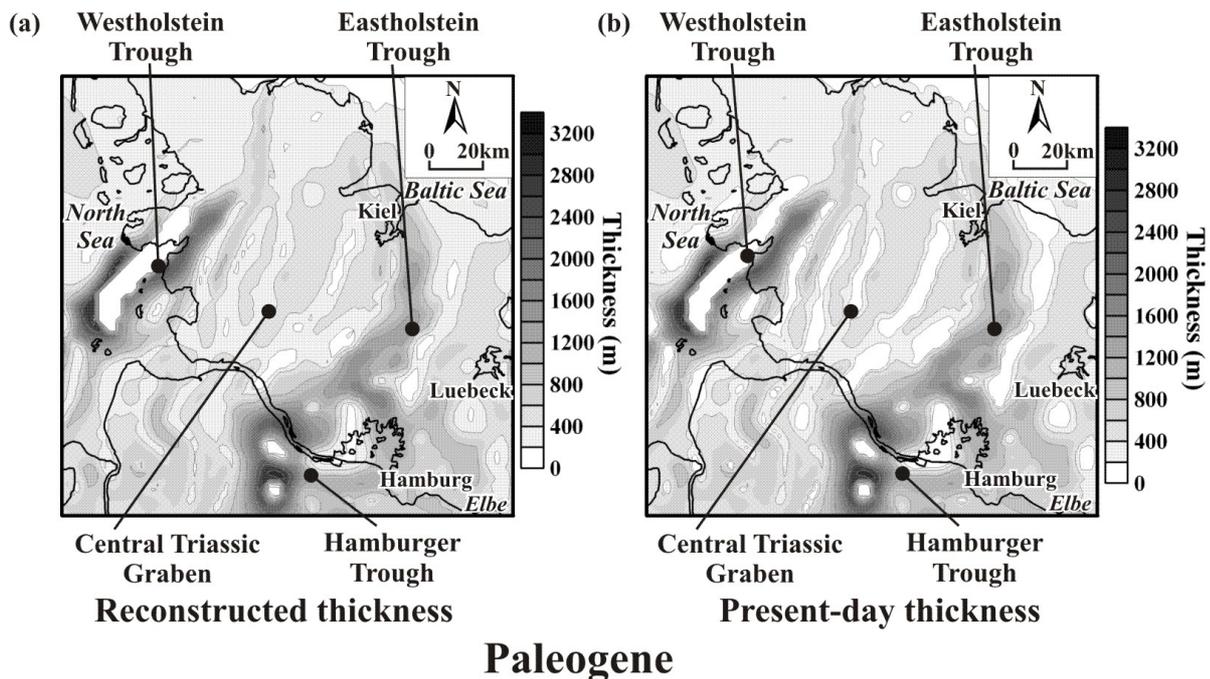

Figure 5.9. Thickness maps of the Paleogene: (a) reconstructed to the end of the Paleogene; and (b) present-day.

5.3.3. Results of the modelling

The results of reverse modeling are shown in Figs. 5.10 and 5.11 (see enlardged versions in Appendix B). 3D views of the top of the Permian salt at the different stratigraphic levels are plotted in Fig. 5.10, in order to allow easier visual perception of changes in geometry of salt structures through time. The obtained results show substantial change of the salt structure distribution from the end of theTriassic (Fig. 5.10f) to present-day (Fig. 5.10a). The results support the conclusion that initial salt movements took place during Middle-Late Triassic within the central part of the GG (Fig. 5.10f). Fig. 5.10f also indicates the development of mainly shallow salt anticlines within the marginal troughs in the Triassic. Following its initiation, strong salt tectonics occurred at the margins of the former Triassic Graben in the Jurassic (Fig. 5.10e). During the Cretaceous-Tertiary, the salt structures were affected by additional growth mainly within the marginal troughs (Figs. 5.10a-d). The evolution of salt structures can be explained in more details by changes of salt thickness, as derived during the reverse modelling. Fig. 5.11 illustrates the modelled thickness of Permian salt for the present-day state and for different stages of backstripping. One of the most remarkable results of the 3D structural model is related to the expansion of the depletion zone or reduced thickness of the Permian salt, which is shown by white colour in Fig. 5.11. It is clearly seen that the Permian salt layer was almost depleted within the central part of the basin in the Triassic (Fig. 5.11f). A small area of the reduced thickness of the salt is also seen west of Hamburg (Fig. 5.11f), indicating Triassic salt movements within the Hamburger Trough. The marginal troughs (West-, Eastholstein and Hamburger) are characterized by locally increased salt thickness, which can be related to salt anticlines. During the Jurassic, the reduction of the salt layer extended onto the SW and NE margins of the Central Triassic Graben (Fig. 5.11e). The zone of reduced thickness within the Hamburger Trough became wider in comparison to Triassic times (cf. Figs. 5.11f and 5.11e). The difference between the salt distribution in the Jurassic (Fig. 5.11e) and in the Cretaceous (Figs. 5.11c, d) is smoothed or even not visible in most parts of the basin, proving low salt activity in the Cretaceous, which was already inferred from the interpretation of seismic lines in Chapter III. Only some inessential reductions of the salt thickness are recognizable within the Westholstein and Hamburger Troughs in addition to those, which are observed in the Jurassic. The next stage of the strong broadening of the area of highly reduced salt thickness

- 87 -
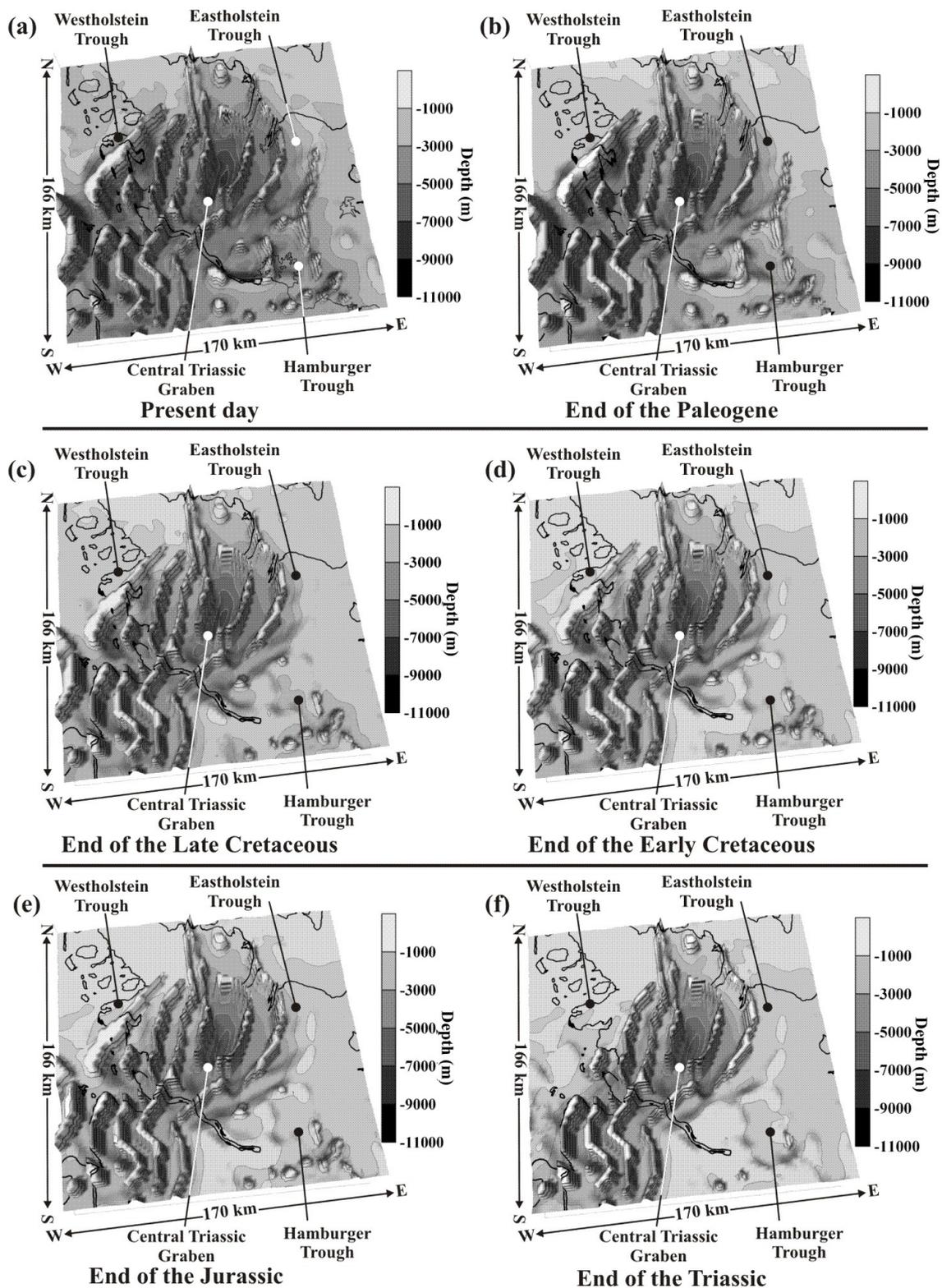
Figure 5.10. 3D views on the top of the Permian salt at the different stratigraphic levels as result of reverse modelling. Evolution of salt structures is shown from the end of the Triassic (f) to present-day (a).
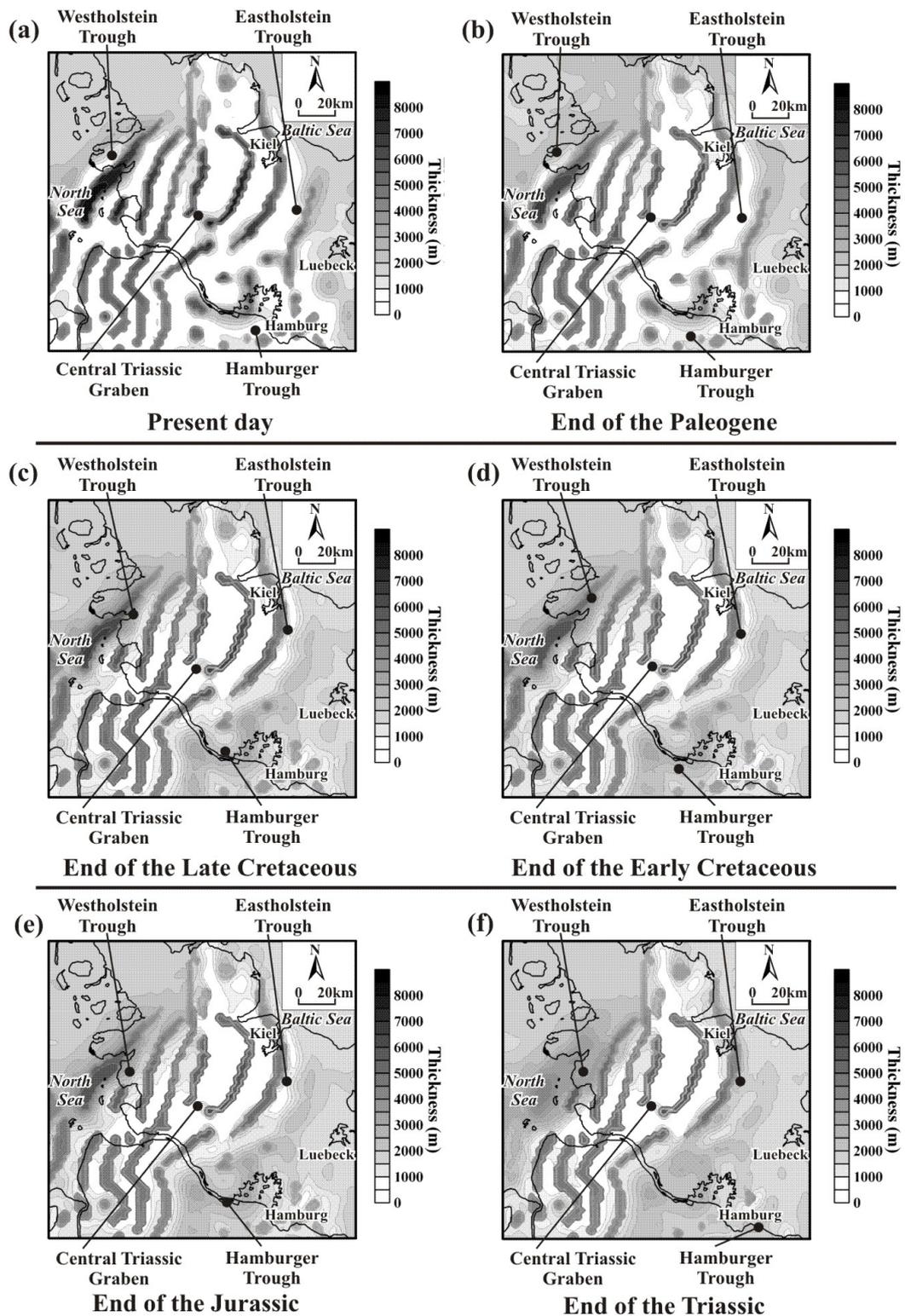
Figure 5.11. Isochore maps of the Permian salt representing thickness distribution of the salt from the end of the Triassic (f) to present-day (a) based on reverse modelling. Gradual movements of the depletion zone of Permian salt from the central part of the original Central Triassic Graben (f) towards its margins (a) is shown by white colour.

is shown in Fig. 5.11b. The map of salt thickness at the end of the Paleogene demonstrates that the depletion of the Permian salt layer occurred mainly within the marginal troughs. During the Paleogene, the thickness of the salt was strongly reduced within the West- and Eastholstein Troughs. On the other hand, depletion of the salt layer within the Hamburger Trough was stronger on the western and eastern parts of this trough than in the central part (Fig. 5.11b). Fig. 5.11a demonstrates further expansion of the salt depletion zone towards the basin flanks during the Quaternary-Neogene.

The 3D geometries of the reconstructed salt structures in Fig. 5.10 are reflected in the reduction of the salt thickness (Fig. 5.11) from the end of the Triassic to the present-day. In other words, the 3D reverse modelling provides evidence for depletion of the Permian salt layer from the central part of the basin towards the basin flanks. Reverse modelling is in agreement with the predicted development of salt structures, which was inferred from seismic lines and present-day sediments distribution in the GG (see Chapters III and IV).

According to the results of the 3D reverse structural modelling, the formation of the deep Central Triassic Graben and the subsequent Jurassic-Cenozoic marginal troughs was partially controlled by gradual depletion of the Permian salt layer through time.

5.4. Results of 3D forward modelling

The modelling approach aims to reconstruct the original Permian salt distribution immediately after deposition. The concept of the 3D forward modelling is illustrated by a 2D schematic diagram in Fig. 5.12. Fig. 5.12a represent the present state of the model. The reconstruction of the initial thickness of salt was carried out in the following sequence. The first step is backstripping of the Meso-Cenozoic sediments and the Permian salt (Fig. 5.12b). After that, the isostatic response of the salt base without sediment infill was calculated (Fig. 5.12c). The restoration of the Permian salt layer above the backstripped and isostatically balanced base of salt is the third step of modelling (Fig. 5.12d). The reconstruction of the initial salt thickness takes into account that the Permian salt partially extruded during the Keuper and was redeposited due to superficial dissolution. The quantity of Permian salt redeposited during the Keuper can be approximately derived from lithostratigraphic and
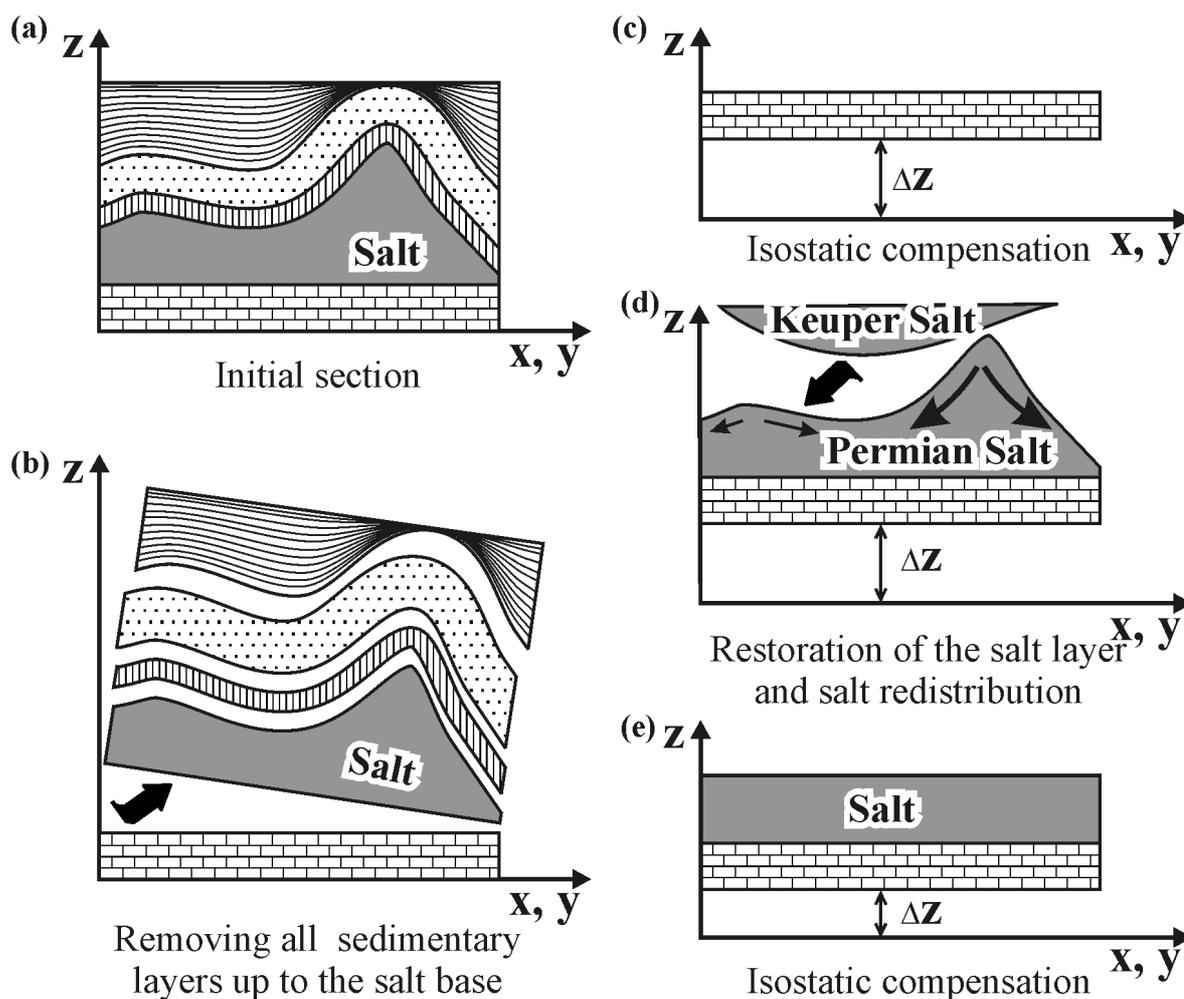
Figure 5.12. Schematic diagram showing different steps of the forward modelling.

structural features of the Keuper succession, which are described in details in Chapters II and III. The amount of salt in the Keuper has been estimated as twenty percentages of the thickest part of the section which occupies the central part of the GG (Fig. 5.13b). Subsequently, the redeposited Permian salt (20% of thickest Keuper) was added to the Permian salt (Fig. 5.12d). The next step is the redistribution of the total Permian salt onto the restored base like a viscous fluid until the salt layer was in hydrostatic equilibrium (Fig. 5.12d) and, finally, the calculation of an isostatic response due to the new load conditions which caused by renewed distribution of salt (Fig. 5.12e).

The obtained initial thickness is displayed in Fig. 5.13c. It shows a spatial correlation between two modelled maxima of the initial salt thickness distribution (Fig. 5.13c)
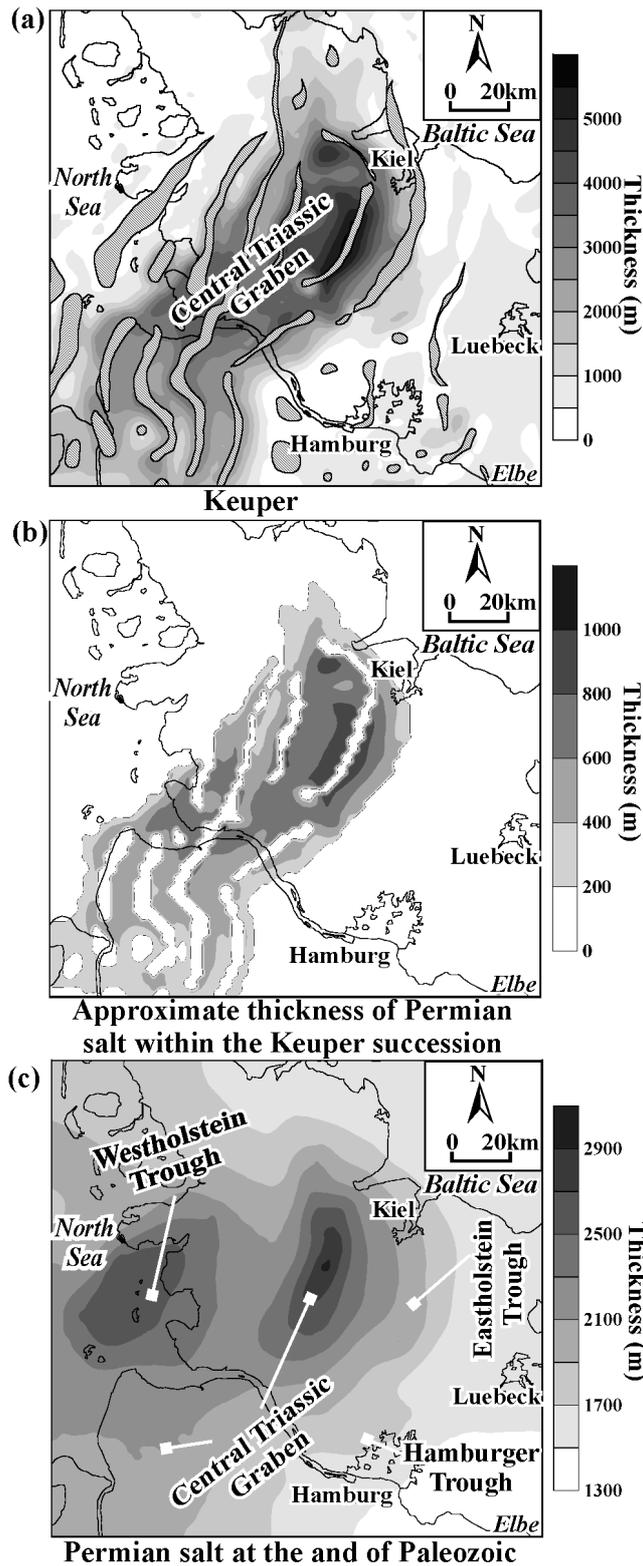
Figure 5.13. (a) Thickness map of the uppermost Middle Triassic and Upper Triassic (Keuper); (b) suggested thickness of the Permian salt within the Keuper strata; (d) reconstructed map of initial salt thickness obtained from 3D salt redistribution within the studied area.

and present-day depth minima within the Westholstein trough and the central part of the GG (Fig. 4.2c). The modelled two maxima of initial salt thickness are correlated with the present-day salt distribution, which is characterized by the largest salt walls within the Westholstein Trough and in the Central Triassic Graben (Figs. 5.10a and 5.11a). The initial salt thickness varies from 1300 m at the flanks of the basin up to 3000 m within the central part. On the basin scale, a clear NNE-SSW trend of the GG is recognizable due to the presence of two NNE-SSW extended maxima of Permian salt thickness. The regional trend of the restored salt distribution points to a westward continuation of the Permian salt basin (Fig. 5.13c). The initial salt thickness varies from 1300 m at the flanks of the basin up to 3000 m within the central part. On the basin scale, a clear NNE-SSW trend of the GG is recognizable due to the presence of two NNE-SSW extended maxima of the Permian salt thickness. The regional trend of the restored salt distribution points to a westward continuation of the Permian salt basin (Fig. 5.13c). In addition, the map displayed in Fig. 5.13c shows that the relative low degree of salt-tectonic activity within the flanks of the basin may have been predetermined by relatively thin initial salt thickness. Thus, the initial thickness of the Permian salt may have controlled the structural style of the basin. Where salt was thick, salt diapirs were formed and the overburden was subjected to high-amplitude folding. Where salt was relatively thin, simple salt pillows and shallow anticlines developed.

Because the modelling approach assumes the volume of salt to be constant through time, the initial thickness of the Permian salt bears an error in the sense that a possible salt loss due to underground dissolution is not considered. The significance of this process is highlighted by Clark et al. (1999) and Cartwright et al. (2001) in the North Sea basin. Most probably, considerable superficial dissolution did occur not only in the Keuper but also in later times. On the other hand, some of the dissolved salt re-entered the system via redeposition during the Keuper – a process considered in the modelled salt volume. However, these aspects of the salt dissolution are too complex, preventing a reliable estimate of the dissolved Permian salt and therefore, have been postponed to future studies.

5.5. Summary

The results of the modelling reveal the thickness distribution of the Permian salt within the GG from the end of the Permian (Fig. 5.13c) to present-day (Fig. 5.11). Three phases of strong growth of the salt structures have been identified by 3D reverse modelling.

A major phase of growth occurred during the Triassic within the central part of the basin (Figs. 5.10f and 5.11f), which can be related to almost W-E extension in the Keuper. This activation of salt tectonics was followed by a Jurassic pulse of salt movements (Figs. 5.10e and 5.11e) which temporally correlates with an extensional event in the Pompeckj Block and the Lower Saxony Basin. The third, Paleogene-Neogene tectonic event caused significant growth and amplification of the salt structures mainly at the margins of the basin (Figs. 5.10 a, b and 5.11 a, b). This event is extensional with a possible horizontal component of tectonic movements. These three phases of salt tectonics were separated by intervals associated with very low degree of salt mobility in the Early and Late Cretaceous (Figs. 5.10 c, d and 5.11 c, d). Therefore, the results of the modelling indicate a good correlation between the main phases of salt movements and tectonic events in the area under consideration.

It is important to note that the restoration method has several sources of errors. The results of the salt redistribution depend strongly on the input data set, such as reconstructed thickness maps for reverse modelling and the shape of the base of the Permian salt for forward modelling. The method also depends how correctly the amount of Permian salt is determined. In order to avoid possible mistakes, the reconstructed thickness maps were established by using all available data, the shape of the salt base was predefined with some approximation beneath the salt structures and strong extrusion and dissolution of the Permian salt during Keuper was taken into account. Some errors of the modelling can occur as a result from an imprecisely constructed salt base beneath the salt structures and possible additional salt dissolution during the Mesozoic and Tertiary. Additionally, the re-established distribution of the Keuper sediments has to be corrected for postdepositional Keuper salt movements at the post Triassic evolution stage of the GG. All these uncertainties require individual investigations by use of additional data (seismic lines and deep wells), and therefore a unique solution of these uncertainties cannot be achieved in the present study. For instance, the prestack migration has to be applied to all seismic lines crossing salt walls in order to resolve a seismic image beneath salt structures; additional borehole data and seismic lines are needed for accurate correlation of reflections within the areas which are strongly affected by salt tectonics and so on. For that reason, some simplifications were used in the modelling process. In any case, the results of the modelling will not avoid all quantitative errors, and have to be considered as a first approximation. Therefore, 3D

structural modelling provides quantitative results in spite of some simplification due to a deficit of the existent and/or available geological and geophysical data.

In summary, it can be stated that the development of the depletion zone of the Permian salt through time (Fig. 5.11) is in agreement with the observed distribution of the maximum subsidence centres of the different stratigraphic units (Fig. 4.13). In the central part of the GG, the depletion occurred already in the Triassic and it is perfectly correlated with the thickest Triassic (cf. Figs. 5.11f and 4.13). During the Jurassic, Cretaceous and Tertiary, the areas of depleted Permian salt shifted towards the basin flanks and the same occurred with the centres of maximum subsidence. Only minor isolated salt pillows remained within the central part of the basin and have locally fed salt walls and diapirs during post Triassic time. The sedimentation centres for each time stage are always located above the zone of the reduced or depleted Permian salt. Thus, the results of the modelling show that salt withdrawal may have played an important role during the Meso-Cenozoic evolution and that the effects of the salt-driven subsidence during the Meso-Cenozoic may be considered a main reason for the formation of the deep Central Triassic Graben and the subsequent Jurassic-Cenozoic marginal troughs.

Chapter VI

CONCLUSIONS

In the present work, the structure and evolution of the GG have been investigated in relation to salt tectonics. The main purpose was to examine the interplay between tectonic and salt induced processes. In order to resolve the role of salt tectonics during the evolution of the GG, one-dimensional analysis of the borehole data, two-dimensional interpretation of seismic lines and three-dimensional structural model and modelling were carried out.

The integrated study shows that the sedimentary cover of the GG contains several salt-rich sequences within the Permian and Triassic intervals. The most important are the salt-rich Rotliegend, the relatively pure Zechstein salt, and the salt-rich Keuper. It was revealed that the Zechstein salt is the main component involved in the diapiric movements that have influenced the regional evolution of the GG. Rotliegend salt is not significantly disturbed within the flanks of the basin where it is still characterized by flat-laying strata. However, the Rotliegend salt could have played an important role in the formation of salt structures in the central part of the GG, where it contributes in addition to the Zechstein salt to the total volume of some salt structures. Thus, the Rotliegend salt may have been much thicker within the central part than on the flanks of the basin. The role of the Keuper salt is also important but mostly restricted to the area of the Central Triassic Graben where its thickness is significant.

Three main phases of growth of the salt structures have been identified by the analysis of the seismic pattern. A major phase of growth occurred during the Keuper extension in response to normal faulting of the salt base. This activation of salt tectonics was followed by a Jurassic pulse of salt movements, which temporally correlate with an extensional event in the Pompeckj Block and the Lower Saxony Basin. The third, Paleogene-Neogene tectonic event caused significant growth and amplification of the salt structures mainly at the margins of the basin. This event is extensional with a possible horizontal component of the tectonic movements. These three phases of salt tectonics were separated by intervals associated with minor salt mobility, especially in the Late Cretaceous.

Triassic extensional faults have been identified on the salt base below salt walls and diapirs which formed in the same time interval. This fault activity most likely controlled the location and orientation of the NNE-SSW elongated salt walls. In this case, the formation of

the salt walls and diapirs was triggered by salt movements above active extensional faults in the Keuper. During the Jurassic and the Cenozoic, the tectonic events played a minor role in the initiation of the formation of salt structures, but aided in their growth.

During the Late Jurassic to Early Cretaceous the area around the Glueckstadt Graben was affected by relative uplift with regional erosion of the elevated relief. This relative uplift coincides with contemporaneous rifting in adjacent areas, the Central Graben, Broad Fourteens basin, Central and Western Netherlands Basin, and the Lower Saxony Basin. Furthermore, the area of the Glueckstadt Graben remained a rather stable high and the Lower Cretaceous indicates minor subsidence within the Central Triassic Graben. The small amount of the eroded Keuper sediments, the presence of truncated toplaps in Jurassic strata and the absence of visible unconformities at the NW flank of the basin suggest that the present-day thinning of the Jurassic sequence could reflect the proximal depositional limit with little Late Jurassic-Early Cretaceous erosion near rising salt structures. Thus, the erosional features did not extensively modify the thickness distribution of the depositional sequences in the Jurassic. Furthermore, the present-day remains of thick Jurassic still represents the areas of intensive subsidence, which was strongly controlled by the withdrawal of the Permian salt from the source layer.

During the Late Cretaceous and Tertiary, the area of the CEBS was affected by inversion related to the Alpine Orogeny. However, there is no major effect observable within the Graben area in terms of seismic stratigraphy or significant variations of sedimentary patterns. Furthermore, the GG was not inverted during the Late Cretaceous and Tertiary, when up to 4.5 km of sediments were eroded in the Lower Saxony Basin (Petmecky et al, 1999) and along the southern margin of the NE German Basin (Scheck et al., 2002). In contrast to other parts of the CEBS, the rise of salt in almost N-S-striking salt walls indicates an E-W directed extension. This is consistent with the assumed regional stress field during Late Cretaceous-Early Tertiary inversion within other parts of the CEBS. For this period, the stress field is characterized by N-S compression and E-W extension that is generally derived from the regional structural analysis within Central Europe (Ziegler, 1990b). The Glueckstadt Graben was parallel to the principal strain direction and therefore was not prone to an inversion in the Late Cretaceous-Early Tertiary.

Initially Permian salt may have been up to 3000 m thick within the central part of the basin and about 1300-1900 m at the flanks. Possibly, the initial thickness distribution of the

Permian salt controlled the structural style of the basin regionally. Where salt was thick, salt diapirs and walls formed. Where salt was relatively thin, simple salt pillows and shallow anticlines developed.

According to results of the 3D structural modelling, the formation of the deep Central Triassic Graben and the subsequent Jurassic-Cenozoic marginal troughs was strongly controlled by salt structures and their development through time. In summary, it can be stated that the centre of sedimentation was moving away from the central part of the of the initial Graben structure towards its margins due to gradual withdrawal of Permian salt. In this sense, the Glueckstadt Graben was formed at least partially as a "basin-scale rim syncline" during post-Permian times. Therefore, the results show that salt withdrawal may have played an important role during the Meso-Cenozoic evolution and that the effects of the salt-driven subsidence during the Meso-Cenozoic may be considered a main reason for formation of the deep Central Triassic Graben and the subsequent Jurassic-Cenozoic marginal troughs.

This study shows that more or less east-west directed stresses caused the formation of the Triassic graben structures between the Tornquist Zone and the Elbe Fault System within the CEBS (Figs. 1.1 and 1.2). In addition, the available data indicate that the originally thick Permian salt deposits provide another important mechanism of subsidence, which has its own dynamics, once initialized, and which reacts very sensibly as far as it is affected in some way by the general stress field. However, the questions concerning the potential localization of strain in the sedimentary cover above the salt layer is still unsolved, although, some evidence for stress and strain partitioning was provided by Marotta et al. (1999). However, it can be stated that salt dynamics certainly involves its own mechanisms with regard to a changing external stress fields and may cause essential interpretation problems in many regions. Open questions are still remained concerning the structure of the deep crust and the depth position of the Moho within the area under consideration due to an absence of the regular coverage by deep seismic lines.

REFERENCES

Abramovitz , T., Landes, M., Thybo, H., Brian Jacob, A.W., Prodehl, C., 1999. Crustal velocity structure across the Tornquist and Iapetus Suture Zones – a comparison based on MONA LISA and VARNET data. Tectonophysics 314, pp. 69-82.

Abramovitz , T., Thybo, H., 1999. Pre-Zechstein structures around the MONNA LISA deep seismic lines in the southern Horn Graben area. Bulletin of the Geological Society of Denmark, v. 45, pp. 99-116.

Aichroth, B., Prodehl, C., Thybo, H., 1992. Crustal structure along the central segment of the EGT. Tectonophysics 207, pp. 43– 64.

Averiev, V., A., 1962. Features of the formation of the salt-dome structures within the south-eastern part of the Dniepr-Donets basin. In: Elina, N., D., Klitochenko., I., F., Pistrak, R., M. (editors). Collected Papers on the Geology of Gas Areas of the USSR. Gostoptechizdat, Moscow, pp. 89–100.11

Bachmann, G., Hoffmann, N., 1997. Development of the Rotliegend basin in Northern Germany. Geologisches Jahrbuch 103, pp. 9-31.

Baldschuhn, R., Binot, F., Fleig, S., Kockel, F., 2001. Geotektonischer Atlas von Nordwest-Deutschland und dem deutschen Nordsee-Sektor. Geologisches Jahrbuch, Reihe A, Heft 153.

Baldschuhn, R., Frisch, U., Kockel, F., (eds.) 1996. Geotektonischer Atlas von NW-Deutschland 1:300000. 4 pp., 65 maps, Bundesanstalt für geowissenschaften und Rohstoffe, Hannover.

Bayer, U., Grad, M., Pharaoh, T., Thybo, H., Guterch, A., Banka, D., Lamarche, J., Lassen, A., Lewerenz, B., Scheck, M., Marotta, A., M., 2002. The southern margin of the East European Craton: new results from seismic sounding and potential fields between the North Sea and Poland. Tectonophysics 360, pp. 301-314.

Bayer, U., Maystrenko, Yu., Hoffmann, N., Scheck-Wenderoth, M., Meyer, H., 2003. 3D structural modelling and basin analysis of the Central European Basin System (CEBS) between the North Sea and Poland. Terra Nostra 3, pp. 1-4.

Bayer, U., Scheck, M., Rabbel, W., Krawczyk, C.M., Götze, H.-J., Stiller, M., Beilecke, Th., Marotta, A.M., Barrio-Alvers, L., Kuder, J., 1999. An integrated study of the NE German Basin. Tectonophysics 314, pp. 285-307.

Benek, R., Kramer, W., McCann, T., Scheck, M., Negendank, J.F.W., Korich, D., Huebscher, H., Bayer, U., 1996. Permo-Carboniferous magmatism of the NE German basin. Tectonophysics, v. 266, pp. 379– 404.

Best, G., Kockel, F., Schoeneich, H., 1983. Geological history of the southern Horn graben. Geol. en Mijnbouw 62, pp. 25-33.

Betz, D., Führer, F., Plein, E., 1987. Evolution of the lower Saxony basin. Tectonophysics 137, pp. 127-170.

Blundell, D., J., 1999. The legacy of the European Geotraverse. Tectonophysics 314, pp. 7-16.

Blundell, D., Mueller, S., Mengel, K., 1992. A Continent Revealed: the European Geotraverse. Camb. In: Blundell, D., Freeman, R., Mueller, St. (eds.), Geodynamics of Europe, Univ. Press. Cambridge, United Kingdom, pp. 215-231.

Boigk, H., 1981. Erdöl und Erdölgas in der Bundesrepublik Deutschland: Erdölprovinzen, Felder, Förderung, Vorräte, Lagerstättentechnik. Germany, Stuttgart: Enke, 330 pp.

Brink, H.J., Dürschner, H., Trappe, H., 1992. Some aspects of the late and post-Variscian development of the Northwestern German Basin. Tectonophysics, 207, pp. 65-95.

Brink, H.J., Franke, D., Hoffmann, N., Horst, W. and Oncken, O., 1990. Structure and evolution of the North German Basin. In: R. Freeman, P. Giese and St. Mueler (Editors), The European Geotraverse: Integrative Studies. European Science Foundation, Strasbourg, pp. 195-212.

Britze, P., Japsen, P., 1991. The Danish Basin.Triassic. Isochore map: Danmarks Geologiske Undersogelse (DGU) Miloeministeriet, Copenhagen, DGU map series no. 31, 1 sheet, scale 1:400000.

Cartwright, J., Stewart, S., Clark, J., 2001. Salt dissolution and salt-related deformation of the Forth Approaches Basin, UK North Sea. Marine and Petroleum Geology, 18, pp. 757-778.

Clark, J., A., Cartwright, J., A., Stewart, S., A., 1999. Mesozoic dissolution tectonics on the West Central Shelf, UK Central North Sea. Marine and Petroleum Geology, 16, pp. 283-300.

Cocks, L.R.M., McKerrow, W.S., Van Staal, C.R., 1997. The margin of Avalonia. Geol. Mag. 134, pp. 627-636.

Dadlez, R., 2003. Mesozoic thickness pattern in the Mid-Polish Trough. Geological Quarterly, 47 (3), pp. 223-240.

Dadlez, R., Narkiewicz, M., Stephenson, R.A., Visser, M.T.M., van Wees, J-D., 1995. Tectonic evolution of the Mid-Polish Trough: modelling implications and significance for central European geology. Tectonophysics 252, pp. 179-195.

Daudre, B., Cloetingh, S., 1994. Numerical modelling of salt diapirism: influence of the tectonic regime. Tectonophysics 240, pp. 59– 79.

DEKORP-BASIN Research Group, Bachmann, G.,H., Bayer, U., Dürbaum, H.,J., Hoffmann, N., Krawczyk, C.,M., Lück, E., McCann, T., Meissner, R., Meyer, H., Oncken, O., Polom, U., Prochnow, U., Rabbel, W., Scheck, M., Stiller, M., 1999. The deep crustal structure of the Northeast German basin: New DEKORP-Basin'96 deep-profiling results. Geology, 27, pp. 55-58.

Dohr, G., Bachmann, G.H., Grosse, S., 1989. Das Norddeutsche Becken. Niedersächsische Akademie der Geowissenschaften Veröffentlichungen, 2, pp. 4-47.

EUGENO-S Working Group, 1988. Crustal structure and tectonic evolution of the transition between the Baltic Schield and the North German Caledonides (The EUGENO-S Project). Tectonophysics, 150, pp. 253-348.

Evans, D., Graham, C., Armour, A., Bathurst, P., 2003. The Millennium Atlas: Petroleim geology of the central and northern North Sea. The Geological Society of London, London, 990 pp..

Evans, D., Graham, C., Armour, A., Bathurst, P., 2003. The Millennium Atlas: Petroleim geology of the central and northern North Sea. The Geological Society of London, London, 990 pp..

Garetsky, R.G., Ludwig, A.O., Schwab, G., Stackebrandt, W. (eds.), 2001. Neogeodynamics of the Baltic Sea depression and adjacent areas. Brandenburgische Geowissenschaftliche Beiträge, 1-2001, 47 pp, 8 maps.

Gast, R., 1988. Rifting im Rotliegenden Niedersachsens. Die Geowissenschaften, 4, pp. 115-122.

George, G., T., Berry, J., K., 1997. Permian Upper Rotliegend synsedimentary tectonics, basin development and palaeogeography of the southern North Sea, in Ziegler P, Turner P, and Daines S R eds., Petroleum geology of the southern North Sea: Geological Society of London Special Publication 123, pp. 31–61.

Gregersen, S., Voss, P., TOR Working Group, 2002. Summary of project TOR: delineation of a stepwise, sharp, deep lithosphere transition across Germany-Denmark-Sweden. Tectonophysics, 360, pp. 61-73.

Guglielmo, G.J., Vendeville B.C., Jackson M.P.A., 1999. Isochores and 3-D visualization of rising and falling salt diapirs. Marine and Petroleum Geology, 16, pp. 849-861.

Ismail-Zadeh, A., Tsepelev, I., Talbot, C., Korotkii, A., 2004. Three-dimensional forward and backward modelling of diapirism: numerical approach and its applicability to the evolution of salt structures in the Pricaspian basin. Tectonophysics, 387, pp. 81-103.

Jaritz, W., 1980. Einige Aspekte der Entwicklungsgeschichte der nordwestdeutschen Salzstöcke. Zeitschrift der Deutschen Geologischen Gesellschaft, 131, 8 Abb., pp. 387-408.

Jordt, H, Faleide, J., I., Bjerlykke, K, Ibrahim, M., T., 1995. Cenozoic sequence stratigraphy of the central and northern North Sea Basin: tectonic development, sediment distribution and provenance areas. Marine and Petroleum Geology, 12, pp. 845-879.

Kaus, B.J.P., Podladchikov, Y.Y., 2001. Forward and reverse modeling of the three-dimensional viscous Rayleigh–Taylor instability. Geophysical Research Letters 28, pp. 1095–1098.

Kockel, F., 1988. Teufenplan Basis Miozän. Bundesanstalt für Geowissenschaften und Rohstoffe, Hannover, 1 map.

Kockel, F., 2002. Rifting processes in NW-Germany and the German North Sea Sector. Geologie en Mijnbouw, 81, pp. 149-158.

Kockel, F., 2003. Problems of diapirism in northern Germany. Geologos 6, pp. 57-88.

Koyi, H., 1998. The shaping of salt diapirs. Journal of Structural Geology, 20, pp. 321-338.

Koyi, H., Jenyon, M. K., Petersen, K., 1993. The effects of basement faulting on diapirism. Journal of Petroleum Geology, 16 (3), pp. 285–312.

Krawczyk, C.M., Eilts, F., Lassen, A., Thybo, H., 2002. Seismic evidence of Caledonian deformed crust and uppermost mantle structures in the northern part of the Trans-European Suture Zone, SW Baltic Sea. Tectonophysics 360, pp. 215-244.

Krzywiec, P., 2004. Triassic evolution of the Klodawa salt structure: basement-controlled salt tectonics within the Mid-Polish Trough (Central Poland). Geological Quarterly 48, pp. 123–134

Lamarche, J., Scheck-Wenderoth, M., 2005. 3D structural model of the Polish Basin. Tectonophysics, Tectonophysics 397, pp. 73-91.

Lockhorst, A. (ed.), 1998. NW European Gas Atlas-Composition and Isotope Ratios of natural Gases. GIS application on CD-ROM by the British Geological Survey, Bundesanstalt für Geowissenschaften und Rohstoffe, Danmarks og Gronlands Geologiske, Undersogelse, Netherlands Instituut voor Toegepaste geowetenschappen, Panstwowy Instytut Geologiczny, European Union.

Marotta, A.M., Bayer, U., Thybo, H., 1999. A 2-D flexural model for crustal deformation below the NE German Basin. Abstract Volume of EUG10, 1999, Strasbourg.

Marotta, A.M., Bayer, U., Thybo, H., 2000. The legacy of the NE-German Basin – reactivation by compressional buckling. Terra Nova 12, pp. 132-140.

Marotta, A.M., Bayer, U., Thybo, H., Scheck, M., 2002. Origin of the regional stress in the North German basin: results from numerical modelling. Tectonophysics 360, pp. 245-264.

Maystrenko, Yu., Bayer, U., Scheck-Wenderoth, M., 2005. The Glueckstadt Graben, a sedimentary record between the North and Baltic Sea in north Central Europe. Tectonophysics, in press.

Meissner, R., Thybo, H., Abramowitz, T., 2002. Interwedging and inversion structures around the Trans-European Suture Zone in the Baltic Sea, a manifestation of compressive tectonic phases. Tectonophysics 360, pp. 265-280.

Nielsen, L., Balling, N., Jacobsen, B.H., MONA LISA Working Group, 2000. Seismic and gravity modelling of crustal structure in the Central graben, North Sea. Observations along MONA LISA profile 3. Tectonophysics, 328, pp. 229-244.

Petmecky, S., Meier, L., Reiser, H., Littke, R., 1999. High thermal maturity in the Lower Saxony Basin: intrusion or deep burial?. Tectonophysics 304, pp. 317–344.

Pharaoh, T., C., 1999. Paleozoic terranes and their lithospheric boundaries within the Trans-European Suture Zone (TESZ): a review. Tectonophysics 314, pp. 17–41.

Pharaoh, T.C., England, R.W., Verniers, J., Zelazniewicz, A. 1997. Introduction: geological and geophysical studies in the Trans-European Suture Zone. Geol. Mag. 134, pp. 585-590.

Plein, E., 1990. The Southern Permian Basin and its Paleogeography. In: Sediments and environmental geochemistry – Selected aspects and case histories. Springer-Verlag Berlin Heidelberg, pp. 124-133.

Poliakov, A.N.B., van Balen, R., Podladchikov, Yu., Daudre´, B., Cloetingh, S., Talbot, C., 1993. Numerical analysis of how sedimentation and redistribution of surficial sediments affects salt diapirism. Tectonophysics 226, pp. 199– 216.

Roemer, M.-M., Neugebauer, H.J., 1991. The salt dome problem: a multilayered approach. Journal of Geophysical Research 96, pp. 2389–2396.

Sannemann, D., 1968. Salt-stock families in northwestern Germany. In: Braunstein, J., O'Brien, G., „Diapirism and diapirs". AAPG publ., pp. 261-270.

Sannemann, D., 1983. Migration of salt-induced structures. In: Bally, A.W. (ed.) Seismic expression of structural styles: a picture and work atlas. AAPG, Vol 2, series 15.

Scheck, M., 1997. Dreidimensionale Strukturmodellierung des Nordostdeutschen Beckens unter Einbeziehung von Krustenmodellen. STR97/10 GeoForschungsZentrum Potsdam, 125 pp.

Scheck, M., Bayer, U., 1999. Evolution of the Northeast German Basin – inferences from 3D structural modelling and subsidence analysis. Tectonophysics 313, pp. 145-169.

Scheck, M., Bayer, U., Lewerenz, B., 2003. Salt movements in the Northeast German Basin and its relation to major post-Permian tectonic phases—results from 3D structural modelling, backstripping and reflection seismic data. Tectonophysics 361, pp. 277–299

Scheck, M., Bayer, U., Lewerenz, B., 2003. Salt redistribution during extension and inversion inferred from 3D backstripping. Tectonophysics 373, pp. 55– 73.

Scheck, M., Bayer, U., Otto, V., Lamarche, J., Banka, D., Pharaoh, T., 2002. The Elbe fault System in North central Europe – a basement controlled zone of crustal weakness. Tectonophysics 360, pp. 281-299.

Scheck-Wenderoth, M., Lamarche, J., 2005. Crustal memory and basin evolution in the Central European Basin System—new insights from a 3D structural model. Tectonophysics, in press.

Schmeling, H., 1987. On the relation between initial conditions and late stages of Rayleigh–Taylor instabilities. Tectonophysics 133, pp. 65–80.

Sclater, J., G., Christie, P., A., F., 1980. Continental stretching: an explanation of the post-Mid-Cretaceous subsidence of the central North Sea basin. Journal of Geophysical Research 85-B7, pp. 3711-3739.

Šimkevičius, P., Katinas, V., Norkūnaitė, L., Voitichovaitė, J., 2001. Mineralogical composition of the Triassic-Lower Jurassic boundary rocks in the South-eastern Baltic region. Lithosphere, 5, pp. 36-48.

Sliaupa, S., 2004. RW disposal prospects in Lithuania. http://esd.lbl.gov/IAEAnetworktraining/ session_summaries/pdfs/Sess_04_Sliaupa.pdf.

Stephenson, R.A., Narkiewicz, M., Dadlez, R., van Wees, J-D., Andriessen, P., 2003. Tectonic subsidence modelling of the Polish Basin in the light of new data on crustal structure and magnitude of inversion. Sedimentary Geology 156, pp.59–70.

Stovba, S., M., Maystrenko, Yu., P., Stephenson, R., A., Kusznir, N., J., 2003. The formation of the south-eastern part of the Dniepr–Donets Basin: 2-D forward and reverse modelling taking into account post-rift redeposition of syn-rift salt. Sedimentary Geology 156, pp. 11-33.

Talbot, C., J., Medvedev, S., Alavi, M., Shahrivar, H., Heidari, E., 2000. Salt extrusion at Kuh-e-Jahani, Iran, from June 1994 to November 1997. In: Vendeville B, Mart Y, Vigneresse J-L (Eds.), Salt, Shale and Igneous Diapirs in and Around Europe, Special Publications, Geological Society, London, 174, pp. 93– 110.

Talbot, C.J., 1995. Molding of salt diapirs by stiff overburdens. In: Jackson, M.P.A., Roberts, D.G., Snelson, S. (Eds.), Salt Tectonics—A Global Perspective, Memoir, American Association of Petroleum Geologists, Tulsa, 65, pp. 61– 75.

Thybo, H., 2001. Crustal structure along the EGT profile across the Tornquist Fan interpreted from seismic gravity and magnetic data. Tectonophysics 334, pp. 155– 190.

Trusheim, F., 1960. Mechanism of salt migration in North Germany. Bull. AAPG, 44, pp. 1519-1540.

Van Hoorn, B., 1987. Structural evolution, timing and tectonic style of the Sole Pit inversion. Tectonophysics 137, pp. 239-284.

Van Wijhe, D. H., 1987. Structural evolution of inverted basins in the Dutch offshore (North Sea). Tectonophysics, 137, pp. 171-219.

Vejbaek, O., V., Britze, P., 1994. Top of the pre-Zechstein rocks. Sub- and supercrop map: Danmarks Geologiske Undersogelse (DGU) Miloeministeriet, Copenhagen, DGU map series no. 45, 1 sheet, scale 1:750000.

Vendeville, B. C., Jackson, M. P. A., 1992. The rise of diapirs during thin-skinned extension. Marine and Petroleum Geology, 9, pp. 331-353.

Woidt, W.-D., 1978. Finite element calculations applied to salt dome analysis. Tectonophysics 50, pp. 369– 386.

Ziegler, P., 1992. European Cenozoic rift systems. Tectonophysics 208, pp. 91-111.

Ziegler, P., A., 1990a. Collision related intra-plate compression deformations in western and central Europe. Journal of Geodynamics 11, pp. 357-388.

Ziegler, P.,1990b. Geological atlas of Western and Central Europe. 2nd ed. Geol. Soc. Publ. House, Bath, Shell International Petroleum Mij., B.v., 239 pp.

Appendix A
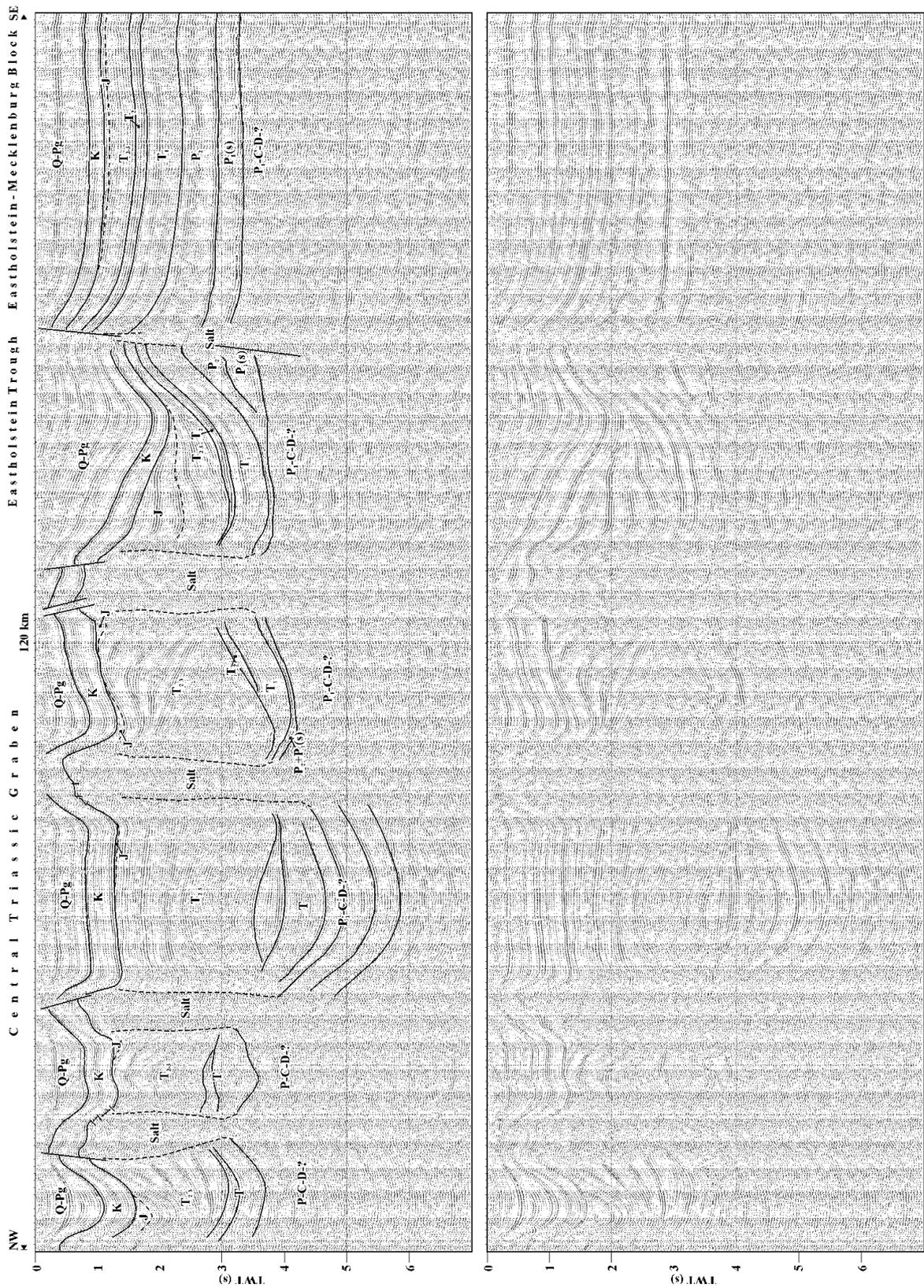
Examples of seismic images and their interpretation

Appendix B

Results of the 3D revese modelling

Seismic line 1

Seismic line 2

Seismic line 4

Seismic line 3

Seismic line 5

Seismic line 6
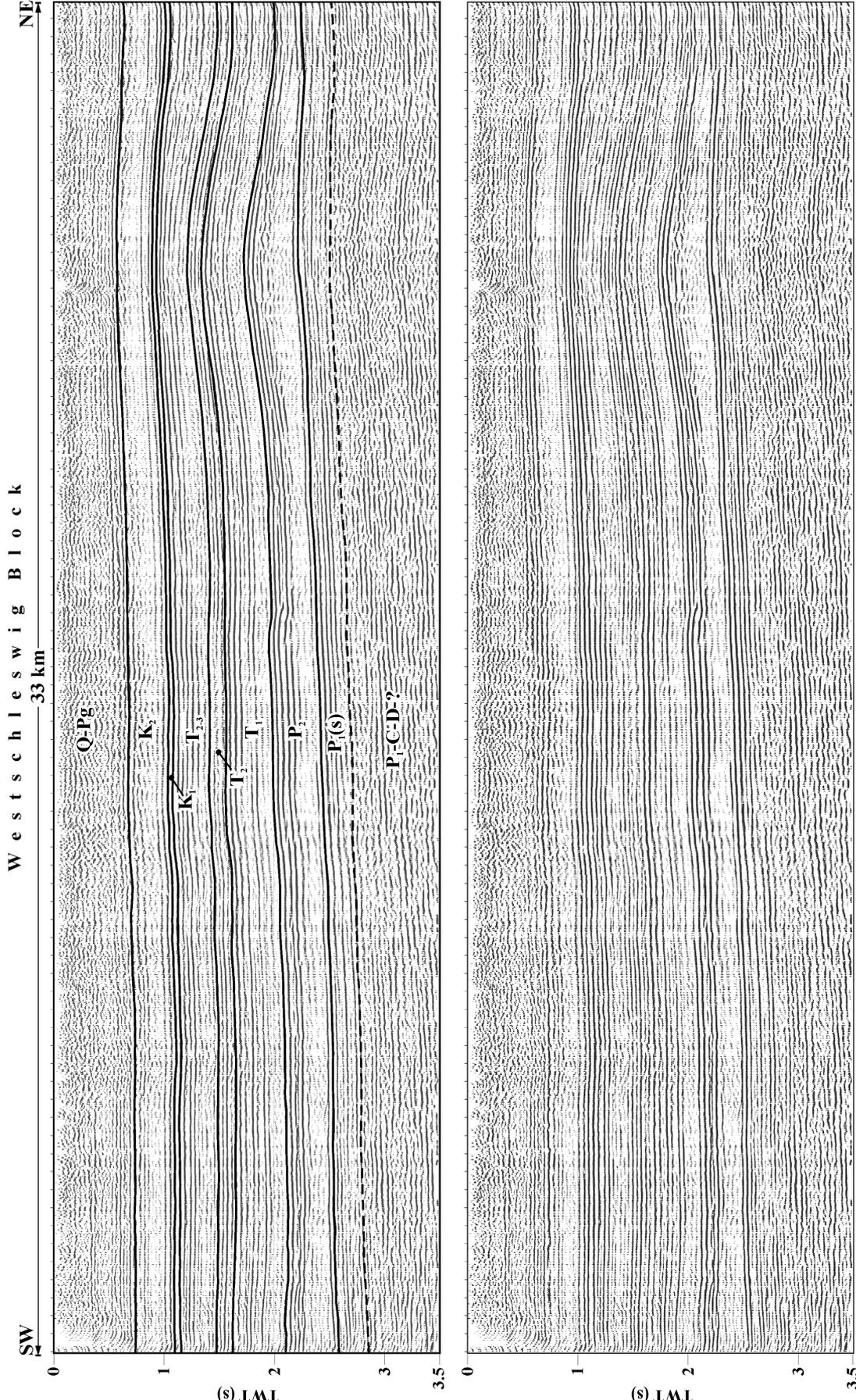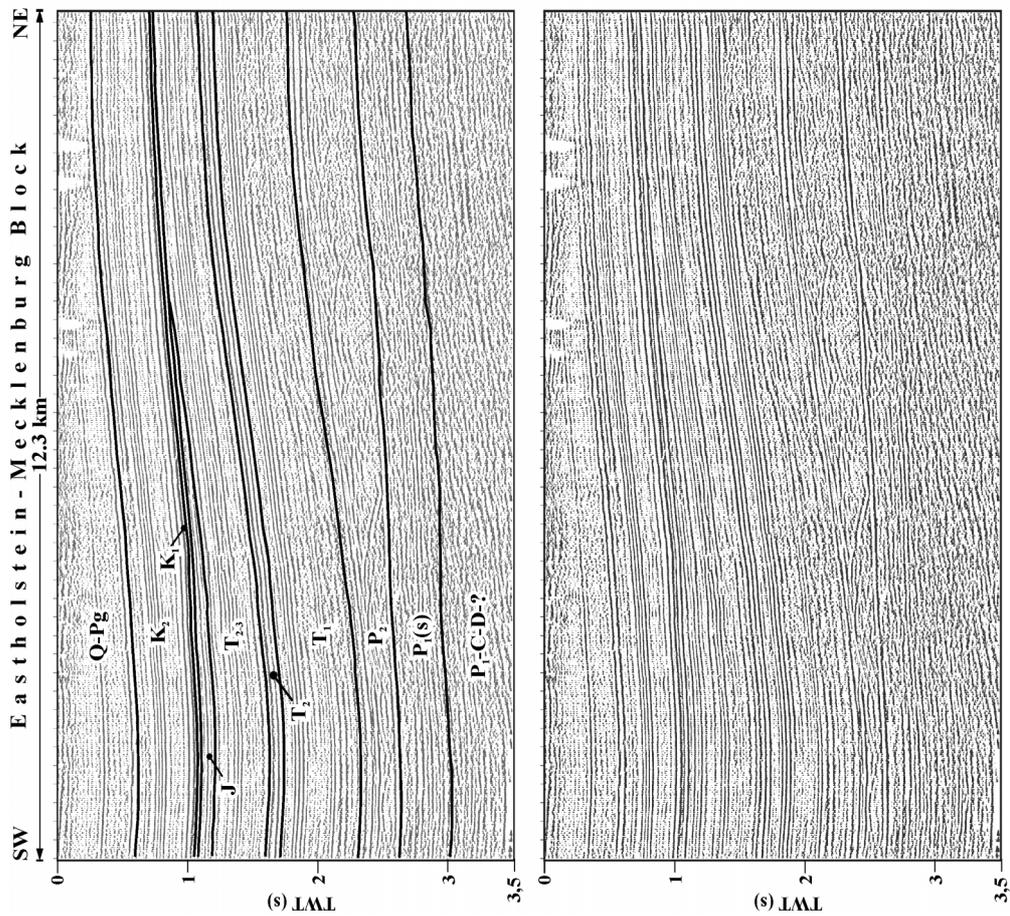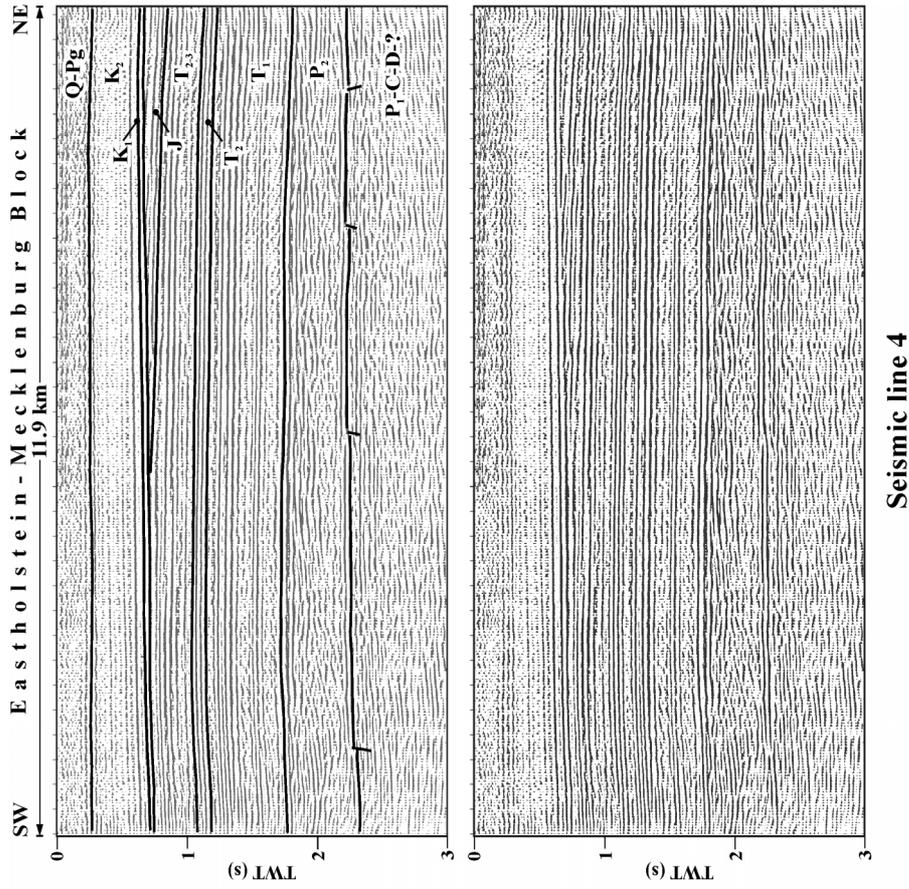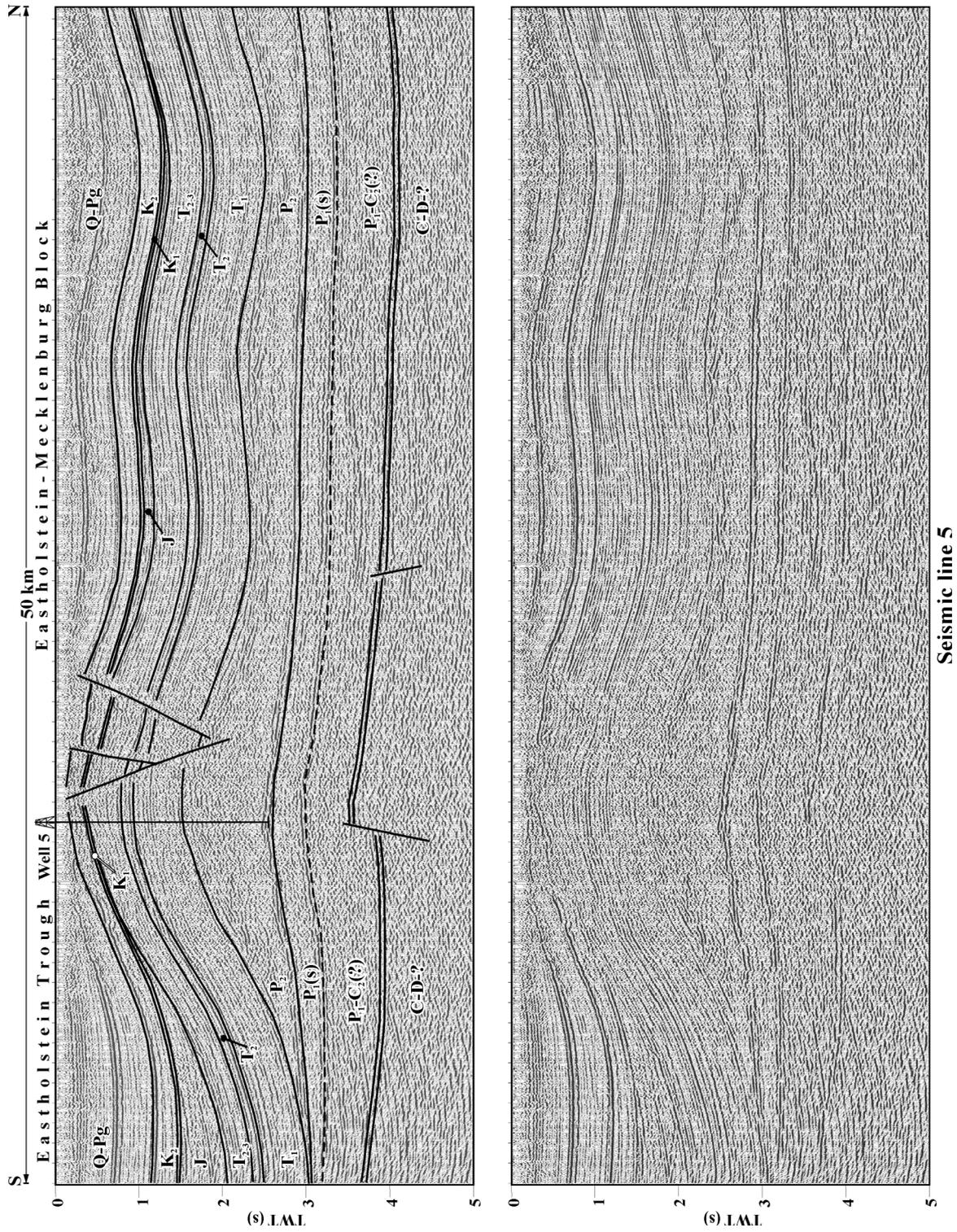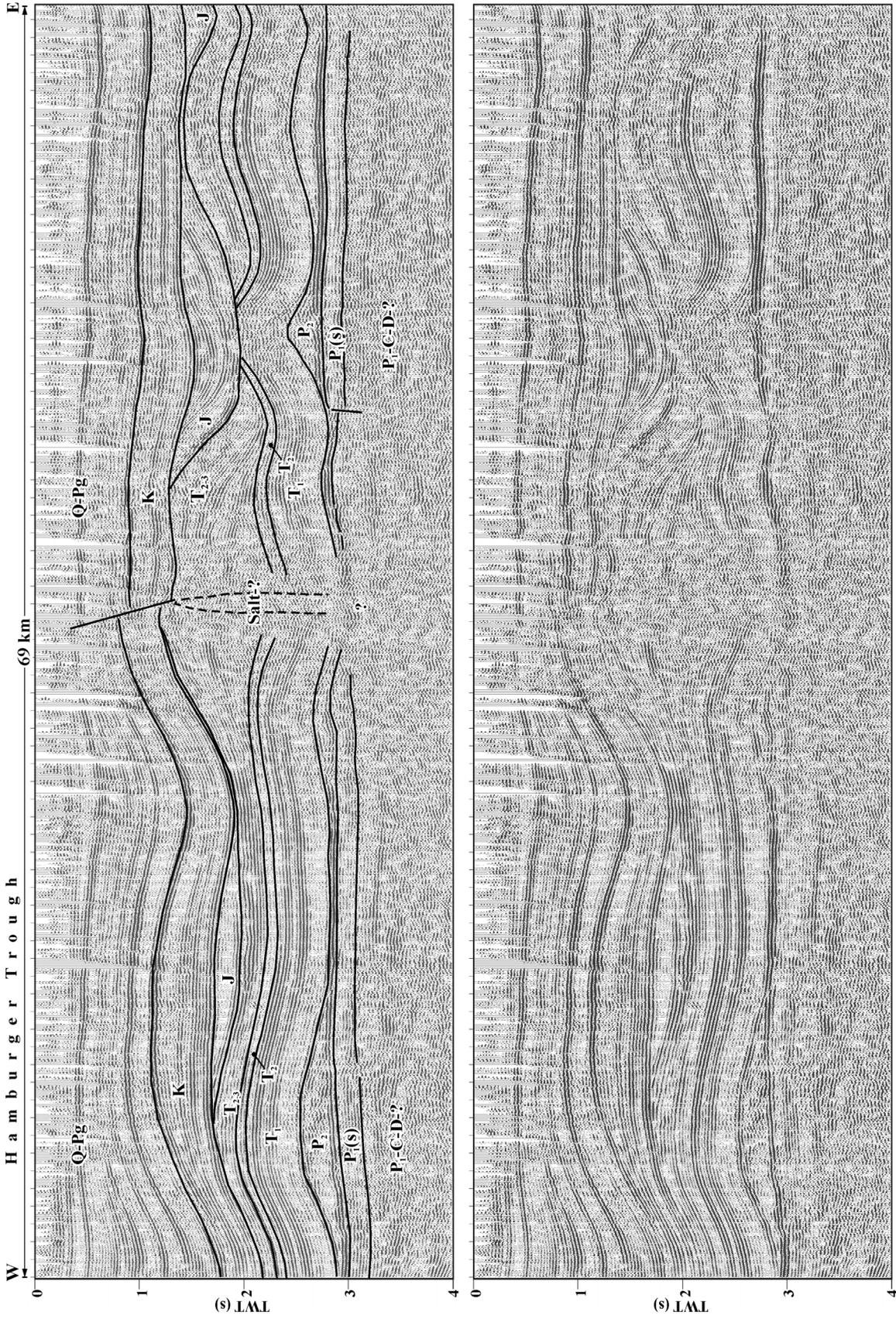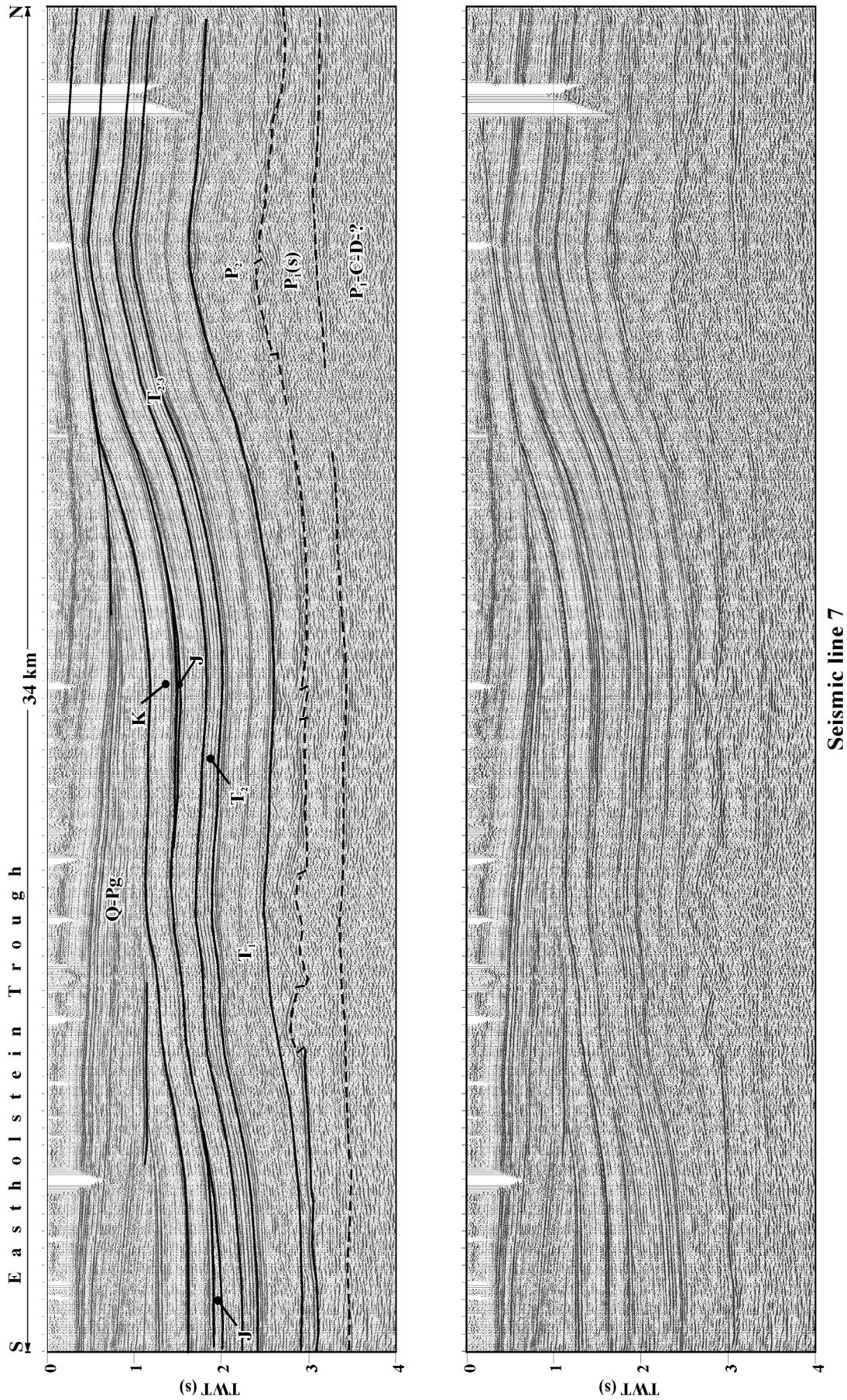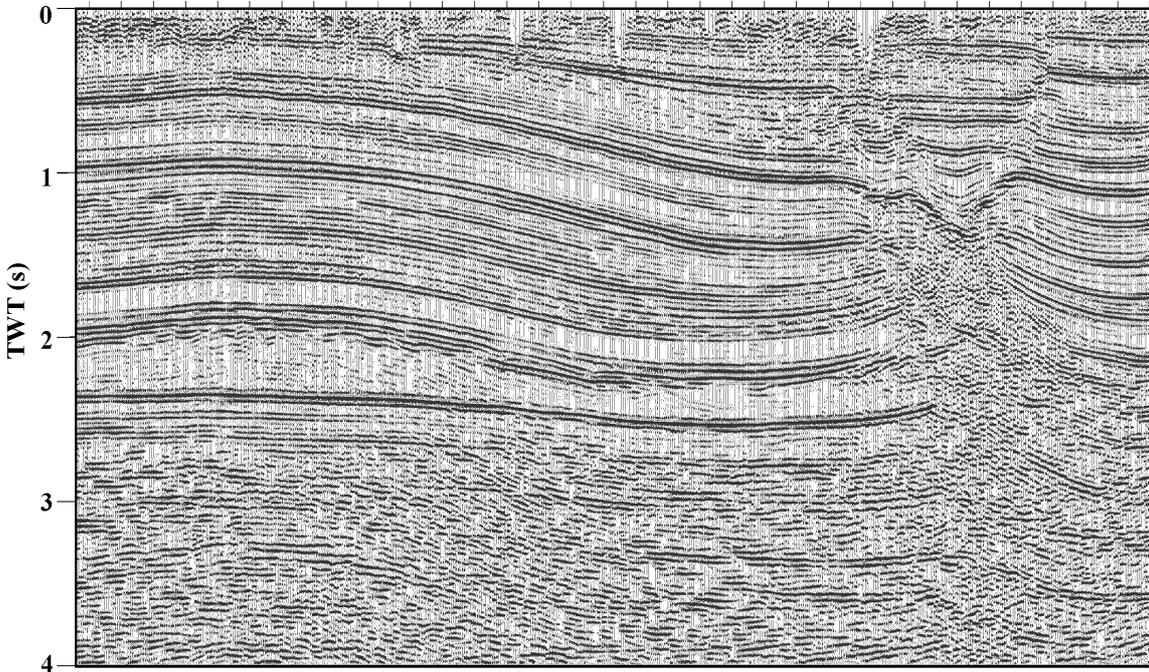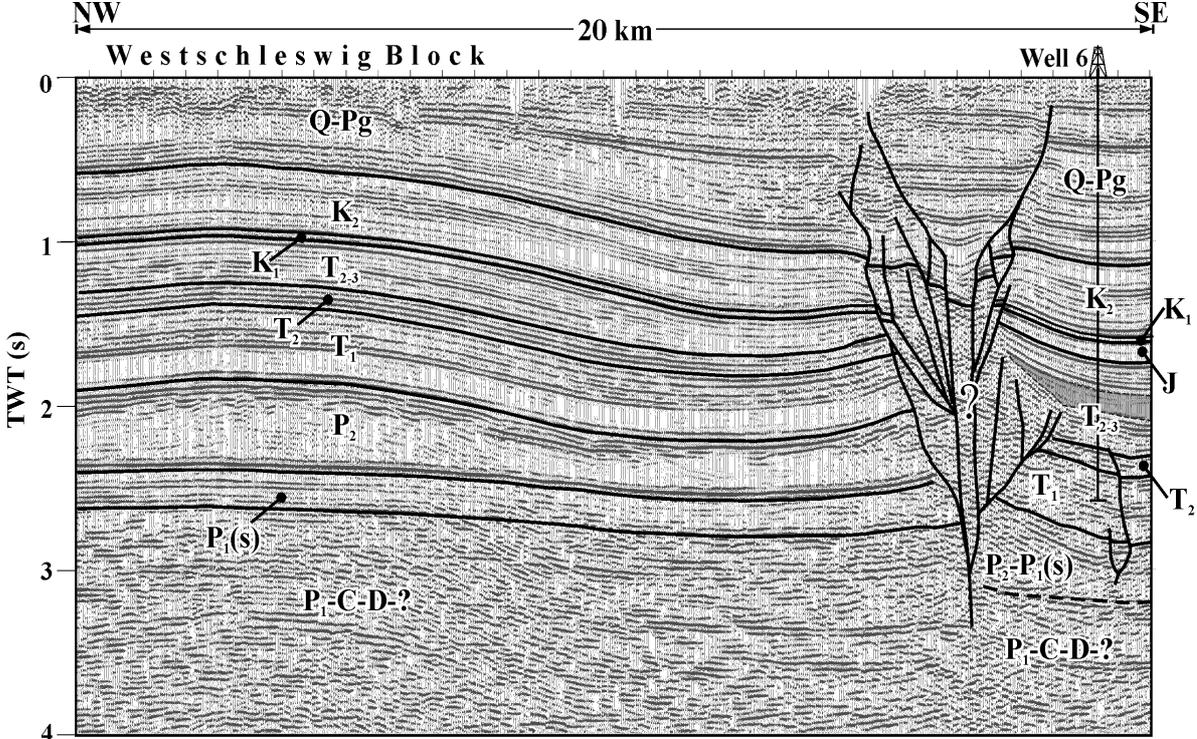
Seismic line 7

Seismic line 8

Seismic line 9
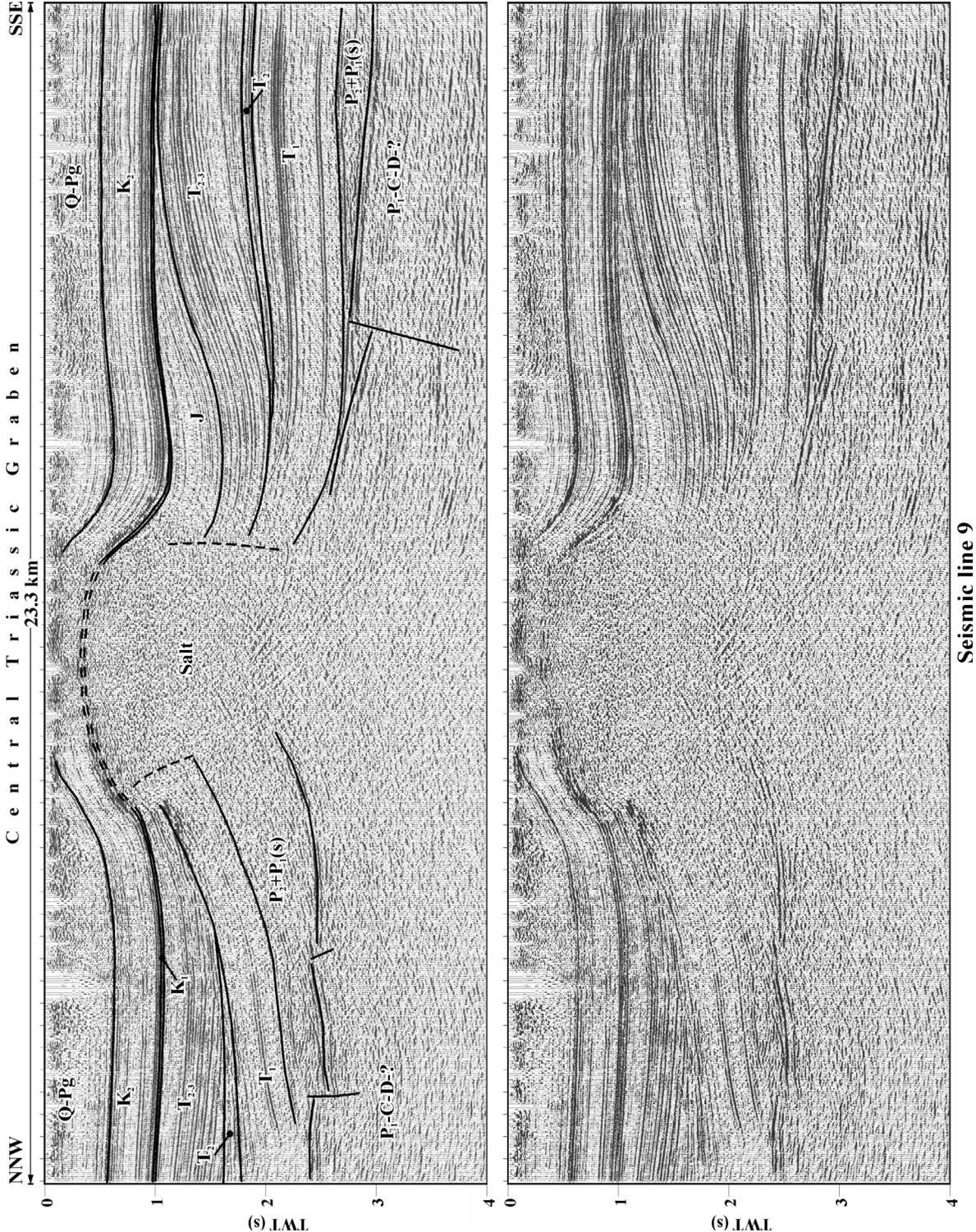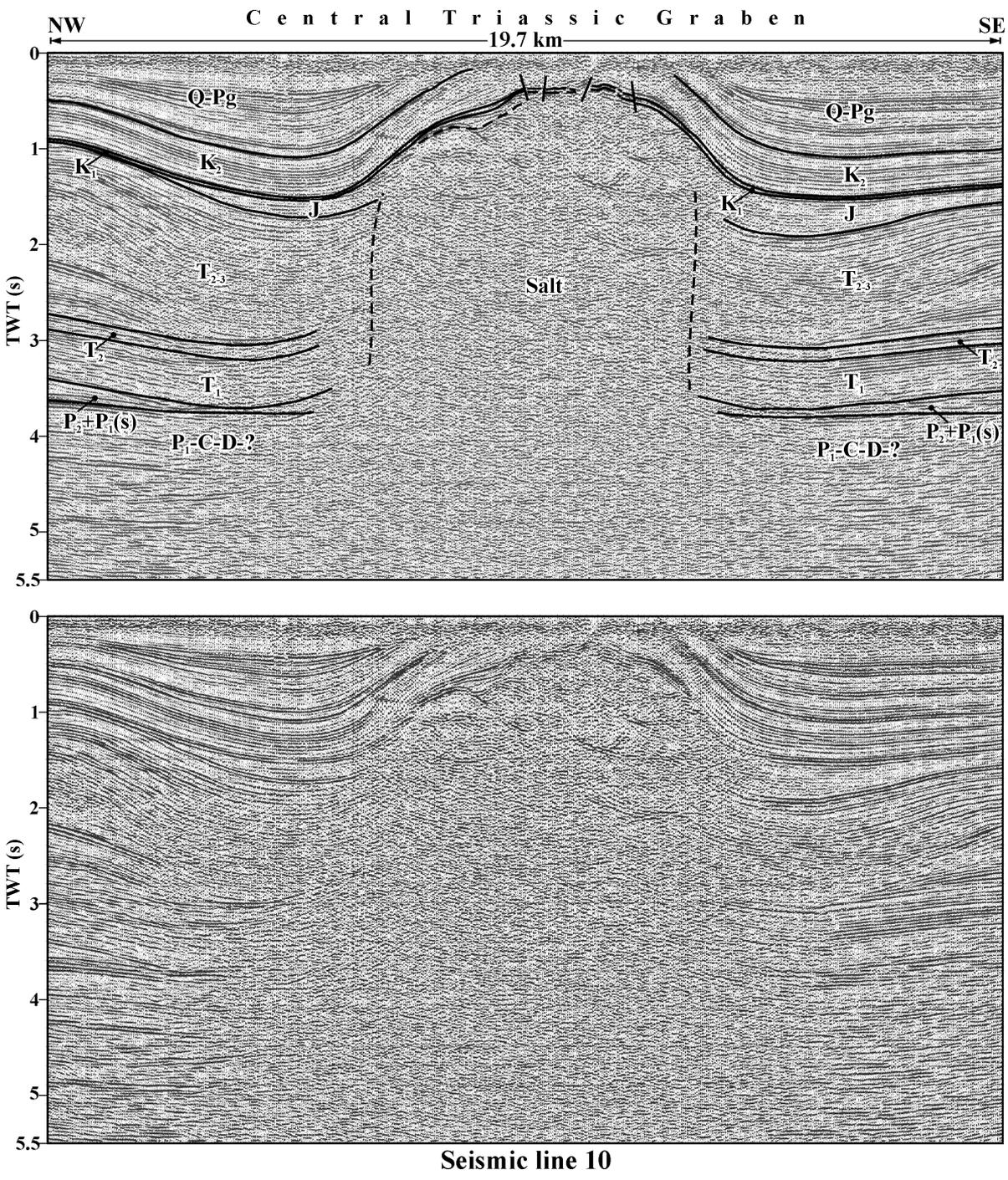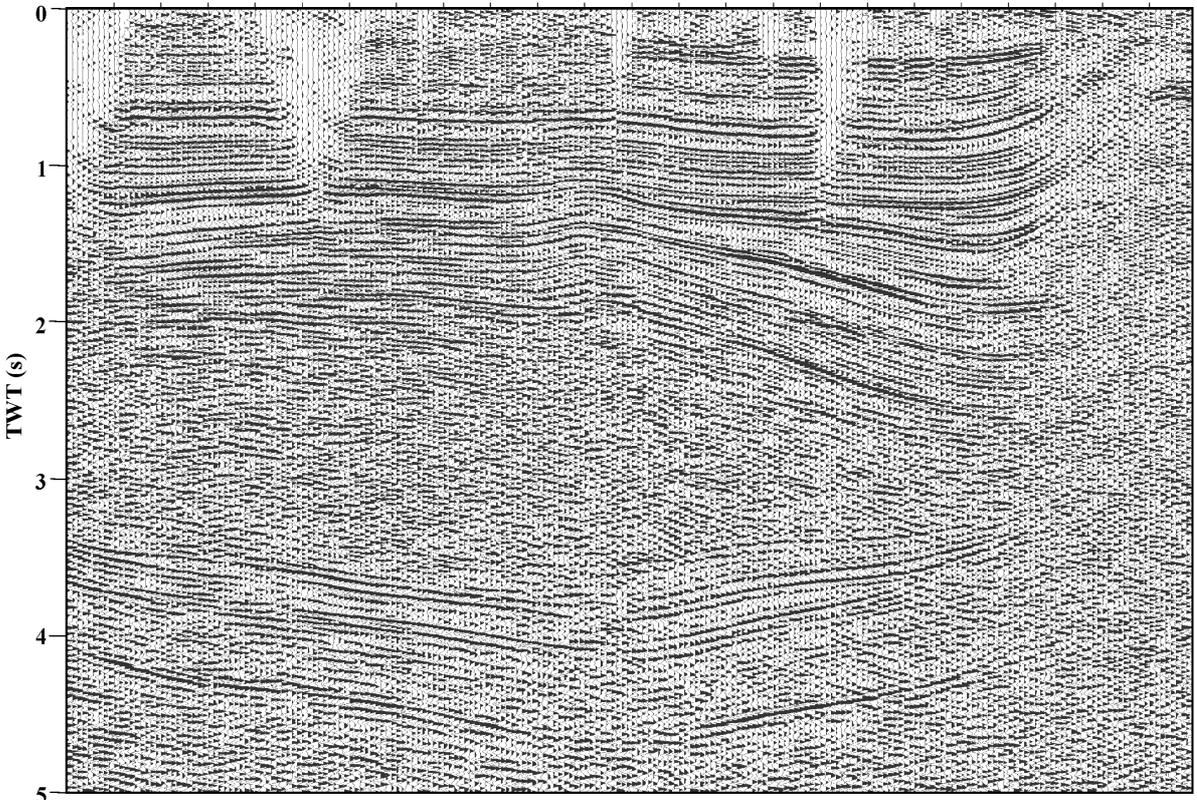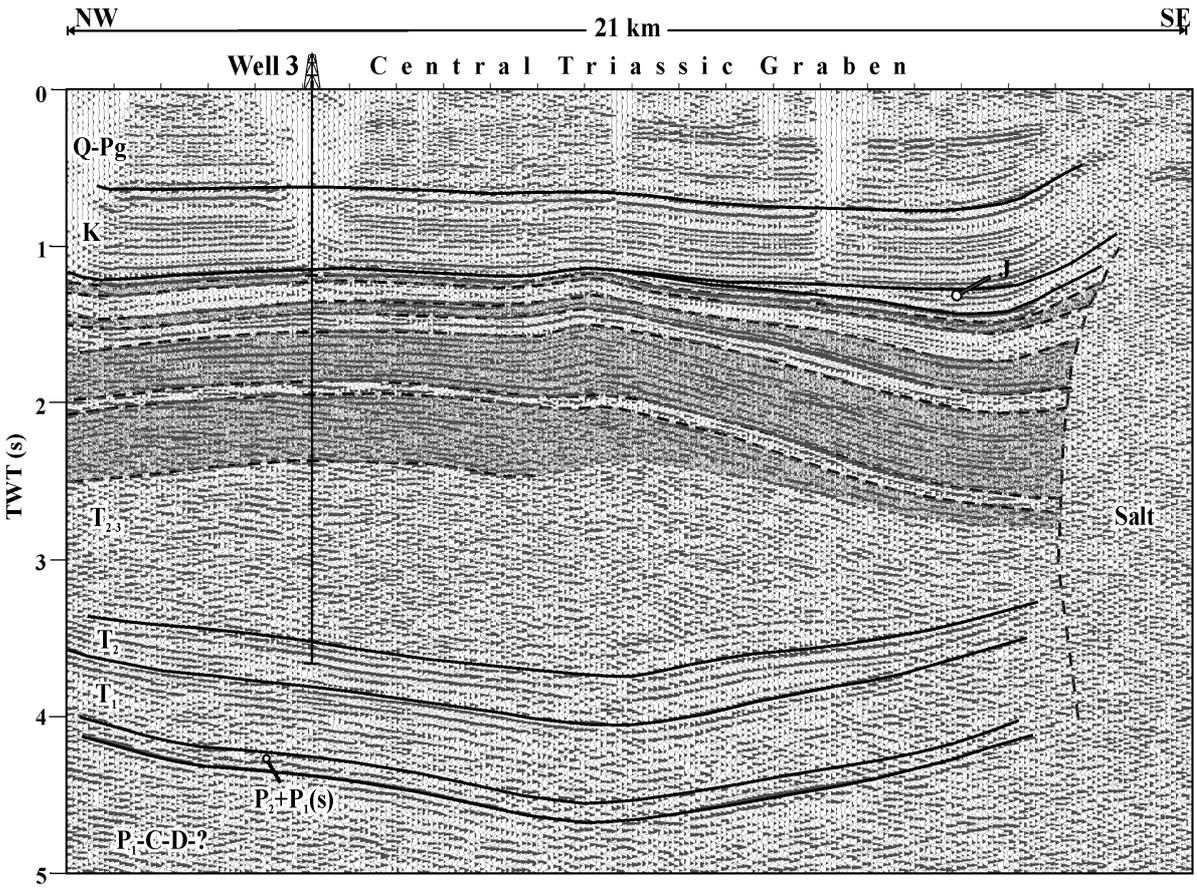
Seismic line 10
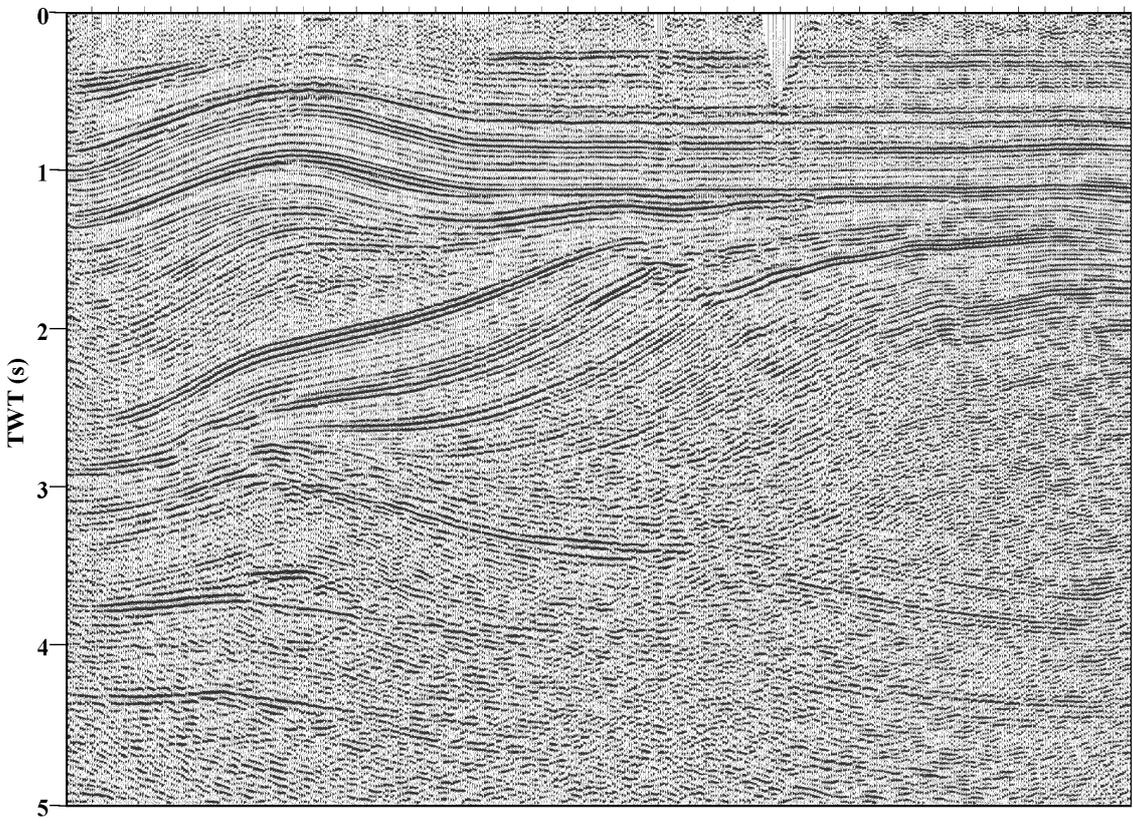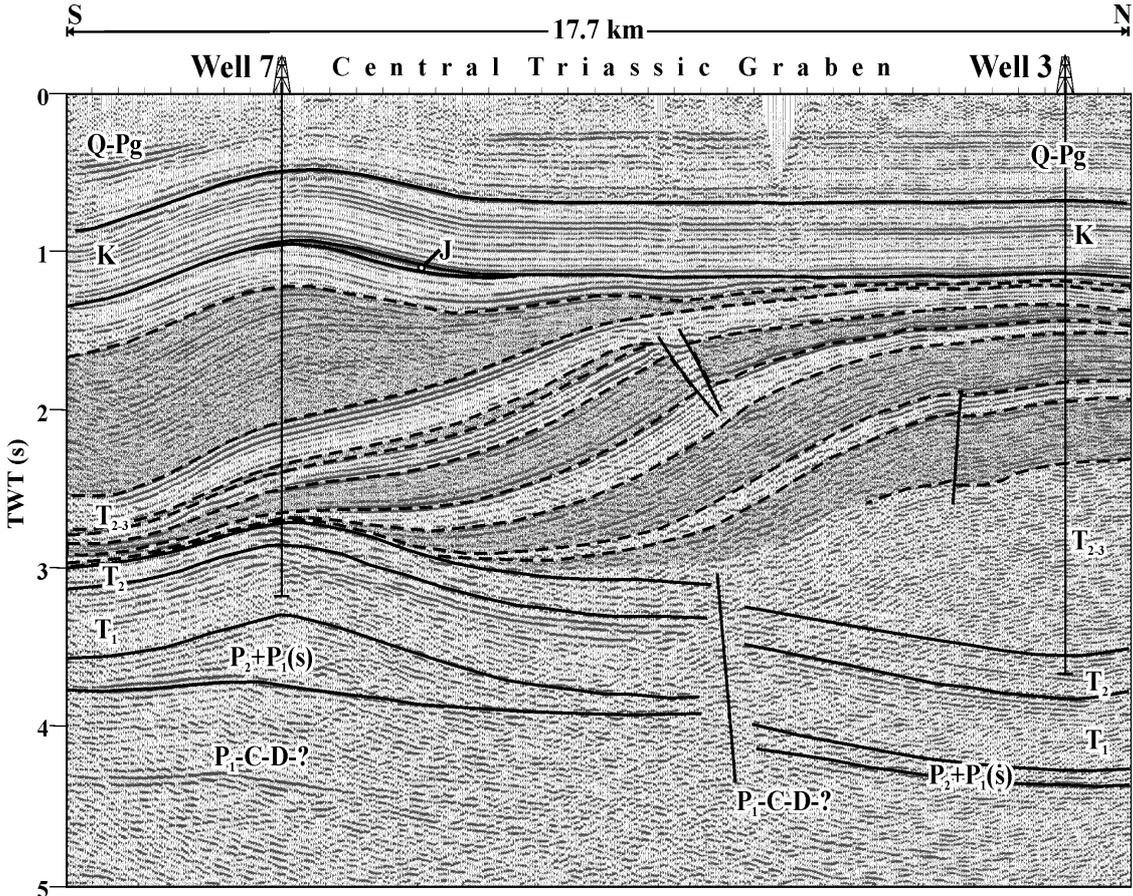
Seismic line 11

Seismic line 12
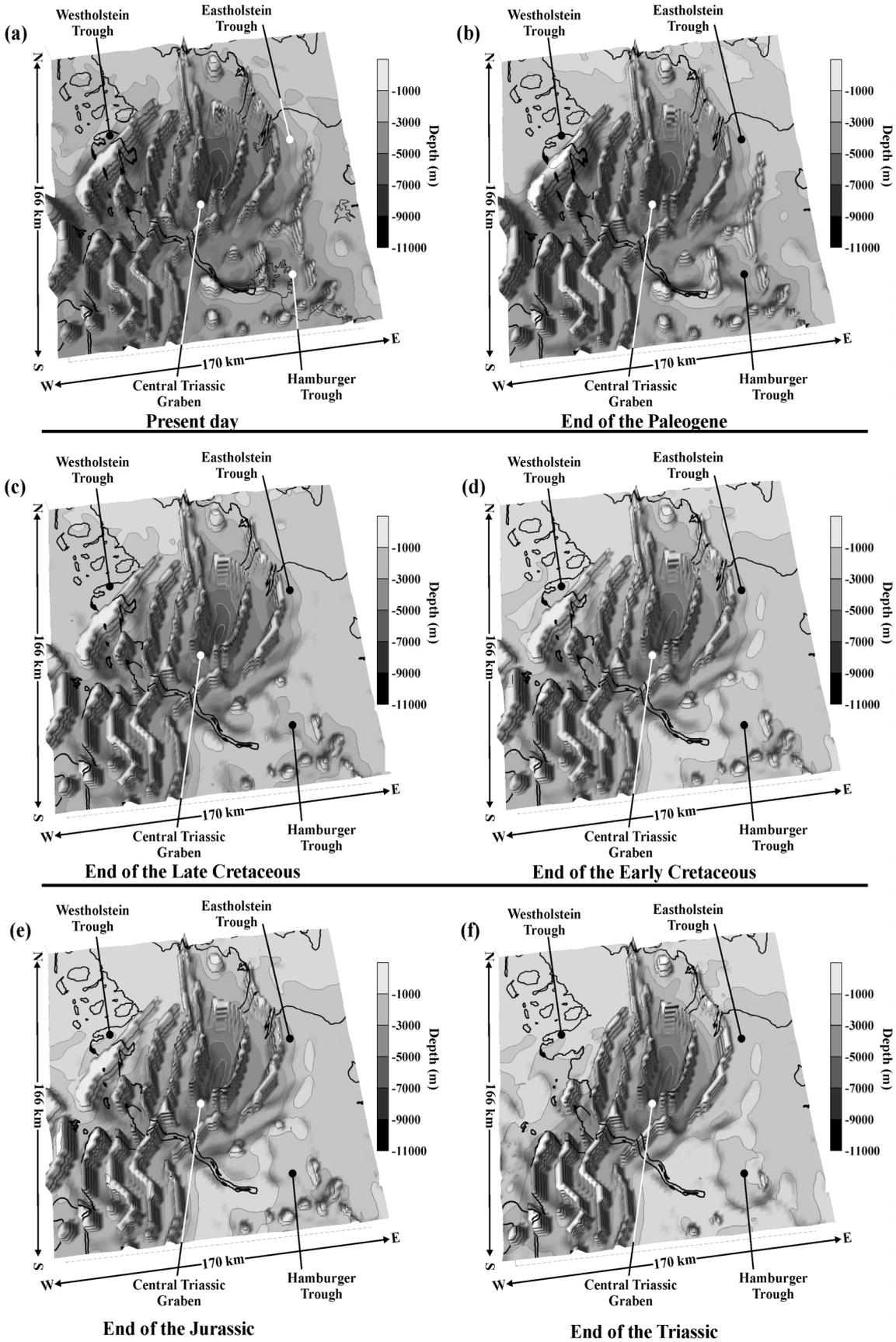
**3D views on the top of the Permian salt at the different stratigraphic levels.
Results of reverse modelling.**
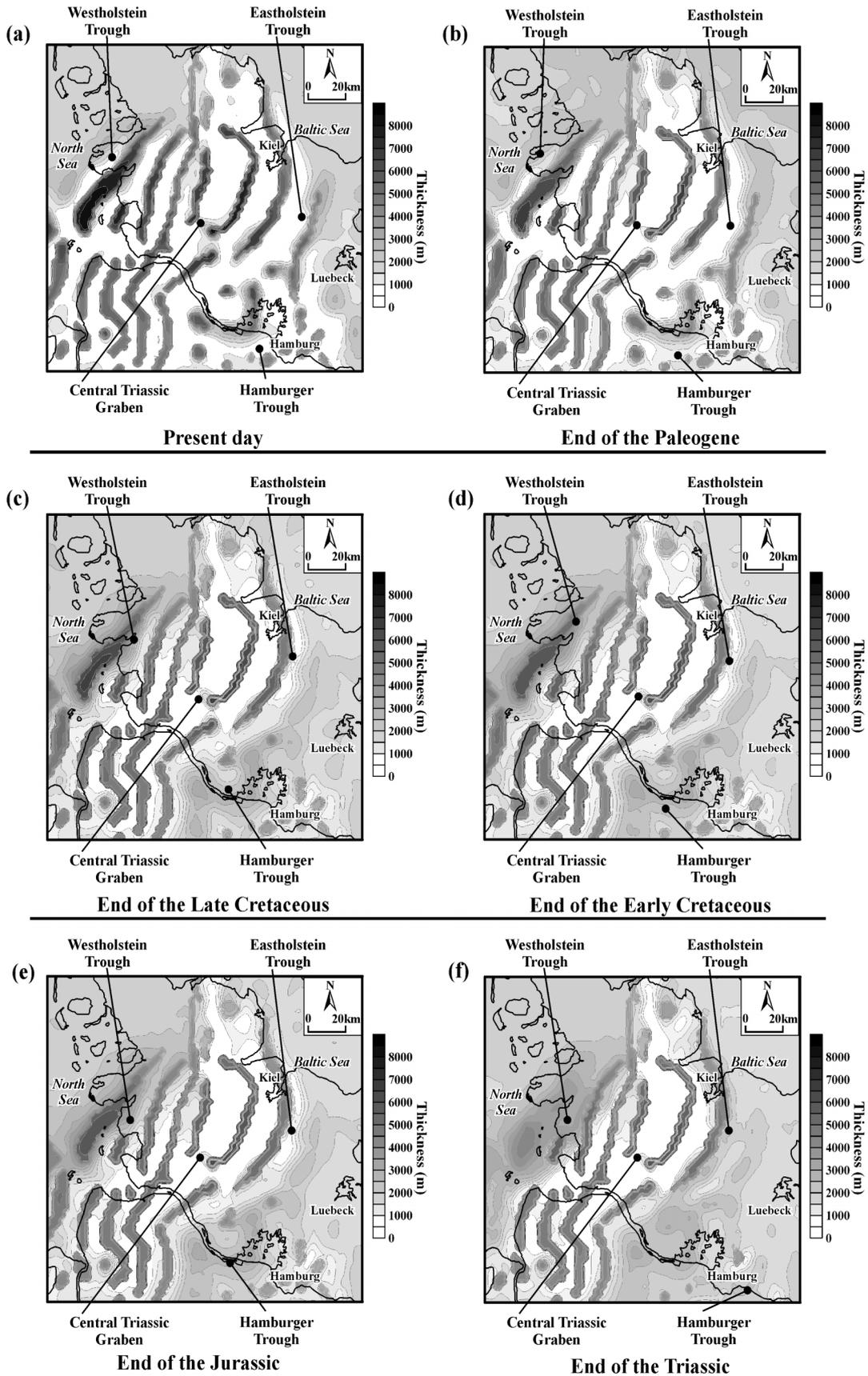
Isochore maps of the Permian salt representing thickness distribution of the salt from the end of the Triassic (f) to present day (a) based on reverse modelling

ERKLÄRUNG

Hiermit versichere ich, dass ich die Dissertation selbständig verfasst und keine anderen als die angegebenen Hilfsmittel verwendet habe. Daten, Materialien und Informationen, die ich durch andere erhalten habe, sind in der Arbeit kenntlich gemacht.

Diese Arbeit hat in gleicher oder anderer Form noch keiner Prüfungskommission (-behörde) vorgelegen.

Mit Genehmigung erfolgte Vorabveröffentlichungen von Teilergebnissen sind der Arbeit beigelegt.

Berlin,

<div align="center">

Curriculum Vitae

</div>

1. Personal Data

Surname: Maystrenko
First Name: Yuriy
Date of Birth: 12 May 1973
Place of birth: Rudnya, Kyiv oblast, Ukraine, USSR
Nationality: Ukrainian
Family status: married

2. Education

1990-1995:   Undergraduate student, Chair of Geophysics, Faculty of geology, Kyiv State University, Kyiv, Ukraine.
1999-2003:   Post-graduate student, Institute of Geophysics, National Academy of Science of Ukraine, Kyiv, Ukraine.

3. Professional Experience

1995 – 1996:   Geophysicist of the regional data interpretation group, State Geophysical Enterprise Ukrgeofisika, Kyiv, Ukraine.
1996 – 2001:   Geophysicist, Technology Center, State Geophysical Enterprise Ukrgeofisika, Kyiv, Ukraine.
2001-2002:   Scientist in the DFG project „International DOBRE project (DOnbas Basin region that includes deep seismic REfraction and REflection profiling)“, GeoForschungsZentrum, Potsdam, Germany
2002 – present: Scientist in the DFG-SPP 1135 project „3D structural modelling and basin analysis of the Central European Basin System between North Sea and Poland“, GeoForschungsZentrum, Potsdam, Germany.
Visiting Researcher:
February 2002: Free University, Faculty of Earth Sciences, Amsterdam, the Netherlands.

Address:

Yuriy Maystrenko
GeoForschungsZentrum Potsdam
Telegrafenberg, C426
D-14473 Potsdam, Germany
Phone: +49(0)331 288-1783
Fax: +49(0)331 288-1349
E-mail: yuram@gfz-potsdam.de

Home address:

Yuriy Maystrenko
Bisamkiez, 22
14478 Potsdam
Germany

List of publications

Publications related to this Ph.D. thesis are marked by a star.

Articles:

Stovba, S.M., Maystrenko, Yu. P., 2000. Features of SE Dniepr-Donets Basin formation by 2D forward and reverse tectonic modelling. Geophysical Journal, Vol. 22, No. 2: 70-84 (in Russian).

Maystrenko, Yu. P., Stovba, S.M., Sovich, T.A., 2001. Some data on the geological structure of the Zmeynuy-Vilkov area of highs from interpretation of regional reflection profiles in the Black Sea. In: The raw stocks of the Crimea and surrounding territories of the Black sea (oil&gas): Simferopol, "Tavria-Plus"–200 p., p.p. 108-113 (in Russian).

Stovba, S.M. and Maystrenko, Yu.P., 2001. Late Devonian extension of the crust as one of the causes of the heterogeneity formation in the crystalline rocks on the flanks of the Dniepr –Donets Basin. Geophysical Journal, v. 23, No. 6: 67-74 (in Russian).

DOBREflection-2000 and Dobrefraction'99 Working Groups (including Maystrenko Yu.), 2002. DOBRE Studies Evolution of Inverted Intra-cratonic Rifts in Ukraine. EOS (Transactions, American Geophysical Union), v. 83, n. 30, pp. 323, 326-327.

Stovba, S.M., Maystrenko, Yu.P., Stephenson, R.A., Kusznir, N.I., 2003. The formation of the south-eastern part of the Dniepr-Donets Basin: 2-D forward and reverse syn-rift and post-rift modelling. Sedimentary Geology, V. 156, pp. 11-33.

Maystrenko Yu., Stovba S., Stephenson R., Bayer U., Menyoli E., Gajewski D., Huebscher Ch., Rabbel W., Saintot A., Starostenko V., Thybo H., Tolkunov A., 2003. Crustal-scale pop-up structure in cratonic lithosphere: DOBRE deep seismic reflection study of the Donbas fold belt, Ukraine. Geology, V. 31, no. 8, pp. 733–736.

Saintot, A., Stephenson, R., Stovba, S., Maystrenko, Yu., 2003. Structures associated with inversion of the Donbas Foldbelt (Ukraine and Russia). Tectonophysics, V. 373, pp. 181-207.

*Maystrenko, Yu., Bayer, U., Scheck-Wenderoth, M., 2005. The Glueckstadt Graben, a sedimentary record between the North and Baltic Sea in north Central Europe. Tectonophysics, V. 397, pp. 113-126.

*Maystrenko, Yu., Bayer, U., Scheck-Wenderoth, M., 2005. Structure and evolution of the Glueckstadt Graben due to salt movements. International Journal of Earth Sciences, in press.

Abstracts:

Samoylyuk, O.P., Maystrenko, Yu.P., 1998. Construction of the chronostratigraphic diagram along the lines of regional seismic reflection profiles in the Dniepr-Donets basin. Oil&gas of Ukraine. Collected papers. After 5th International scientific-practical conference "Oil and Gas of Ukraine - 98", Poltava, Ukraine, Vol., pp. 243-244 (in Russian).

Maystrenko, Yu. P., Stovba, S.M., Sovich, T.A., 2000. Some data about the structure of the Kilian-Zmeinian area of high by interpretation of regional reflection profiles. Abstracts of the International scientific conference of the young scientists and specialists "Oil and gas geology and geophysics of Ukraine – look in the new millennium", Chernigiv, Ukraine, pp. 117-118 (in Russian).

Maystrenko, Yu. P., Stovba, S.M., 2000. Processes of the Devonian rifting within some areas of the Northern flank of Dniepr-Donets basin. Abstracts of the International scientific conference of the young scientists and specialists "Oil and gas geology and geophysics of Ukraine – look in the new millennium", Chernigiv, Ukraine, pp. 48-50 (in Russian).

Maystrenko, Yu. P., Stovba, S.M., Sovich, T.A., 2000. Some data about the structure of the Kilian-Zmeinian area of high by interpretation of regional reflection profiles. Abstracts of the 2-nd International Conference on "Tectonics and oil-gas bearing of Azov-Black sea regions due to continents passive outskirts oil-gas bearing", Gurzuf, Crimea, Ukraine, pp. 48-54 (in Russian).

Maystrenko, Yu.P., Stovba, S.M., 2000. Dniepr-Donets Basin: some features of the Late Devonian rift stage. Geophysical Journal, Vol. 22, No. 4: 111.

Maystrenko, Yu.P., Stovba, S.M., Sovich, T.A., 2000. Structure of the Zmeinian-East-Vilkovian uplift zone, Black Sea, Ukraine, from regional seismic reflection profiles. Geophysical Journal, Vol. 22, No. 4: 112.

Maystrenko, Yu.P., Stovba, S.M., 2000. Extension within north flank of Dniepr-Donets Basin during the rift stage. Oil&gas of Ukraine. Collected papers. After 6th International scientific-practical conference "Oil and Gas of Ukraine - 2000", Ivano-Frankivsk, Ukraine, Vol. 1. 256-261 (in Russian).

Stovba, S.N., Turchanenko, N.T., Sovich, T.A., Maystrenko, Yu.P., Kalatalo, T.V., 2000. The structure and phases of the evolution of the transzone from Dniepr-Donets trough to Donets Foldbelt. Oil&gas of Ukraine. Collected papers. After 6th International scientific-practical conference "Oil and Gas of Ukraine - 2000", Ivano-Frankivsk, Ukraine, Vol. 1. 319-321 (in Russian).

Maystrenko, Yu., Bayer, U. and Stovba, S., 2001. Structural Interpretation of the Seismic reflection line "DOBREflection 2000" from the Ukrainian Shield (Priazovian Massif) to the Donbas-area // Abstracts of a joint meeting of the URALIDES, GEORIFT, TESZ, and SW-IBERIA Projects on "Variscides-Craton-Uralides: Linkage between Orogenic and Intraplate Processes". EUROPROBE. Devonian-Triassic "Time-Slice" Symposium. Moscow, Russia, p.16-17.

Bayer, U., Stovba, S., Maystrenko, Y., Stephenson, R., Tolkunov, A. and the DOBREflection Working Group, 2002. DOBREflection: An Exceptional Example of Basin Inversion in the East-European Craton // European Geophysical Society,

XXVII General Assembly, CD-ROM: Geophysical Research Abstracts, vol. 4, 2002; Abstract Number: EGS02-A-01640. Nice, France.

Maystrenko, Y., Stovba, S., Bayer, U., Stephenson, R., Tolkunov, A. and the DOBREflection Working Group, 2002. Donbas Foldbelt: An Exceptional Example of Basin Inversion // European Geophysical Society, XXVII General Assembly, CD-ROM: Geophysical Research Abstracts, vol. 4, 2002; Abstract Number: EGS02-A-04203. Nice, France.

Tolkunov, A., Stovba S., Stephenson, R., Maystrenko, Y., Bayer, U., and the DOBREflection Group, 2002. The structure of the Donbas Foldbelt (Ukraine) from DOBREflection-2000 // 64th EAGE Annual Conference & Exhibition. Florence, Italy (auf englisch).

*Bayer, U., Hoffmann, N., Scheck, M., Meyer, H., Maystrenko, Y., 2002. 3D structural modelling and basin analysis of the Central European Basin System (CEBS) between the North Sea and Poland // Workshop of the German Research Foundation (DFG) – SPP „Dynamics of sedimentary systems under varying stress conditions by example of the Central European Basin System", p. 1-2. Schloss Eringerfeld, Germany.

*Bayer, U., Hoffmann, N., Maystrenko, Yu., Scheck-Wenderoth, M., Meyer, H., 2003. 3D structural modelling and basin analysis of the North-Western German Basin (area around the Glueckstadt Graben) // EGS-AGU-EUG Joint Assembly, CD-ROM: Geophysical Research Abstracts, vol. 5, 2003; Abstract Number: EAE03-A-01048. Nice, France.

*Bayer, U., Hoffmann, N., Maystrenko, Y., Scheck-Wenderoth, M., Meyer, H., 2003. 3D structural modelling and basin analysis of the North-Western German Basin (area around the Glueckstadt Graben) // Workshop of the German Research Foundation (DFG) – SPP 1135 „Dynamics of sedimentary systems under varying stress conditions by example of the Central European Basin System". Hamburg, Germany.

Maystrenko, Yu., Bayer, U., Stovba, S., Stephenson, R., Saintot, A., 2003. 2D Reverse Tectonic Modelling along the DOBRE-2000 deep seismic reflection profile and its northern continuation in the Donbas Foldbelt, Ukraine // International geophysical conference and exhibition "Geophysics of the 21st century – the leap into the future", CD-ROM: PS14, Poster N 17. Moscow, Russia.

*Bayer, U., Maystrenko, Yu., Hoffmann, N., Scheck-Wenderoth, M., Meyer, H., 2003. The structure of the Upper Triassic (Keuper) sequence based on the deep borehole data and interpretation of seismic lines within Glueckstadt Graben // International geophysical conference and exhibition "Geophysics of the 21st century – the leap into the future", CD-ROM: PS6, Poster N 7. Moscow, Russia.

*Bayer, U., Maystrenko, Yu., Hoffmann, N., Scheck-Wenderoth, M., Meyer, H., 2003. 3D structural modelling and basin analysis of the Central European Basin System (CEBS) between the North Sea and Poland. Terra Nostra. Heft Nr. 2003/03, p. 1-4.

*Maystrenko, Yu., Bayer, U., Scheck-Wenderoth, M., 2004. Meso-Cenozoic evolution and structure of the Glueckstadt Graben by well data, seismic lines and 3D-structural model, NW Germany // 1st EGU General Assembly, CD-ROM: Geophysical

Research Abstracts, vol. 6, 00097, 2004; Abstract Number: SRef-ID: 1607-7962/gra/EGU04-A-00097. 25-30 April 2004. Nice, France.

Bayer, U., Gajewski, D., Maystrenko, Yu., 2004. Strain localization in basin inversion – a comparison between the deep seismic lines DOBREflection and DEKORP Basin'96. Abstracts book, p. 11. // Inversions-Workshop of the German Research Foundation (DFG) – SPP 1135. 26 June 2004. Hannover, Germany.

*Maystrenko, Yu., Bayer, U., Scheck-Wenderoth, M., 2004. Meso-Cenozoic evolution of the Glueckstadt Graben according to results of 3D-structural modelling and interpretation of seismic lines, NW Germany. Schriftenreihe der DGG, Heft 34, Kurzfassungen der Vorträge und Poster, p. 261. // GeoLeipzig 2004, Geowissenschaften sichern Zuckunft. 29.09-01.10 2004, Leipzig, Germany.

Yegorova, T., Bayer, U., Maystrenko, Yu., Scheck-Wenderoth, M., Thybo, H., 2004. Gravity signals in the CEBS. Terra Nostra, 05, pp. 118-121.

*Maystrenko Yu., Bayer U., Scheck-Wenderoth M., 2005. The Glueckstadt Graben: structure and evolution caused by salt movements, and its relation to other Triassic subsidence centers within the Central European Basin System // General Assembly, CD-ROM: Geophysical Research Abstracts, Vol. 7, 02553, 2005, SRef-ID: 1607-7962/gra/EGU05-A-02553. 24 – 29 April 2005, Vienna, Austria.

Scheck-Wenderoth M., Mazur S., Maystrenko Y., Lamarche J., Bayer U., 2005. The main players in Mesozoic deformation of the Central European Basin System // General Assembly, CD-ROM: Geophysical Research Abstracts, Vol. 7, 06579, 2005, SRef-ID: 1607-7962/gra/EGU05-A-06579. 24 – 29 April 2005, Vienna, Austria.

Yegorova T., Bayer U., Thybo H., Maystrenko Y., Scheck-Wenderoth M., Lyngsie S., 2005. Gravity signals in the Central European Basin System // General Assembly, CD-ROM: Geophysical Research Abstracts, Vol. 7, 00972, 2005, SRef-ID: 1607-7962/gra/EGU05-A-00972. 24 – 29 April 2005, Vienna, Austria.